

# ***ROSETTA***

## **Radio Science Investigations (RSI)**

### **Experiment User Manual**

**Reference: RO-RSI-IGM-MA-3081**

**Issue: 4**

**Revision: 2**

Rheinisches Institut für Umweltforschung, Abt. Planetenforschung  
Universität zu Köln  
Aachenerstr 209  
D-50931 Köln

Prepared by:

---

Silvia Tellmann, Experiment Manager

Approved by:

---

Martin Pätzold, Principal Investigator

ROSETTA RSI: **Rosetta Radio Science Investigations**  
**Experiment User Manual**

Document **RO-RSI-IGM-MA-3081**

Issue: 4

Revision: 2

Date: 25.04.2016

Page: 2 of 144

---

PAGE LEFT FREE

# Contents

1	Introduction.....	10
1.1	Purpose.....	10
1.2	Scope.....	10
1.3	Applicable Documents.....	10
1.4	Referenced Documents.....	10
1.5	Abbreviations.....	11
2	An Introduction to Radio Science .....	14
2.1	Introduction .....	14
2.2	Background.....	14
2.3	Technique .....	17
3	Mission Characteristics.....	20
3.1	Scientific Objectives of the Rosetta RSI Experiment.....	20
	Primary Scientific Objectives .....	20
	Secondary Scientific Objectives .....	21
3.1.1	Gravity: Cometary Mass and bulk density.....	21
3.1.2	Gravity: Cometary Gravity Field Coefficients.....	23
3.1.3	Gravity: Cometary Moments of Inertia.....	24
3.1.4	Gravity: Cometary Orbit.....	25
3.1.5	Nucleus: Surface (Bistatic Radar) .....	25
3.1.6	Nucleus: Internal Structure.....	27
3.1.7	Nucleus: Size and Shape.....	27
3.1.8	Coma: Plasma and Dust Content.....	27
3.1.9	Coma: Mass Flux .....	28
	Asteroids: Mass and Bulk Density.....	28
3.1.10	.....	28
3.1.11	Solar Corona.....	31
3.2	Overview of the Instrument: Space Segment.....	31
3.2.1	General .....	31
3.2.2	Definition of Radio Links.....	32
3.2.3	Radio Link Budget.....	33
3.2.4	Radio Link Mode and Scientific Objective Cross Reference .....	34
3.3	Overview of the Instrument: Ground Segment .....	35
3.3.1	Overview .....	35
3.3.2	Ground Stations .....	35
3.3.3	Ground Station Capabilities.....	35
3.3.4	Observed Quantities .....	36
3.4	Data Products.....	39
3.4.1	Introduction .....	39
3.4.2	Data types.....	39
3.4.3	Data required from ESOC and JPL.....	39
3.4.4	Data Volume Calculation.....	46
3.4.5	End-to-End performance.....	48
4	Experiment Operations.....	53
4.1	Definitions and Configurations.....	53
4.1.1	Spacecraft and Ground Station configurations.....	53
4.1.2	ONES.....	53

4.1.3	ONED.....	54
4.1.4	TWOS.....	55
4.1.5	TWOD.....	55
4.2	RSI Operational Procedures.....	57
4.2.1	PCx Passive or Active Checkout Number x.....	57
4.2.2	CMD Center of mass determination.....	58
4.2.3	DOT Doppler Tracking.....	58
4.2.4	GMC Gravity Mapping Campaign.....	59
4.2.5	OCP Occultation Operations Procedures.....	59
4.2.6	BRP Bistatic Radar Procedures.....	60
4.2.7	AST Asteroid Flyby Procedures.....	60
4.2.8	SCP Solor Corona Procedure.....	60
	HGA Pointing Requirements.....	61
4.3	.....	61
4.3.1	Overview.....	61
4.3.2	Earth inertial pointing.....	61
4.3.3	Comet pointing.....	61
4.3.4	Phase center pointing.....	61
4.4	Mapping of Science Objectives to Operational Procedures.....	63
4.5	Functions: Space Segment.....	64
4.5.1	Design and Functional Description of the RF Subsystem.....	64
4.6	Functions: Ground Segment.....	66
4.6.1	Overview.....	66
4.6.2	Deep Space Network.....	72
5	RSI Interface with RMOC.....	81
5.1	Operation Procedure Request.....	81
5.1.1	EPS syntax.....	81
5.2	Data retrieval.....	94
5.3	Interface JPL/RSI.....	94
6	Detailed Descriptions of Operational Procedures.....	96
6.1	Overview.....	96
6.2	PCx: Passive Checkout Number x.....	97
6.2.1	Objective.....	97
6.2.2	Operations.....	97
6.3	CMD: Center of Mass Determination.....	100
6.3.1	Objective.....	100
6.3.2	Operations.....	100
6.4	Doppler Tracking: DOT.....	104
6.4.1	Objective.....	104
6.4.2	Operation.....	105
6.5	GMC: Gravity mapping Campaign.....	109
6.5.1	Objectives.....	109
6.5.2	Description.....	109
6.5.3	Operations.....	110
6.6	OCP: Occultation Operations Procedure.....	113
6.6.1	Objectives.....	113
6.6.2	Description.....	113
6.6.3	Operations.....	114
6.7	BRP: Bistatic Radar Procedure.....	121

6.7.1	Objective .....	121
6.7.2	Description .....	121
6.7.3	Operations.....	121
6.8	SCP: Solar Conjunction Procedure .....	126
6.8.1	Objectives .....	126
6.8.2	Description .....	126
6.8.3	Operations.....	126
6.9	AST: Asteroid Flyby Procedures .....	129
6.9.1	Objective .....	129
6.9.2	Description .....	129
6.9.3	Operations.....	129
7	Flight Operation Procedures (FOP); Sequence-of-Events.....	134
7.1	Definitions .....	134
7.1.1	Format of FOP file names .....	134
7.1.2	RSI FOP procedures .....	134
7.1.3	Format of Command Sequence Files.....	135
7.1.4	Command sequence files.....	135
8	Commissioning Results .....	136
8.1	NEVP Commissioning.....	136
8.2	Passive Checkout Results.....	136
9	References .....	137

## List of figures

Figure 3.1-1: Accuracy of comet nucleus mass determination .....	22
Figure 3.1-2: Velocity perturbation due to the gravity field coefficients $C_{20}$ and GM. ....	23
Figure 3.1-3: Distance Earth-Churyumov-Gerasimenko and Sun-Churyumov-Gerasimenko as function of time .....	24
Figure 3.1-4: Monostatic and bistatic radar .....	27
Figure 3.2-1: Block diagram of the Rosetta radio subsystem .....	32
Figure 3.2-2: Radio link modes between the orbiter and the ground station on Earth. Upper panel: one-way X-band downlink. Lower panel: Two-way radio link where the uplink is transponded back phase-coherently at a dual-frequency downlink. The frequency stability is governed by an hydrogen maser located at the ground station.....	33
Figure 3.4-1: Total Doppler noise as a function of integration time.....	51
Figure 3.4-2: Orbital Velocity and Spacecraft revolution period as function of distance to comet center of mass .....	52
Figure 4.5-1: Block diagram of the Rosetta radio subsystem .....	64
Figure 4.6-1: IFMS block diagram .....	67
Figure 4.6-2: IFMS Open-Loop Digital Data Processing Part for RSI .....	68
Figure 4.6-3: IFMS internal signal processing. The 8 bit resolution will be replaced by a 12 bit resolution. ....	69
Figure 4.6-4: DSN Network.....	73
Figure 4.6-5: DSN subsystem schematics.....	74
Figure 4.6-6: DSN open loop receiver block diagram .....	76
Figure 6.4-1: Required tracking time as a function of Doppler integration time to resolve perturbing acceleration from the Doppler noise background for $2\sigma$ and a $10\sigma$ signal.....	108

## List of tables

Table 3.1-1: Rosetta asteroid flyby parameters .....	30
Table 3.2-1: Radio link modes and RSI science objectives .....	34
Table 3.4-1: Doppler velocity error budget .....	52
Table 4.2-1 RSI Pointing Requests .....	61
Table 4.3-2 Pointing Request Parameters.....	62
Table 4.4-1: Mapping of Science Objectives to Operational Procedures.....	63
Table 4.6-1: IFMS receiver system scenario 1 .....	69
Table 4.6-2: IFMS receiver system scenario 2 .....	70
Table 4.6-3: IFMS receiver system scenario 3 .....	70
Table 4.6-4: IFMS receiver system scenario 4 .....	71
Table 4.6-5: DSN operational modes .....	79
Table 4.6-6: DSN sampling rates.....	79
Table 4.6-7: DSN Channel assignments.....	79
6.3 CMD: Center of Mass Determination.....	100

## Document Change Record

Issue	Rev.	Section	Date	Changes	Author
Draft	0	All	12. Sep. 00	Initial version	mpa
1	0	all	12.12.2000	all sections	mpa
1	1	2	10.10.2001	section 2 added	mpa
		3.1	10.10.2001	Figures updated	mpa
		3.4.2	10.10.2001	section updated IFMS scenarios updated and added	mpa
		3.4.3	10.10.2001	section added	mpa
		4.1 4.4	10.10.2001	section added Ops Timeline extended	mpa
		5.1-5.9	10.10.2001	sections updated	mpa
		5.10	10.10.2001	Grand total data volume section added	mpa
		6	10.10.2001	section included	mpa
	2	all 5,7	20.03.2002	minor revisions, nomenclature ground-segment configs revised detailed HGA pointing request added	mpa
2	0	All	15-May-02	Document restructured	mpa
2	1	2,4,5,6,7	16.07.02	Numbering updated, FCP-tables rewritten, DSN description added	mpa
2	2	3 4  5 6 7	25.08.02	Section 3.4.3 open-loop data volume updated Section 4.1.3, table 4.1-2 updated Section 4.1.4, Table 4.1.-3 deleted Section 4.4.1 editing Section 4.4.1 4.5, Table 4.5-1 to 4.5-5 updated section 5.3 editing chapter 6 all sections updated chapter 7 all FOP tables corrected and updated	ah
2	3	6.3	09.10.2002	Table 6.3-2 updated FOP TVT PROC-1 to PROC-7 updated Some editing	ah
3	0	6.1	31.03.2003	EPS section included	lc
4	0	All	13.01.2006	New target comet included, Commissioning results included, update of several chapters	st
4	1	All	20.01.2006	Updated mainly the sequences and asteroid flybys	st
4	2	3.3.2.1 3.4.3.1.2 3.4.3.2.1 3.4.3.2.2	25.04.2016	Update of groundstation description Update Section included Section included	jo

## Distribution List

Recipient	Institution	No. of copies
<b>RSI Team</b>		
Martin Pätzold	IGM	1
Kaare Aksnes	ITA	1
John D. Anderson	JPL	1
Sami W. Asmar	JPL	1
Jean-Pierre Barriot	CNES	1
Michael K. Bird	RAIUB	1
Hermann Bönhardt	ESO	1
Eberhard Grün	MKP	1
Bernd Häusler	UniBW	1
Wing-H. Ip	NUTw	1
Essam Marouf	SJSU	1
Trevor Morley	ESOC	1
Fritz M. Neubauer	IGM	1
Hans Rickman	AOU	1
Silvia Tellmann	IGM	1
Nick Thomas	MPAe	1
Bruce T. Tsurutani	JPL	1
<b>Rosetta Project</b>		
Viney Dhiri	ESTEC	1
Paolo Ferri	ESOC	1
Armelle Hubault	ESOC	1
Detlef Koschny	ESTEC	1
Elsa Montagnon	ESOC	1
Gerhard Schwehm	ESTEC	1
Kristin Wirth	ESTEC	1

# 1 Introduction

## 1.1 Purpose

This document presents the Experiment User Manual for the RSI experiment. It is intended as a reference for the implementation of RSI science operations during the ROSETTA mission.

## 1.2 Scope

The document defines the science objectives, describes the observational methods, and the configuration and operational modes of the RSI experiment, with regard to the space and ground station segments. The document describes the Scientific objectives, maps these to the RSI operations, depicts the configurations and functions of the space- and ground segments of the RSI experiment and defines the interface with ground. Section 6 is intended as an additional reference: Here the characteristics of the experiment are listed by individual operational procedures.

## 1.3 Applicable Documents

The following documents are applicable to this document:

	Reference Number	Title
[1]	GRST-TTC-GS-ICD-0518-TOSG	IFMS-to-OCC Interface Control Document
[2]	MEX-MRS-IGM-RS-3014	IFMS User Requirement Document
[3]	SOP-RSSD-SP-002	Science operations for planetary missions EPS PTR SSD
[4]	RO-EST-TN-3053	ROSETTA Mission Scenarios - Pointing
[5]	ROS-RSI-IGM-IS-3079	Archive Generation, Validation and Transfer Plan
[6]	ROS-RSI-IGM-IS-3087	Radio Science File Naming Convention and Radio Science File Formats

## 1.4 Referenced Documents

The following documents are referenced by this document:

	Reference Number	Title
[7]	RO-ESC-IF-5002	Rosetta SGCID Vol. 1
[8]	MR-IFMS-ICD-FTP-OCC	IFMS-OCC ICD
[9]	<i>RO-RSI-IGM-TN-3057</i>	RSI Technical Note: Jitter
[10]	RO-RSI-IGM-RS-3014	MaRS IFMS Requirement Specifications
[11]		Archival Tracking Data File ATDF TRK 2-25 Original Data Record ODR RSC 11-13 Radio Science Receiver RSR

		0189-Science
[12]	DSN810-5	Deep Space Network / Flight Project Interface Design Book, Document 810-5, JPL, Pasadena, CA.
[13]	ROS-RSI-IGM-TR-3117	Rosetta Radio Science Investigations: Report on NEVP Commissioning Operations March, May, September and October 2004
[14]	RO-EST-RS-3169	ROSETTA Spacecraft Housekeeping Parameter Delivery on the DDS
[15]	RO-EST-TN-3215	How to find Spacecraft Housekeeping Parameters on the DDS
[16]	RO-ESC-IF-5003	Rosetta Mission Control System; DDID Data Delivery Interface Document
[17]	ROS-RSI-IGM-RP-3123	Report on RSI Commissioning and Passive Checkout Results

## 1.5 Abbreviations

ADEV	Allan Deviation
AGC	Automatic Gain Control
AOU	Astronomical Institute, Uppsala University
AST	Asteroid Flyby Procedures
ATDF	Archival Tracking Data File
AVAR	Allan Variance
BRP	Bistatic Radar Procedures
BVA	High performance, low phase noise type of quartz oscillator
CEB	Ceberos
CMD	Center of Mass Determination
CNES	Centre National d'Etude Spatiale
DOT	Doppler Tracking Procedure
DSA	Deep Space Antenna
DSN	Deep Space Network
DTM	Digital Topographic Model
DUT	Device under test
EM	Engineering Model
EDF	Experiment Description File
EPS	Experiment Planning System
EQM	Electrical Qualification Model
ESA	European Space Agency
ESO	European Southern Observatory
ESOC	European Space Operations Centre
FCP	Flight Control Procedure
FM	Flight Model
FOM	Flight Operations Manual
FS	Flight Spare
GMC	Gravity Mapping Campaign
G/S	Ground Station
HDEV	Hadamard Deviation
HGA	High Gain Antenna
HRSC	High Resolution Stereo Camera
HVAR	Hadamard Variance
IFMS	Intermediate Frequency Modulation System
IGM	Institut für Geophysik und Meteorologie, Universität zu Köln
ITA	Institute of Theoretical Astrophysics, Oslo University
JPL	Jet Propulsion Laboratory
LCP	Left Circular Polarization

LGA	Low Gain Antenna
LHC	Left Handed Circulated Polarization
LOS	Line-of-Sight
MaRS	Mars Express orbiter Radio Science Experiment
MKP	Max-Planck-Intitut für Kernphysik
MLG	Malargue
MPAe	Max-Planck Institut für Aeronomie
MPTS	Multi-Protocol Transport Service
NASA	National Aeronautics and Space Administration
NEVP	Near Earth Verification Phase
NNO	New Norcia
OCP	Occultation Operations Procedure
ONES	One-way single-frequency mode
ODF	Orbit Data File
ODR	Original Data Record
OPR	Operation Procedure Request
PA	Power Amplifier
PCx	Payload Passive or Active Checkout Number x
PFM	Proto Flight Model
PLL	Phase-lock loop
PSD	Power Spectral Density
RAIUB	Radioastronomisches Institut der Universität Bonn
RCP	Right Circular Polarization
RF	Radio Frequency
RFDU	Radio Frequency Distribution Unit
RHC	Right Handed Circulated Polarization
RSI	Radio Science Investigation
RSR	Radio Science Receiver
RX	S-band Receiver
S/C	Spacecraft
SCP	Solar Corona Procedure
SGICD	Surface Ground Interface Control Document
SJSU	San Jose State University
SNR	Signal-Noise-Ratio
SOHO	Solar and Heliospheric Observatory
SoM	School of Mathematics, University of Wales
SOWT	Science Operations Working Team
STAT	Science Time Analysis Tool
S-TX	S-Band Transmitter
TBD	To be defined
TBC	To be confirmed
TBW	To be written
TCXO	Temperature controlled crystal oscillator
TT&C	Telemetry Tracking & Comanding
TNF	Tracking and Navigation File
TWOD	Two-way dual-frequency mode
TWOS	Two-way single-frequency mode
TWTA	Travelling wave tube amplifier
UniBW	Universität der Bundeswehr
USO	Ultra Stable Oscillator
VCXO	Voltage controlled crystal oscillator
X-TX	X-band Transmitter

ROSETTA RSI: **Rosetta Radio Science Investigations**  
**Experiment User Manual**

Document **RO-RSI-IGM-MA-3081**

Issue: 4

Revision: 2

Date: 25.04.2016

Page: 13 of 144

---

PAGE LEFT FREE

## 2 An Introduction to Radio Science

### 2.1 Introduction

Initially conceived as an exploratory tool, radio science techniques have provided considerable knowledge of the atmospheres and gravity of the planets – many of them originally unanticipated. Radio Science techniques are applied to the study of planetary and cometary surfaces, planetary rings and surfaces, and gravity, as well as the solar corona.

### 2.2 Background

*Radio Science* is the general study of phenomena affecting the propagation, scattering, and reception of electromagnetic transmissions in the wavelength regime longward of roughly 0.1 millimeters. A broad array of phenomena and the techniques used in studying them fall in this category, including much of electromagnetism in the natural world. The distinction between ‘radio science’ and ‘electromagnetics,’ as used especially in an engineering sense, is the emphasis in the former on study of phenomena observed in nature. In the context of planetary study and exploration, however, the term radio science has come generally to indicate a focus on the use of radio signals traveling between spacecraft and an Earth terminal for scientific investigation of planets and their environs. This specialized usage arises from the historical development of space applications. Thus, for example, topside sounding and passive reception of natural emissions properly would be ‘radio science’ in a terrestrial context, but these topics likely would be identified in terms of the specific techniques when applied in space. In the context of planetary studies the term radio science also includes the scientific application of radio tracking data in the precise determination of a spacecraft’s orbit and scientific information that can be derived from such information. Radio signals provide an extremely precise measurement of the radio path between the ground station and the spacecraft, and such measurements in turn are employed to infer important characteristics of planetary systems.

Early missions incorporating radio science investigations include the Mariners, Pioneers, and Viking, as well as Soviet projects. Examples of recent and current radio science investigations include those conducted with Voyager (Eshleman et al. 1977; Tyler 1987), Ulysses (Bird et al., 1994, 1996; Pätzold et al., 1995, 1996), Giotto (Pätzold et al., 1991a; 1991b; 1993, 2001a), Galileo (Howard et al. 1992), Magellan (Tyler et al., 1991, 1992a), Mars Observer (Tyler et al. 1992b), and Mars Global Surveyor (Tyler et al. 2000, 2001; Bougher et al., 2004; Hinson et al., 2004a,b). Missions carrying radio science investigations currently en route or planned include Cassini (Bird et al., 1995, 2005), Rosetta (Pätzold et al., 2000a), Mars Express (Pätzold et al., 2004) and Venus Express (Häusler et al., 2006).

Radio science investigations fall into three broad categories of experimentation and observation.

First, for the study of planetary or cometary environments, the orbit or trajectory of the spacecraft is arranged so that the spacecraft passes behind the planetary body as seen from the tracking station on the Earth. In this instance the spacecraft is said to be ‘occulted’ by the planet during those intervals when the

atmosphere or body of the planet lies between the radio source and receiver. In a typical occultation experiment conducted with an orbiter, the spacecraft sequentially passes behind the ionosphere, the neutral atmosphere, and body of the planet as seen from the tracking station, and then reemerges in the reverse sequence. During an occultation event one 'senses' the media of interest—atmosphere and ionosphere—by the effect of the gas on the radio signal. The method can be extended to any one of several separable 'atmospheres' including the planetary rings and magnetospheres, as well as the relativistic gravitational effects of stars (Eshleman, 1973) or the dust and cometary environment of a comet's nucleus. In conducting such observations the geometry and other experimental conditions must be controlled so that the only significant unknown factors are the properties of the medium along the radio path.

Second, oblique incidence scattering investigations using carom paths between spacecraft, a planetary or satellite surface, and an Earth station can be used to explore the surface properties through study of the microwave scattering function. This technique was first described by Fjeldbo (1964). Such investigations are referred to as 'bistatic radar' after the military nomenclature for radar systems in which the transmitter and receiver are separated by significant angular distances or ranges. In this instance the first experiment in space was conducted on the moon with Luna-11 (Yakovlev & Efimov, 1966). The oblique scattering geometry afforded by the Lunar Orbiter-1, which orbited the moon in 1966, provided the signal source for the first US mission and signals from Explorer-35 also contained echos from the lunar surface (Tyler et al., 1968b). As it happened, the plane of the spacecraft spin axis and the antenna polarization made it possible to measure the Brewster angle of the lunar crust, leading to an unambiguous value for the relative dielectric constant of lunar soil between 2.9 and 3.1, and thereby confirming that a future landing spaceship would be on firm (lunar) ground.

Third, when the radio path is well-clear of occulting material, the spacecraft can be treated as a classical 'test particle' falling in the gravity field of the planetary system with the component of its velocity along the line-of-sight to the tracking station measured by the Doppler effect. In contrast with occultation experiments, which sense the effect of the medium along a path between two known points, gravity experiments are based on determining the motion of the spacecraft in response to the variations in mass distribution within a planet or its satellites. This is a classical physics laboratory experiment carried out on planetary scales. Our global knowledge of Earth's gravity comes from such studies. Our only knowledge of the gravity field of Mercury results from the three flybys of Mariner 10 (Howard et al., 1974, Anderson et al., 1987). Similarly, recent observational inferences as to the internal structures of the Galilean satellites, for example that there is an ocean on Europa, are based on the behavior of the trajectory of Galileo spacecraft during close flybys (Anderson et al., 1992; e.g. Anderson et al., 1997). A precise determination of the total mass of Uranus and Neptune from the Voyager 2 flybys (Tyler et al., 1986, 1989) has led to the conclusion that there is not need for a 'Planet X' to explain the orbits of these bodies (Standish, 1993). The method has been extended to small bodies as well, for example in the mass determination of asteroid Mathilde (Yeomans et al., 1997) and gravity field of asteroid Eros (Yeomans et al., 2000) and was done for the Stardust flyby at comet P/Wild-2 in 2004 (Anderson et al., 2004). At Mars, techniques similar to those used for asteroids can be applied to a precise determination of the masses

of Phobos and Deimos and are planned for Mars Express during close encounters (Pätzold et al., 2004; 2006) and with Rosetta for the Lutetia flyby in 2010.

These three techniques—radio occultation, bistatic radar, and determinations of gravity from radio tracking—have roots and counterparts in classical astronomy: (i) Classical stellar occultation observations make use of the chance passage of a planet between Earth and a star. Such an occurrence permits determination of the existence or absence of an atmosphere by observing the extinction of starlight as the planet obscures the star (v., e.g., Elliot et al., 1989). When an atmosphere is present some of its properties can be determined. Stellar occultation has been extended to the study of planetary rings by observing the degree extinction as a function of radius (v., e.g., Elliot and Nicholson, 1984). Sometimes the unexpected occurs; the rings of Uranus were discovered by this technique by investigators attempting to understand the planet's upper atmosphere. (ii) Measurements of the classical scattering phase function, *i.e.*, the angular distribution of scattered energy flow, are the optical predecessor of bistatic radar, in which the source typically is the sun and observations are made with terrestrial telescopes. (iii) Early determinations of the small-scale properties of the lunar surface, for example, were carried out in this manner. Classical Earth-based measurements of the motions of natural satellites are used to determine the low-order gravity fields of planets. When available, radio science methods provide much greater accuracy and dynamic range than these classical approaches. The power of radio science methods as compared with the classical techniques arises from the use of coherent radio signals that permit the measurement of radio frequency phase and deterministic polarization as precise tools for probing planetary environments. An additional, fundamental distinction between the classical approaches and those of radio science is the ability of the investigation geometry to be controlled through manipulation of the spacecraft relative to the Earth, thereby considerable flexibility in the selection of the geometric experimental parameters. Future missions in which such experiments are organized utilizing transmission between or among multiple satellites in orbit about the same planet would permit complete control of experimental conditions. An early such occultation experiment, GPS/MET, has been conducted in Earth orbit using the GPS constellation of satellites as signal sources with reception on a low-Earth orbiter (Kursinski et al. 1997a, 1997b; Ware et al. 1996).

Short of in situ measurements by entry probes, radio occultation studies of atmospheres provide the most detailed information available on the vertical structure of the neutral atmosphere, the ionosphere, and atmospheric waves. In principle, vertical structure as fine as a few meters can be discerned, and a resolution as fine as 100 m has been demonstrated for Mars. Recent analyses of MGS radio occultations at Mars have shown that a sequence of radio occultation measurements can provide adequate sampling and accuracy to provide a useful determination of atmospheric fields; wind velocity, temperature, and pressure can all be determined as a function of altitude (Hinson et al., 2004a, 2004b). An unusual aspect of this is the use of the occultation determination of the atmospheric parameters in terms of the absolute radius, thereby enabling the use of new techniques to address problems in atmospheric dynamics. For example, the gradient wind equation can be used to determine absolute winds vs. altitude across a path connecting two nearby occultation points (Hinson et al., 1999). Radio occultation measurements strongly complement and extend the use other spacecraft and Earth-based remote sensing techniques, such as infrared spectroscopy, which provide detailed information on

atmospheric constituents and low vertical resolution structure over wide regions by instrumental scanning. The best results are obtained when radio occultation and these other observations are combined.

Bistatic radar observations of the Moon, Venus, and Mars extend and complement Earth-based radar astronomy studies of these objects. For example, the fundamental nature of the lunar surface as a consolidated soil was first demonstrated by a combination of terrestrial radar astronomy and bistatic radar methods. Likewise, determination of the particle sizes in the rings of Saturn was based on a forward scattering experiment for observing the diffraction pattern of the ring particles; refined experiments of this type are planned for Cassini when it reaches Saturn. Similarly, the existence of exotic phase changes in materials at the upper levels of Cytherian mountains was demonstrated by observing variations in polarization from Maxwell Montes with a bistatic scattering experiment conducted with the Magellan spacecraft. Most recently, verification of the typical nature of the Mars Polar Lander target sites on centimeter to decimeter scales was provided by bistatic scattering observations with Mars Global Surveyor.

Radio tracking studies of gravity are uniquely suited to determination of interior structure of planets, for those cases for which the appropriate geometrical conditions can be obtained. To date, the intense radiation field of Jupiter's magnetosphere and the hazard of planetary rings at Saturn and Uranus have prevented close approach to these planets by spacecraft, thereby limiting the utility of this technique at the outer planets. While in these cases the best information to date is obtained by classical methods, suggested missions that would fly interior to the radiation belts of Jupiter, say, hold considerable promise for solving the puzzle of that planet's interior organization. When practical, spacecraft methods are superior in all instances for determination of total system mass, the internal distribution of mass of various bodies, and the masses of individual satellites.

## 2.3 Technique

Radio science instrumentation combines equipment on the ground with on-board spacecraft hardware required to create and maintain a highly stable and precise radio link. Most commonly, two-way radio signals have been generated on the ground and transmitted 'uplink' through the large antennas of the NASA Deep Space Network. These transmissions are received by spacecraft transponder, shifted in frequency, and then re-transmitted 'downlink' to the Earth where they are received either at the original site or at a second site, possibly located on another continent. Transponder design is such that the frequency of the downlink signal is coherently related to the received uplink frequency by a known integer ratio. Because the downlink signal frequency is derived precisely from that of the uplink, it is possible to measure changes in the radio path length by comparison of the received, downlink signal with the ground oscillator that generated the uplink signal originally. An increase in the radio path length decreases the phase of the received downlink signal relative to the ground oscillator, while a decrease in path length has the opposite effect. As hydrogen maser clocks are used for the fundamental frequency reference on the ground, measurement of the downlink phase provides an extremely precise method of determining changes in the round trip propagation time to the spacecraft. A one-hertz difference between the frequencies of the uplink and downlink signals means

that the total radio path length is changing at the rate of one wavelength per second; larger or smaller frequency differences correspond to proportionally larger or smaller rates of path length change. Overall, the short term accuracy of the measurement procedure depends on the signal-to-noise ratio achieved and, ultimately, on the stability of the ground station oscillator over the round trip flight time of the radio signals to the spacecraft and back (Eshleman and Tyler, 1975; Lipa and Tyler, 1979).

On the ground, stations for communication over interplanetary distances are built around the large antennas of 20–100 m diameter. These stations are used primarily for uplink transmission of commands and downlink reception of spacecraft data (Yuen, 1983). On spacecraft, however, typical antenna sizes are limited to only a few meters at most, and the transmitted downlink signal power ranges from about 1 to less than 100 W. As mentioned, hydrogen maser atomic clocks are used for the ground station frequency reference, while microwave frequencies in the 2 (S-band) and 8 (X-band) Gigahertz range, corresponding to 12–13 cm and 3–4 cm wavelengths, respectively, are used for the radio signals. Either band can be used separately or both used simultaneously. Use of dual frequencies is advantageous since this permits direct separation of the effects of neutral and ionized gases on the basis of differences in the dispersive characteristics of the two media. Frequency changes as small as about 0.001 hertz can be measured, corresponding to a fractional accuracy in the range of a few parts in  $10^{14}$  (Tyler et al., 1992a). In the absence of other effects, this leads to an accuracy in the measurement of spacecraft velocity, for example, in the range of 30 micrometers/second when the 8 Gigahertz band is used. Under the best conditions accuracies better than 10 micrometers/second have been achieved. The use of a two-way, uplink/downlink radio path is suitable for study of gravity and for spacecraft navigation purposes. Because it relies on the reception by the spacecraft transponder of an uncorrupted uplink signal, in general the two-way technique can be used reliably only under free-space uplink propagation conditions (Tyler, 1987).

Occultation observations exhibit considerable signal dynamics, with simultaneous variations in signal frequency and amplitude, as well as the presence of near-forward scattering and diffraction when the radio path passes near a planet's surface.

Observed signals obtained from bistatic scattering experiments are characteristically broadened relative to the illuminating signal as a result of the combination of angular spreading of the waves by the scattering process and the relative motion of the spacecraft and ground station with respect to the planet's surface. Unlike occultation observations, much of the information regarding the surface properties is in the polarization and amplitude of the scattered signal; typically there is no coherent component in the scattered fields.

Thus, both occultation and bistatic scattering observations produce dynamic signals occupying a considerably greater bandwidth than the transmitted illuminating waveform. For this reason, the measurement of these signal characteristics requires capture of the time-sampled waveform at a sufficient sampling rate to avoid frequency aliasing effects. This is accomplished with open-loop receivers pre-programmed to track the expected spectral window. The dynamical characteristics of the occultation and scattered signals preclude reliable use of phase-locked loop techniques for reliable radio occultation measurements.

ROSETTA RSI: **Rosetta Radio Science Investigations**  
**Experiment User Manual**

Document **RO-RSI-IGM-MA-3081**

Issue: 4

Date: 25.04.2016

Revision: 2

Page: 19 of 144

---

## 3 Mission Characteristics

### 3.1 Scientific Objectives of the Rosetta RSI Experiment

The primary scientific objectives of RSI, addressing the scientific objectives as defined in the Rosetta AO, are divided into the following categories: Gravity Field and Dynamics, Cometary Nucleus, and Cometary Coma. The secondary scientific objectives of RSI are studies which are not covered by the ESA prime scientific objectives, but will significantly enhance the science return of the mission.

#### *Primary Scientific Objectives*

Doppler data provide time-resolved measurements of the spacecraft motion and the plasma state and thus may be used for physical investigation of the nucleus and the inner coma of comet P/Churyumov-Gerasimenko. In particular, the following scientific objectives may be addressed by an analysis of dual-frequency one-way or two-way radiometric tracking data, together with information provided by other Rosetta experiments, e.g. Remote Imaging System (OSIRIS):

#### *Gravity Field and Dynamics*

- Cometary mass and bulk density
- Cometary gravity field coefficients
- Cometary moments of inertia and spin state
- Cometary orbit, lightshift, thermal properties of the nucleus
- Asteroid mass and bulk density

#### *Cometary Nucleus*

- Size and shape (from S/C occultation observations)
- Internal structure (from nucleus sounding)
- Dielectric constant and roughness of the surface (from bistatic radar experiment)
- Rotation, precession and nutation rates (from bistatic radar)

#### *Cometary Coma*

- Distribution of mm - dm size particles (from coma sounding)
- Plasma content of the inner coma (from coma sounding)
- Gas and dust mass flux (from non-gravitational perturbations of the *Rosetta* S/C)

Regarding investigations of the cometary gravity field and its internal structure, shape models derived from Rosetta imagery may be used for the construction of theoretical gravity models and compared with the observed gravity field coefficients. Image data will, furthermore, provide information on the orientation and rotation of the nucleus, required for the determination of the cometary gravity field and the moments of inertia.

## **Secondary Scientific Objectives**

During its cruise to comet P/Churyumov-Gerasimenko, the Rosetta spacecraft will pass through five solar conjunctions and additionally another two conjunctions during the primary mission. It is proposed to perform radio sounding observations of the solar corona during solar conjunctions, respectively:

### *Solar Corona Science*

- Electron content of the inner corona, solar wind acceleration, search for coronal mass ejections, turbulence

### **3.1.1 Gravity: Cometary Mass and bulk density**

Determination of the cometary mass and bulk density is a fundamental objective required to assess the validity and accuracy of various cometary models. Extensive simulation studies, in preparation for the Near Earth Asteroid Rendezvous (NEAR) mission to asteroid 433 Eros, demonstrate that orbiting a small asteroid will require a gravity field extraction process fundamentally different from previous gravity studies of the planets or moons (Scheeres, 1995; Miller et al., 1995). Upon arrival at the comet, the nucleus size, shape, mass, activity and spin state will be poorly known. P/Churyumov-Gerasimenko is significantly smaller than 433 Eros but its nucleus radius is expected to be about 2000 m (Lamy et al., 2003) and four times larger than P/Wirtanen. The expected gravity attraction shall therefore be 60 times stronger than at Wirtanen at the same assumed distance and bulk density. This will allow a more precise mass and density determination at low orbits. First estimates for the Wirtanen mission have been published by Pätzold et al. (2001b).

An initial flyby during the Rosetta approach phase should enable a mass determination to an accuracy of 1%. The current size estimate (accounting also for an albedo between 3% to 4%) of the nucleus radius of  $(1.98 \pm 0.02)$  km (Lamy et al., 2003) suggest a flyby distance within 100 km for different nucleus models (Fig. 3.1-1).

Injection into a bound high orbit allows iterative improvements of the mass determination down to the sub-permille level. Compared to the Wirtanen mission this may be already achieved within 30 km orbital radius (Wirtanen was 7 km).

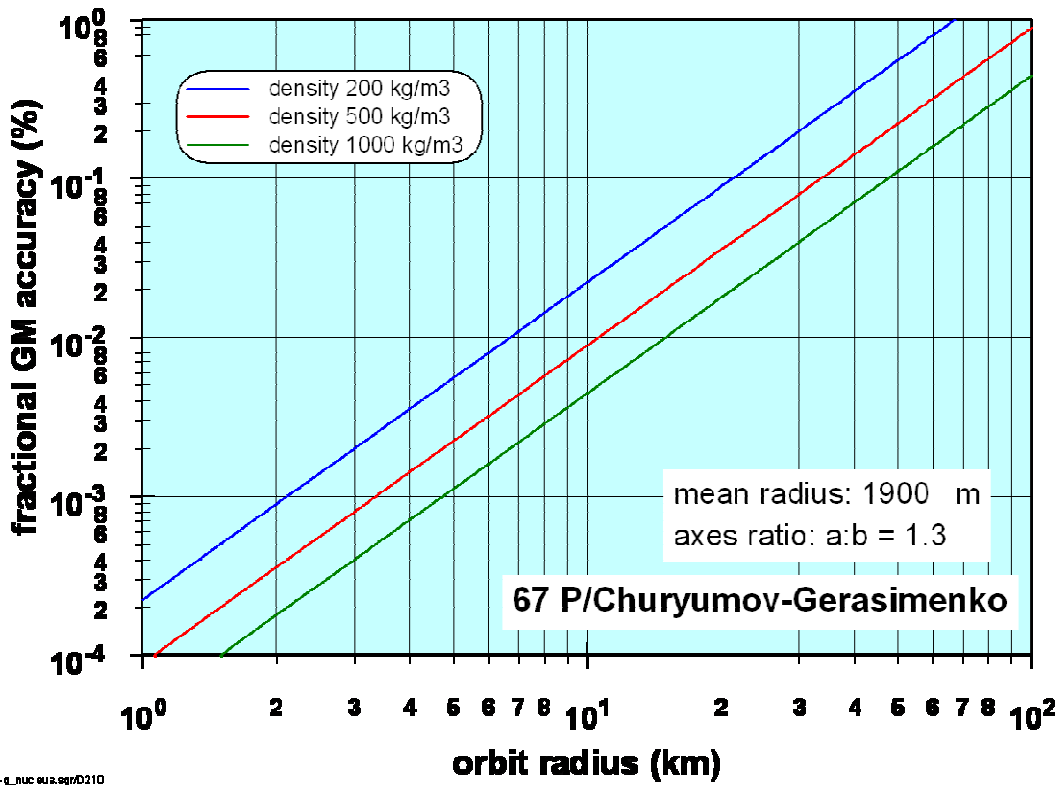


Figure 3.1-1: Accuracy of comet nucleus mass determination

### 3.1.2 Gravity: Cometary Gravity Field Coefficients

The second order and degree gravity coefficient ( $C_{20}$ ) can be estimated using the shape model (from imaging observations) and assuming constant density. The result is a constraint on the true gravity field.

The most stable low orbits for the spacecraft will be in equatorial, retrograde orbits about the comet (no outgassing perturbations assumed). Beginning with these orbits, the second-order gravity field can be solved for in the orbit determination process. Higher-order gravity coefficients might be determined from low polar terminator orbits (Figure 3.1-2). This strategy also assumes that cometary outgassing does not induce significant accelerations upon the spacecraft. Initial estimates of comet Wirtanen have shown that early activity even beyond 3 AU, however, might generate radial accelerations due to outgassing that could mask the effects of higher gravity harmonics (Gill et al., 1996, Pätzold et al. 2001b). The determination of the higher harmonics would probably only be feasible if a gravity mapping campaign takes place at heliocentric distances well beyond 3 AU when the comet is not very active. In view of the Rosetta mission constraints, such a gravity mapping campaign is best performed at heliocentric distances between 3.5 AU and 3 AU (Figure 3.1-3) before or at the onset of activity. Unfortunately the comet will be near solar conjunction at that time and solar plasma may induce higher noise.

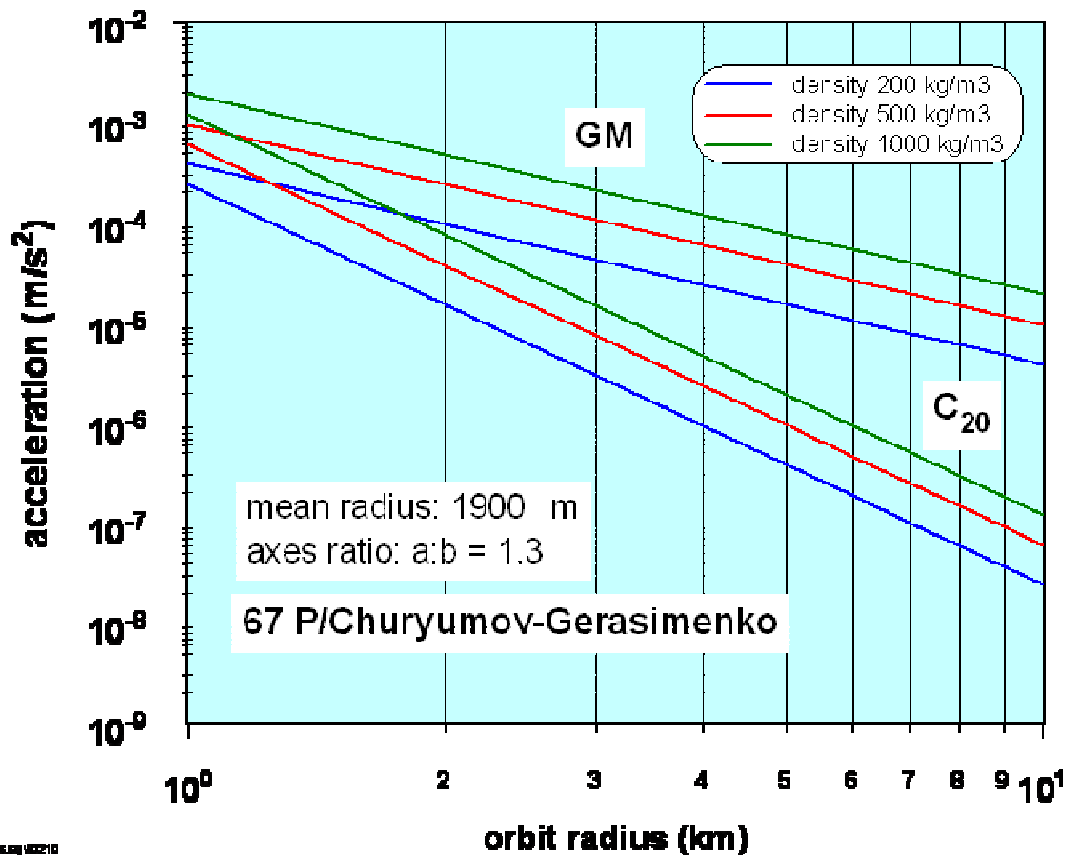
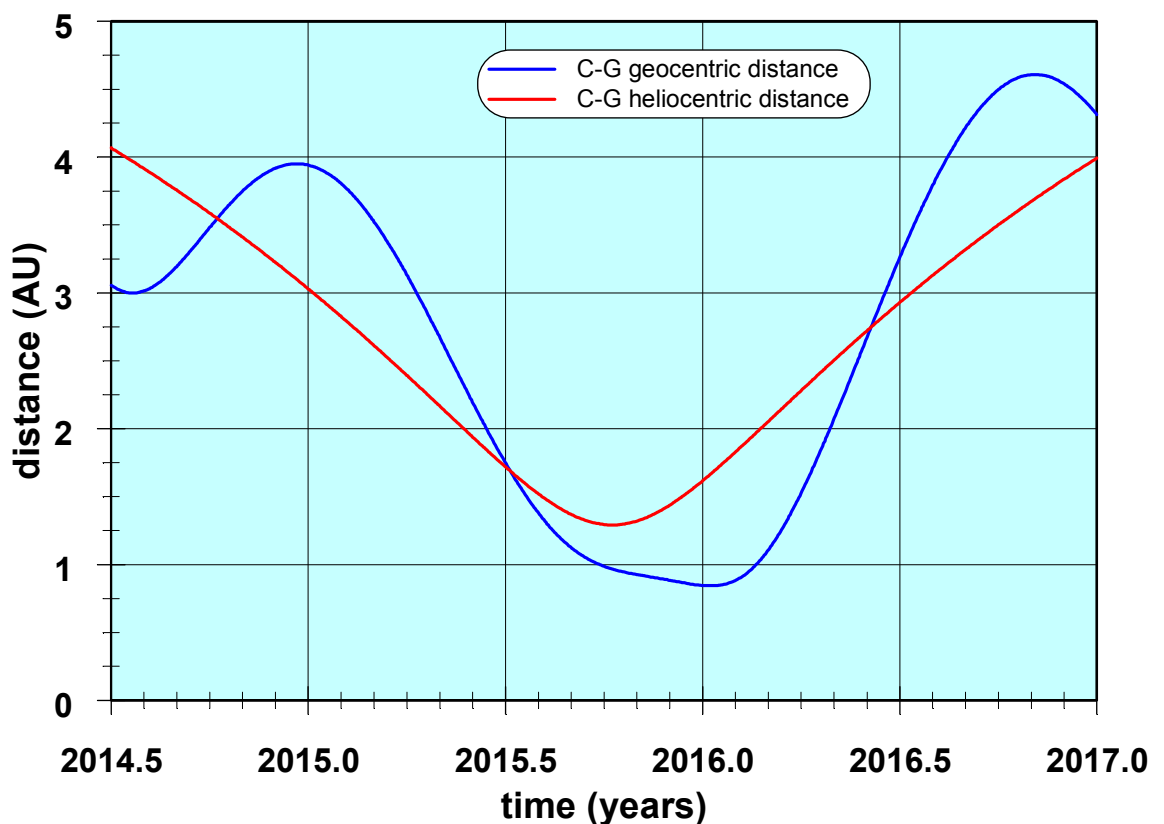


Figure 3.1-2: Velocity perturbation due to the gravity field coefficients  $C_{20}$  and GM.

If the gravity mapping campaign must be delayed to times when the comet is already active, care must be taken to ensure that the spacecraft does not become adversely perturbed by the outgassing streams in a direction toward the Sun. If the spacecraft orbit could be maintained in a terminator orbit nearly perpendicular to the Sun-comet line, the outgassing perturbations would presumably be minimized.

From an improved shape model, the model can be refined and the gravity field can once again be approximated assuming a constant density nucleus. Mass will eventually be known to better than 0.1% (Figure 3.1-1), volume and density better than 3%. The shape gravity model (with constant density) and the true gravity model (from spacecraft tracking) can then be compared to yield information on the mass heterogeneity of the comet nucleus.



c-g\_plot.sgr/d210

Figure 3.1-3: Distance Earth-Churyumov-Gerasimenko and Sun-Churyumov-Gerasimenko as function of time

### 3.1.3 Gravity: Cometary Moments of Inertia

In the likely event that the comet is not in perfect principal axis rotation, a knowledge of the body's second-order gravity coefficients and a determination of its spin state can be used to determine its moments of inertia; these moments provide constraints upon the internal structure of the nucleus.

### **3.1.4 Gravity: Cometary Orbit**

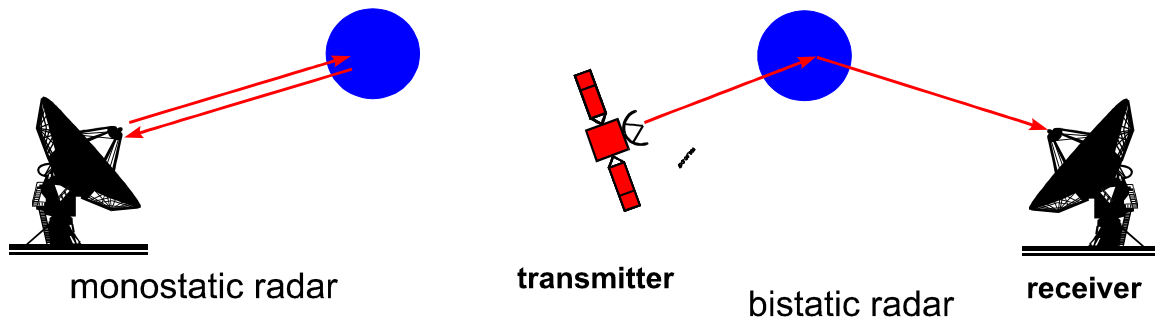
The cometary orbit itself is affected by gas and dust emission during the active phase (typically within 3 AU heliocentric distance). For the original target comet P/Wirtanen it was suspected by Boehnhardt et al. (1996) that the effects of the nongravitational forces of P/Wirtanen may be very different than previously estimated (Marsden and Williams, 1995) in order to explain the discrepancy between the predicted and observed position of the time at the time of its recovery in 1995. Ground-based astrometry of the comet provides only limited spatial accuracy for orbit determination and suffers furthermore, particularly during high activity near perihelion, from the offset between the center of light of the coma and the center of gravity of the nucleus (Yeomans, 1986), the so-called "light shift". The position of a spacecraft very close to the comet can be determined very accurately using Doppler and ranging measurements and the positions of the comet with respect to the spacecraft can be determined using on-board imaging observations. These precise observations of the comet's position, along with the comet's existing astrometric data will allow a significant refinement to this comet's nongravitational acceleration force model.

### **3.1.5 Nucleus: Surface (Bistatic Radar)**

Rosetta is the first spacecraft to use occultation techniques and probably bistatic radar to explore the properties of the comet's surface and its interior. These radio sounding techniques are well established and have been successfully performed for investigations of planetary rings, atmospheres, ionospheres and surfaces (e.g. Marouf et al., 1982; Tyler, 1987; Tyler et al., 1992a). Bistatic radar techniques are presently performed with Mars Express on a routine basis with great success (Simpson et al., 2006) and are planned for Venus Express (Häusler et al., 2006).

A bistatic-radar experiment will measure the scattering properties of the nucleus, hence determine the physical nature of the surface and its material properties. A bistatic radar experiment is distinguished from a monostatic measurement by the spatial separation of transmitter and receiver (Figure 3.1-4). In the Rosetta case the transmitter is the spacecraft, with its High Gain Antenna pointed toward the nucleus surface. The signal is reflected from the surface and received at large ground antennas on Earth. Radar observations of comets were conducted with P/Encke (Kamoun et al., 1982), P/Halley (Campbell et al., 1989), IRAS-Aracki-Alcock (Harmon et al., 1989), Hyakutake (Harmon et al., 1997) and P/Grigg-Skjellerup (Kamoun et al., 1999). Rosetta's orbit around the nucleus enables the measurements of the strength and state of polarization of the X-band radio signal transmitted by Rosetta and scattered by the nucleus over a broad range of spacecraft-comet-Earth angles. Preliminary studies confirm echo detectability over a broad range of observation angles for sufficiently close spacecraft orbits within at most 40 km distance to the nucleus. For a nucleus rotating faster than the spacecraft revolves about the nucleus, the reflected echo spectrum will vary considerably about the center frequency (direct signal), thereby allowing a determination of the rotation and precession rates with sufficient accuracy during a single tracking pass. The shape and strength of the co- and cross-polarized components of the echo spectra can be used to differentiate between asteroid-like diffractive surface scattering (Ostro, 1985; Harmon et al., 1989) and icy-body-like volume scattering (Ostro et al., 1992). Furthermore, for the circularly polarized incident wave, observation of the bistatic

scattering angle at which the co- and cross-polarized components are nearly equal in strength (the echo is roughly linearly polarized) determines the Brewster angle  $\gamma_B$  of the surface material, hence its dielectric constant  $\varepsilon$ . In principle, independent differentiation between an icy conglomerate ( $\gamma_B \sim 50^\circ$ ,  $\varepsilon \sim 1.4$ ) and very dusty ( $\gamma_B \sim 60^\circ$ ,  $\varepsilon \sim 3$ ) surfaces can thus be achieved. Similar bistatic radar observations were used to determine  $\varepsilon$  of the lunar crust (Tyler and Howard, 1973) and the Martian surface (Simpson and Tyler, 1981).



radar2.cdr/D95

Figure 3.1-4: Monostatic and bistatic radar

### 3.1.6 Nucleus: Internal Structure

Because the nucleus is a small body, the interior or the upper layers of the nucleus may be penetrable by microwaves. The refractive properties of the nucleus will modify the propagation of the radio signal that it might be possible to constrain the bulk refractive index of the nucleus. This sounding of the nucleus can be performed during occultations when the S/C is located behind the nucleus.

### 3.1.7 Nucleus: Size and Shape

The size and shape of the nucleus are investigated by occultation experiments prior to, during and after the spacecraft is occulted by the nucleus as seen from the Earth. Accurate measurements of the ingress and egress occultation times determine the length of the occultation chord for a known spacecraft trajectory, hence constraining the size of the nucleus. Repeated measurements for different occultation track geometries constrain the nucleus shape. Occultation observations are most useful when imaging observations are not possible, e.g. for observations of the unlit side or when the limb of the nucleus is obscured by dust.

### 3.1.8 Coma: Plasma and Dust Content

Radar observations of comets Iras-Araki-Alcock (Harmon et al., 1989) and Halley (Campbell et al., 1989) revealed a dust grain size population between a few mm and probably as large as 10 cm distributed about the nucleus out to distances of 1000 km. The wavelengths used by the Rosetta radio subsystem are in the same bands used in the radar studies mentioned above. The total mass intercepted during the Giotto flybys at Halley and Grigg-Skjellerup were dominated by dust grains of a few mm (Pätzold et al., 1991b; 1993). Richter and Keller (1995) studied the influence of the radiation pressure force on the orbital evolution of dust grains up to 10 cm in size around cometary nuclei. They concluded that large grains might survive in stable orbits for an entire orbital revolution of the comet.

One observable of the cometary grain sounding experiment will be the signal attenuation along the ray path from the spacecraft to the Earth, expressed as the optical depth,  $\tau(\lambda)$ . The value for X-band,  $\tau(3.6 \text{ cm})$ , reflects the contribution for all grains larger than a few mm and the differential optical depth,  $\tau(3.6 \text{ cm}) - \tau(13 \text{ cm})$ ,

constrains the contribution to grains in the mm - dm size range (Marouf et al., 1982). The second observable is the power incoherently scattered in the near-forward direction. Because of the motion of the grains relative to Rosetta and the Earth, the scattered signal is Doppler shifted and spread over a finite bandwidth centered on the frequency of the direct ray. The detectability of these observables strongly depends on the abundance and size distribution of the mm and larger size particles. A search by Rosetta for attenuation and near-forward scattering effects during coma occultation events will either determine or set limits on the abundance of such particle sizes using techniques similar to those used to study planetary rings (Marouf et al., 1983, Tyler et al., 1983).

The first radio sounding observations of a cometary ionosphere were performed with the VEGA spacecraft at comet P/Halley. They revealed the mean large-scale electron density distribution and were able to resolve the inner "pile-up" region (Andreev and Gavrik, 1990; Pätzold et al., 1996). Observations at two coherently related frequencies are required to separate the dispersive contribution from the classical Doppler shift.

With Rosetta it is possible to access in particular those coma regions which will not be investigated *in situ*. Preliminary estimates indicate that a differential phase shift is detectable for gas production rates between  $10^{27}$  molecules/s and  $10^{28}$  molecules/s.

### 3.1.9 Coma: Mass Flux

The motion of the Rosetta spacecraft about the nucleus is perturbed by mostly radial accelerations due to gas and dust impinging on its surface. These orbit perturbations are detectable from ground from Doppler shifts of the radio signal. It may thus be possible to determine the combined gas and dust mass flux and its variation with distance from the nucleus, the evolution with heliocentric distance and the variation of coma and jet activity with illumination. The entire cross sectional area of the spacecraft (the solar cell array alone measures about  $60 \text{ m}^2$ ) serves as a detector for the impinging coma material. The impact of individual large dust grains (larger than 1 mm in diameter) may be detectable. In contrast to the Giotto flybys (Pätzold et al., 1991a), however, the main perturbations are expected to be due to gas jets rather than dust grain impacts. Together with the gravity field modeling, RSI is able to constrain the maximum liftable mass and can also provide an estimate of the overall gas and dust production rate.

### 3.1.10 Asteroids: Mass and Bulk Density

The spacecrafts velocity is perturbed by the gravitational field of asteroids during sufficiently close flybys. The spacecraft is accelerated toward the asteroid along its flyby trajectory. The analysis of the resultant velocity changes ultimately yields a measure of its total mass or GM. The bulk density is determined from the mass determination and the volume estimate made by the camera experiment. Mass and bulk density estimates of asteroids have thus far only been obtained from the Galileo flyby at asteroid Ida and from the NEAR flybys at asteroid Mathilde (Yeomans et al., 1997) and Eros (Yeomans et al., 1999, 2000). Asteroid Ida was too small to perturb the flyby trajectory of Galileo above the threshold of detectability. The discovery of

Ida's moon Dactyl, however, provided an unexpected opportunity to estimate Ida's mass and bulk density. Mathilde's bulk density was found to be surprisingly low.

Table 3.1-1: Rosetta asteroid flyby parameters

	Steins	Lutetia
<b>Flyby date</b>	<b>05 September 2008</b>	<b>10 July 2010</b>
<b>Time of closest approach (UTC)</b>	<b>18:30:26</b>	<b>15:24:30</b>
<b>Size</b>	<b>17.5 – 5.5 km (1)</b>	<b>95.8 ± 4.1 km (2)</b>
<b>Density</b>	<b>2000 ± 500 kg/m<sup>3</sup></b>	<b>2000 ± 500 kg/m<sup>3</sup></b>
<b>Asteroid Class</b>	<b>E (2)</b>	<b>C (or M) (2+3)</b>
<b>Flyby velocity</b>	<b>9.0 km/s</b>	<b>15.0 km/s</b>
<b>Minimal flyby distance</b>	<b>600 km</b>	<b>1600 km</b>
<b>Nominal flyby distance</b>	<b>1761 km</b>	<b>3004 km</b>
<b>Angle between relative flyby velocity vector and direction to Earth</b>	<b>52°</b>	<b>43°</b>
<b>Distance Earth-Rosetta</b>	<b>2.4 AU</b>	<b>3.0 AU</b>
<b>Closest Distance between signal and sun</b>	<b>192 RSUN</b>	<b>193 RSUN</b>
<b>Angle between Earth-Sun and Earth-Rosetta</b>	<b>62°</b>	<b>62°</b>

(1) depending on albedo values of 0.04-0.4, Barucci et al. 2005

(2) Barucci et al., 2005

(3) Lazzarin et al., 2004

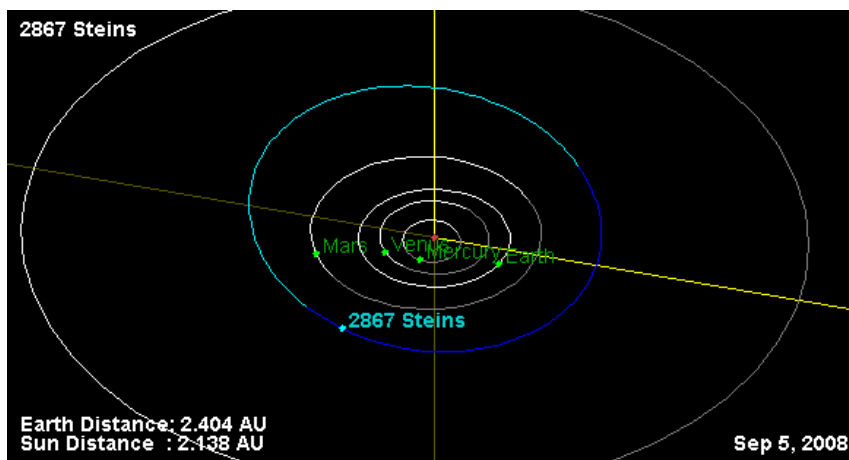


Figure 3.1-5: Planetary configuration at the time of the close fly by at Steins (picture produced by NASA, JPL)

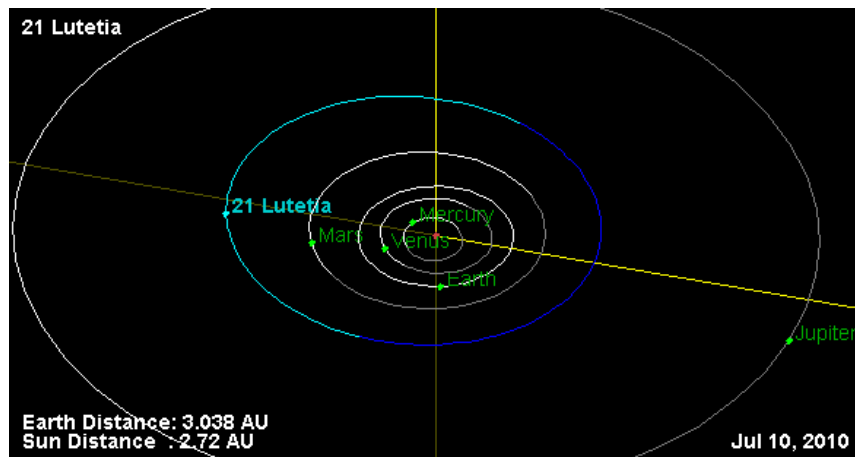


Figure 3.1-6: Planetary configuration at the time of the close fly by at Lutetia  
(picture produced by NASA, JPL)

Rosetta will perform flybys at asteroids Steins and Lutetia on 5 September 2008 and 10 July 2010, respectively. The determination of the mass and bulk density of these bodies depend crucially on the flyby distances. Table 3.1-1 lists the flyby parameters used for estimates of the change in velocity during the simulated flybys. Figure 3.1-5 and Figure 3.1-6 show the planetary configuration at the time of the flybys.

### 3.1.11 Solar Corona

The technique of solar corona sounding is well established and has been successfully performed during superior conjunctions of the Viking, Voyager and Ulysses spacecraft (Muhleman and Anderson, 1981; Anderson et al., 1987; Bird et al., 1994; Pätzold et al., 1995).

## 3.2 Overview of the Instrument: Space Segment

### 3.2.1 General

The ROSETTA Radio Science Investigations (RSI) experiment will make use of the radio link between the orbiter and the ground station(s) on Earth. Frequency, amplitude and polarisation information will be extracted from the radio signal received in the ground station.

A block diagram of the characteristic features of the Rosetta radio subsystem is shown in Figure 3.2-1. The most important elements are the two redundant transponders, the Ultrastable Oscillator (USO) and the antennas.

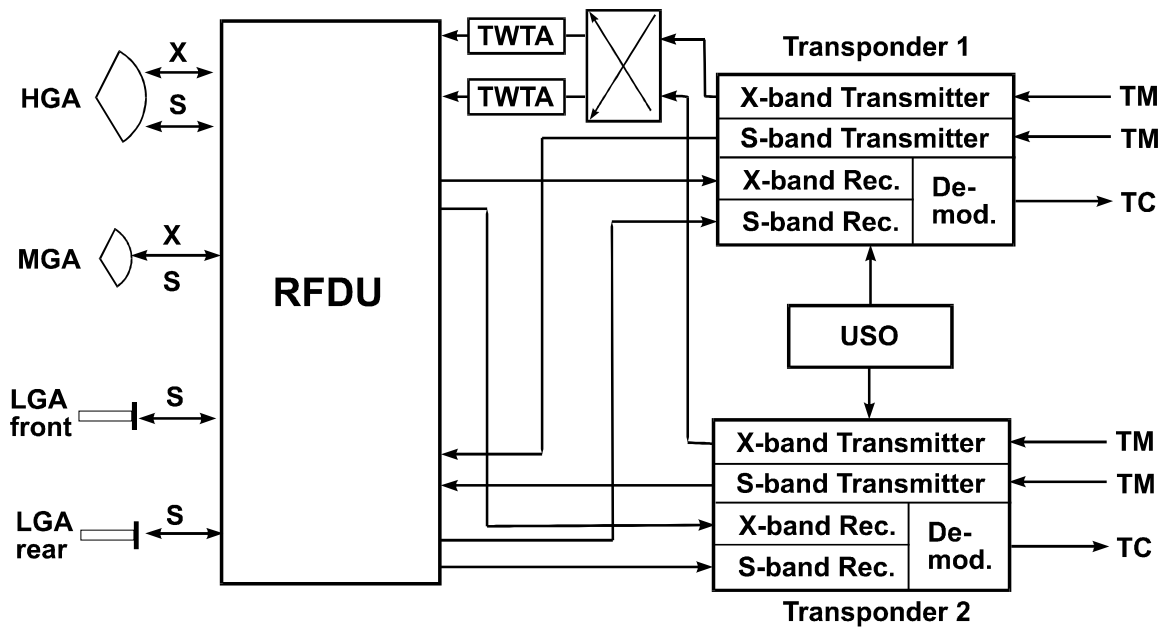


Figure 3.2-1: Block diagram of the Rosetta radio subsystem

Rosetta is capable of receiving and transmitting radio signals via three dedicated antenna systems:

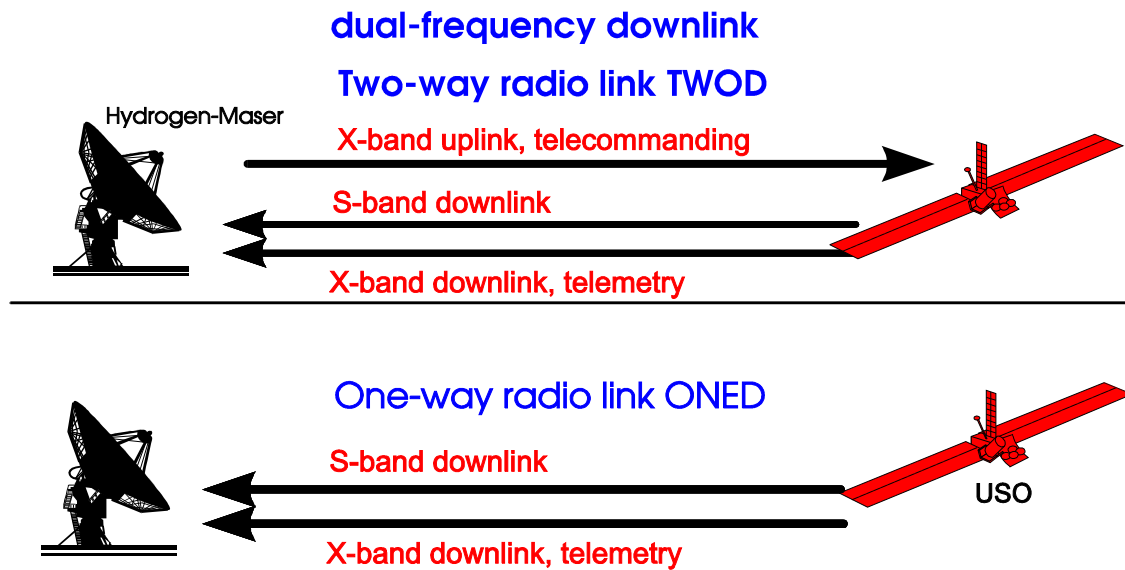
1. High Gain Antenna (HGA), a fully steerable parabolic dish of 2.20 m diameter
2. Medium Gain Antenna (MGA), a fixed parabolic dish of 0.60 m diameter
3. two Low Gain Antennas (LGA), front and rear, S-band only

The transponders consist of an S-band and X-band receiver and transmitter each. The spacecraft is capable of receiving two uplink signals at S-band (2100 MHz) via the LGAs, or non-simultaneously at either X-band (7100 MHz) or S-band via the HGA and transmit via the HGA simultaneously two downlink signals at S-band (2300 MHz) and X-band (8400 MHz) or at S-band only via the LGAs.

The HGA is the main antenna for receiving telecommands from and transmitting telemetry to the ground. The LGAs are used during the commissioning phase just after launch and for emergency operations. The MGA is considered as a back-up.

### 3.2.2 Definition of Radio Links

RSI uses two radio link modes. Figure 3.2-2 shows a schematic of the different radio link modes and Table 3.2-1 combines these modes with the science objectives.



radiokor

Figure 3.2-2: Radio link modes between the orbiter and the ground station on Earth. Upper panel: one-way X-band downlink. Lower panel: Two-way radio link where the uplink is transponded back phase-coherently at a dual-frequency downlink. The frequency stability is governed by an hydrogen maser located at the ground station.

The *two-way radio link* (TWOS, TWOD) is established by transmitting an uplink radio signal X-band to the spacecraft. The received uplink carrier frequency is transponded to downlinks at X-band and S-band upon multiplying by the constant transponder ratios 240/221 and 880/221, respectively, in order that the ratio of the two downlinks is  $880/240 = 11/3$ . This radio mode takes advantage of the superior frequency stability inherent to the hydrogen maser in the ground station on Earth. This mode is used for all RSI gravity science applications, routine tracking observations when in orbit during the escort phase, the sounding of the solar corona and the search for gravitational waves.

The *one-way link mode* (ONES, ONED) is used only during an occultation of the spacecraft by the nucleus as seen from Earth. This enables radio sounding of the immediate vicinity of the nucleus and perhaps even the nucleus itself, should the solid cometary body prove to be penetrable by microwaves. These one-way occultation experiments require an Ultra-Stable Oscillator (USO) added to the radio subsystem. The prime purpose of the USO is to serve as a phase-coherent frequency reference for the simultaneous one-way downlink transmissions at S-band and X-band. The required stability (Allan variance) of the USO is about  $\Delta f / f \approx 10^{-13}$  at 10 - 1000 seconds integration time. The one-way radio link can be transmitted either while receiving a noncoherent uplink or without any uplink contact at all.

This radio subsystem design makes Rosetta one of the best equipped spacecraft (besides Galileo and Cassini) for radio science experiments.

### 3.2.3 Radio Link Budget

Cf. section 4.6

### 3.2.4 Radio Link Mode and Scientific Objective Cross Reference

Table 3.2-1: Radio link modes and RSI science objectives

Science objective	Radio link mode	Uplink	Downlink
Gravity Combined mass flux Asteroid flybys	Two-way	X-Band	X-band & S-band
Solar corona sounding	Two-way	X-Band	X-Band & S-Band
Gravity	Two-way	X-band	X-band & S-Band
Bistatic radar	One-way	-	X-band & S-Band
Occultations: Plasma content Dust grain distribution Nucleus structure	One-way	-	X-band & S-band

### 3.3 Overview of the Instrument: Ground Segment

#### 3.3.1 Overview

Ground stations include antennas, associated equipment and operating systems in the tracking complexes of New Norcia (Perth) (ESA, 35 m), Australia, and the Deep Space Network (NASA, 70 m and 34 m) in California, Spain and Australia. A tracking pass consists of typically eight to ten hours of visibility. Measurements of the spacecraft range and carrier Doppler shift can be obtained whenever the spacecraft is visible. In the two-way mode the ground station transmits an uplink radio signal at X-band and receives the dual-frequency simultaneous downlink at X-band and S-band. The information about signal amplitude, received frequency and polarization is extracted and stored as a function of ground receive time.

#### 3.3.2 Ground Stations

##### 3.3.2.1 European Ground Stations

The ESA Deep Space Antennas consist of the New Norcia station DSA 1, the Cebreros station DSA 2 and the Malargüe station DSA 3.

While DSA 1 hosts a 35 m antenna with an S- and X-band uplink and downlink, DSA 2 and 3 consist of 35 m antennas with X-band transmission and Ka- and X-band reception. The station equipments consist of three ESA IFMS receivers (IFMS 1, IFMS 2, IFMS 3).

##### 3.3.2.2 Deep Space Network

The DSN ground stations provide uplinks at S-band or X-band and a full scale radio science equipment used for most of the NASA missions.

It should be emphasized that the feasibility of the two-way measurements does not depend on the uplink frequency. The two data types, closed-loop and open-loop, can be generated simultaneously regardless of the radio link configuration, one-way or two-way.

The open-loop equipment is capable to receive one frequency at two polarizations (LCP and RCP) or two frequencies at one polarization (LCP or RCP). The reception of two frequencies at two polarization (four channels) each is only feasible at the 70-m ground stations.

#### 3.3.3 Ground Station Capabilities

The following required ground station capabilities are supported by the new IFMS systems at the DSA and the DSN:

1. X-band uplink transmission
2. S-band downlink reception
3. X-band downlink reception
4. S,X-band downlink simultaneous reception
5. Doppler sample rates: 1000, 100, 10, 1, 0.1 samples/sec. (to be selected by RSI)
6. OL sampling of RHC and LHC X-band signals

7. OL sampling of RHC and LHC S-band signals
8. X/S ranging
9. X/X ranging
10. X/S and X/X simultaneous ranging (starting in 2004)
11. ranging sample rates: 1..120 sec., 1 sec. Steps  
Monitoring and recording of S, X-band AGC, sample rates 60, 10, 1, 0.1 samples/s

Digitally recording of RHC and LHC signals at S-band or X-band (starting in 2004)

Digitally recording of RHC signals at S-band and X-band (starting in 2004)

12. Storage of Doppler frequencies and range values in a defined data format :

	Description
IFMS	GRST-TTC-GS-ICD-0518-TOSG [1] IFMS-to-OCC Interface Control Document
DSN	Archival Tracking Data File ATDF TRK 2-25 Original Data Record ODR RSC 11-13 Radio Science Receiver RSR 0189-Science

### 3.3.3.1 Ground Station Frequency Reference Source

A Hydrogen maser frequency standard has frequency stability in the order of  $10^{-15}$ . This stability is required for precise two-way tracking in order to achieve velocity accuracy better than 0.1 mm/s at one second integration time.

### 3.3.3.2 Further Equipment: RS IFMS

For a detailed description of the Radio Science IFMS, refer to MEX-MRS-IGM-RS-3014 [2].

### 3.3.4 Observed Quantities

The received carrier frequencies, the signal amplitudes (received total power) and the polarization of the radio signals is monitored at the ground station. Ground-based radio metric data are recorded using so-called closed-loop receivers:

- amplitude and phase (Doppler) measurements (two-way mode and one-way mode)
- ranging measurements (two-way mode only)
- full polarization measurements (primarily one-way mode)

In general, radio science measurements in the ground stations can be done simultaneously on a non-interference basis with the transmission and/or reception of telecommands and telemetry. The current mission baseline includes the 35 m ESA deep space antennas DSA 1, DSA 2 and DSA 3, which should be operational within the next few years. The NASA Deep Space Network (DSN) with antenna complexes in California, Spain and Australia is considered as a back-up.

The transmission of dual-frequency phase-coherent downlinks at S-band and X-band with the constant ratio 11/3 makes it feasible to separate the dispersive from the nondispersive Doppler effects on the radio link.

The frequency of the radio carrier is shifted according to the relative radial velocity between the transmitter and the receiver (classical Doppler shift).

Furthermore, a phase shift is experienced when the radio wave propagates through an ionized medium (ionospheres, interplanetary medium, solar corona). Excluding oscillator drifts and instabilities, the frequency shift for a one-way (spacecraft-to-Earth) radio link is

$$\Delta f = f_0 - f = -\frac{f_0}{c} \frac{ds}{dt} + \frac{40.31}{c} \frac{1}{f_0} \frac{d}{dt} \int_{S/C}^{Earth} N ds \quad (3-1)$$

where  $ds/dt$  is the rate of change of the distance between transmitter and receiver (relative velocity),  $c$  is the speed of light,  $f_0$  is the carrier frequency, and  $N$  is the electron density. The integral of the electron density along the propagation path  $ds$  of the radio wave from the S/C to Earth is also called the electron content, or column density.

The first term on the right hand side of (3-1) is the classical Doppler shift (linear in  $f_0$ ) and the second term is the dispersive propagation effect of radio waves in ionized media (inversely proportional to  $f_0$ ). A larger classical Doppler shift is measured on the X-band, but the S-band frequency is more sensitive to dispersive frequency shifts. A change in relative velocity of 2 cm/s yields a classical Doppler frequency shift of 0.6 Hz at X-band. A dispersive frequency shift of 0.6 Hz at S-band is produced by a change in electron content by one hexem ( $10^{16}$  electrons/m<sup>2</sup>) within one second.

It is not possible to separate classical and dispersive frequency shifts from the observed total change in frequency  $\Delta f$  at either  $f_S$  or  $f_X$ . However, using (3-1) for the two phase-coherent downlinks at X-band and S-band with a constant transponder ratio of  $880/240 = 11/3$  and calculating the *differential Doppler*

$$\Delta f_S - \frac{3}{11} \Delta f_X,$$

where  $\Delta f_S$  and  $\Delta f_X$  are the observed Doppler shifts at S-band and X-band, respectively, it is possible to isolate the dispersive frequency shift:

$$\begin{aligned} \Delta f_S - \frac{3}{11} \Delta f_X &= -\frac{\frac{d}{dt}S}{c} f_S + \frac{40.31}{c} \frac{1}{f_S} \frac{d}{dt} \int_{S/C}^{Earth} N ds + \frac{3}{11} \frac{\frac{d}{dt}S}{c} f_X - \frac{3}{11} \frac{40.31}{c} \frac{1}{f_X} \frac{d}{dt} \int_{S/C}^{Earth} N ds \\ &= \frac{40.31}{c} f_S \left[ \frac{1}{f_S^2} - \frac{1}{f_X^2} \right] \frac{d}{dt} \int_{S/C}^{Earth} N ds \end{aligned} \quad (3-2)$$

The differential Doppler (3-2), calculated from the observed frequency shifts, is used to determine the changes in electron content. All oscillator drifts are eliminated in this process. This result can further be used to correct each single classical frequency shift for the dispersive propagation effects.

The example above was derived for a one-way link. It can be shown that the calculation of the differential Doppler of a two-way radio link, where the spacecraft transmitted carrier frequencies are derived from the received (and Doppler shifted) uplink frequency, leads to exactly the same relation (3-2). In any case, (3-2) can be used to determine the electron content along the downlink path.

Integration of (3-2) yields the differential phase, which is proportional to the *changes* in electron content along the downlink from the beginning of the tracking pass.

The *absolute value* of total electron content, on the other hand, can be determined from the differential propagation delay by two-way ranging at S-band and X-band:

$$\tau_S - \tau_X = \frac{40.31}{c} \left\{ \frac{1}{f_S^2} - \frac{1}{f_X^2} \right\} \int_{s/c}^{Earth} N ds \quad (3-3)$$

Typically, the Doppler or phase measurements are more sensitive than the ranging measurements by about two orders of magnitude.

## 3.4 Data Products

### 3.4.1 Introduction

A thorough description of the RSI data products from level 1a to level 2 can be found in the Rosetta/Mars Express/Venus Express Archive Plan [5] and the Rosetta/Mars Express/Venus Express File Naming Convention Document [6].

### 3.4.2 Data types

#### 3.4.2.1 Closed-loop data

Closed-loop data acquisition is done with a phase-locked loop receiver at the ground station. Two-way Doppler shifts are extracted by comparing each measure of the downlink carrier frequency from the phase-locked loop with a reference from the ground station frequency reference source, e.g. a hydrogen maser with a frequency stability in the order of  $10^{-15}$  to  $10^{-16}$ . Because this frequency reference source is also used for the generation of the uplink carrier, the accuracy of the frequency determination is as good as the reference source. The Doppler integration time needed to achieve a certain signal to noise ratio controls the time between successive frequency determinations. The amplitude of the radio signal is estimated by the Automatic Gain Control (AGC).

#### 3.4.2.2 Open-loop data

Open-loop data recording is done by filtering and down-converting the received radio carrier signal to baseband where it is A/D converted and stored for subsequent analysis. The open-loop receiver is tuned by a local oscillator. The frequency of the local oscillator is defined by the best available estimate of the carrier frequency transmitted by the spacecraft and applying Doppler corrections due to the relative S/C-to-Earth motion. The drift of the USO output frequency will be known by long term measurements on ground and will be controlled by inflight calibration.

### 3.4.3 Data required from ESOC and JPL

#### 3.4.3.1 Observation data from DSA

The radio science observation data are recorded in the ground station by the IFMS systems. Depending on the ground station configuration up to three IFMS may record radio science data.

The Radio Science IFMS is an integral part of the receiving system at the ESA ground station. Its configuration has to fulfill the requirements of the Radio Science experiments, it can however serve also as a complementary and redundant unit for ESA's prime receiving units.

The following tables show the likely configuration scenarios for the IFMS system. All Doppler and ranging measurements must be performed by the standard ESA IFMS units with two downlink frequencies (TWOD) in order to allow compensation for the ionospheric/interplanetary TEC contribution.

The listed scenarios below show that for all cases requiring the Radio Science IFMS in OL mode operation, no telemetry modulation shall be applied to the downlink carrier analysed by the Radio Science IFMS in order to preserve spectral cleanliness as much as possible. Also, as a highly desirable option, scenarios (e. g. scenario 4) are suggested which require in addition to the Radio Science IFMS either IFMS 1 or IFMS 2.

#### 3.4.3.1.1 IFMS Configurations

IFMS data recording configurations are described in section 4.6.1.1.3.

#### 3.4.3.1.2 IFMS Data files

Closed-loop data:

Receiver system	Data type	
IFMS-1	Doppler 1	Hz
	Doppler 2	Hz
	AGC 1	dBm
	AGC 2	dBm
	Range	s
	Meteo	
IFMS-2	Doppler 1	Hz
	Doppler 2	Hz
	AGC 1	dBm
	AGC 2	dBm
	Meteo	
IFMS-3 (RS)	Doppler 1	Hz
	Doppler 2	Hz
	AGC 1	dBm
	AGC 2	dBm
	Range	s
	Meteo	
Sample rate	1, 10	s <sup>-1</sup>

Before and after the pass a range calibration of the IFMS equipment is requested.

The following data files from each operating IFMS at the ESA ground stations are requested:

**yy1n\_ssss\_YEAR\_DOY\_dk\_dt\_hhmmss\_xxxxx**

Identifier	Explanation	options
yy	Ground station ID	CB = Cebreros MG = Malargüe NN = New Norcia
n	number of the operating IFMS	
ssss	spacecraft acronym	ROSE for Rosetta
YEAR	Year	
DOY	Day of year	
dk	Data kind	OP = operational CL = calibration TS = test
dt	Data type	D1 = Doppler 1 D2 = Doppler 2 G1 = AGC 1 G2 = AGC 2 RG = ranging MT = meteo
hhmmss	Start time in hours, minutes, seconds	
xxxxx	Data set sequence ID	Starting with 00001

### 3.4.3.2 Observation data from DSN

#### 3.4.3.2.1 Tracking and Navigation Files (TNF)

The Tracking and Navigation File (TNF) is the primary output from the DSN closed-loop receiver system. The files comprise nearly 20 block types, each designed to carry data of interest to a particular navigation, telecommunication, or science community. The blocks are described by TNF\_SIS.TXT in the DOCUMENT/DSN\_DOC directory.

#### 3.4.3.2.2 Orbit Data Files (ODF)

Orbit Data Files are edited and partially processed versions of Tracking and Navigation Files (TNF), containing the most important information (range and Doppler) needed by spacecraft navigators and investigators interested in determining gravitational fields of bodies.

**Auxiliary Data**

<b>Data required</b>	<b>Timing</b>	<b>Data source</b>	<b>Freq.</b>	<b>Sampling</b>	<b>Accuracy (Required)</b>
<b>Major S/C events</b> (Orbit Manoeuvres, Eclipse etc)	Planned and Predicted	Ground	Monthly	Event related	Highest feasible
<b>Long range Orbit Prediction</b>	Predict	Ground	Monthly	1 sample/min.	Highest feasible
<b>Near Term Orbit Prediction</b>	Predict	Ground	Weekly	1 sample/min.	Highest feasible
<b>Quick look Orbit Estimation</b>	Post-obs	Tracking Data	Once in 2 days	1 sample/sec.	Highest feasible
<b>Precision Orbit Estimation</b>	Post-obs	Tracking Data	Once in 2 weeks	1 sample/sec.	Highest feasible
<b>Predicted Attitude</b>  Quarternions representation in both s/c orbiting ref.system and inertial reference system	Predict	Ground	Event related	1 sample/min.	Highest feasible
<b>Reconstituted Attitude (Attitude and Rates)</b>  Quarternions representation in both s/c orbiting ref.system and inertial reference system	Post-obs.	S/C Data + Ground	Event related	1 sample/sec.	Highest feasible

Data required	Timing	Data source	Freq.	Sampling	Accuracy (Required)
<b>Rotation Angle of SA (with respect to S/C frame of reference)</b>	Post-obs.	S/C Data	Weekly	1 sample/min	Highest feasible
<b>Pericentre 'TICK'</b>	Predict	Ground	Weekly	Every Orbit	Highest feasible
	Post-obs	Tracking Data	daily	Every Orbit	Highest feasible
<b>Orbit Time Period</b>	Predict	Ground	Weekly	Every Orbit	Highest feasible
	Post-obs	Tracking Data	daily	Every Orbit	Highest feasible
<b>Thruster Firing Times (Start Time &amp; Duration)</b>	Predict & Post-obs.	Ground & S/C	Event related	Every Manoeuvre	millisec
<b>Sun Zenith Angle (Over Pericentre)</b>	Predict	Ground	Weekly		Highest feasible
<b>Times of Earth Occultation Entry and Exit</b>	Predict	Ground	Weekly	Each Earth occultation	seconds
<b>Spacecraft Position at Earth occultation entry and exit</b>	Predict	Ground	Weekly	Each Earth occultation	Highest feasible
	Post-obs.	Tracking Ground	daily	Each Earth occultation	Highest feasible
<b>Longitude &amp; Latitude of occultation entry and exit in the plane-of-sky</b>	Predict	Ground	Weekly	Each Earth occultation	Arc minutes
	Post-obs.	Ground	daily	Each Earth occultation	Arc minutes

<b>Data required</b>	<b>Timing</b>	<b>Data source</b>	<b>Freq.</b>	<b>Sampling</b>	<b>Accuracy (Required)</b>
<b>Solar Zenith Angle at Earth occultation entry and exit</b>	Predict	Ground	Weekly	Each Earth occultation	Arc minutes
	Post-obs	Ground	daily	Each Earth occultation	Arc minutes
<b>Duration of Earth Occultation</b>	Predict	Ground	Weekly	Each Earth occultation	seconds
<b>Spacecraft position as subsatellite point</b>	Predict	Ground	weekly	Event related (approved pericenter pass for gravity)	Highest feasible
	Post-obs.	Tracking & Ground	Daily	Event related (approved pericenter pass for gravity)	Highest feasible
<b>HGA pointing direction Angle wrt NADIR (for gravity)</b>	Post-obs	Ground + S/C	Each event	1 sample/sec	Arc minutes
<b>Angle wrt Earth direction (for bistatic radar)</b>	Post-obs	Ground + S/C	Each event	1 sample/sec	Arc minutes
<b>Quaternions representation in both s/c orbiting ref. System and inertial reference system</b>	Post-obs	Ground + S/C	Each event	1 sample/sec	Arc minutes

### 3.4.3.3 SPICE

SPICE Kernels used by RSI are defined in the Radio Science File Naming Convention.

### 3.4.3.4 Housekeeping Data

The table below summarizes the USO telemetry data and the nominal value of each channel, for the warm-up case and for the steady-state case.

Besides several other Housekeeping parameters are of interest for RSI. A complete list of all these parameters can be found in RO-EST-RS-3169 [14]. Further information about Housekeeping data delivery from the DDS can be found in RO-EST-TN-3215 [15] and RO-ESC-IF-5003 [16].

#### TM conversion Table:

TM Name	TM Raw Unit	TM Conversion	TM Unit
DC Current	V	Raw Value/5	A
DC/DC Voltage	V	Raw Value *3	V
Output Power A	V	<2.5V muted >2.5V enabled	V
Output Power B	V	<2.5V muted >2.5V enabled	V
Oven Temp A	V	<2.4 V to cold 2.4V ... 2.7V nominal >2.7V to hot	V
Oven Temp B	V	<2.4 V to cold 2.4V ... 2.7V nominal >2.7V to hot	V
Lock State A (note 1)	V	0.0V ... 2.5V unlock 2.5V ... 5.0V lock	V
Lock State B (Note 1)	V	0.0V ... 2.5V unlock 2.5V ... 5.0V lock	V
USO TRP		YellowSpring YSI-44907	°C

Note 1): Addition of two signals: LockState + (10V-Utune)/4

#### Nominal values during warm-up:

TM Name	TM Raw min.	TM Raw max.	TM value min	TM value max
DC Current	0.8 V	1.7 V	0.16 A	0.34 A
DC/DC Voltage	3.32 V	3.33 V	9.96 V	9.99 V
Output Power A	1.7 V	2.2 V	1.7 V	2.2 V
Output Power B	1.7 V	2.2 V	1.7 V	2.2 V
Oven Temp A	0 V	2.7 V	0 V	2.7 V
Oven Temp B	0 V	2.7 V	0 V	2.7 V
Lock State A	0.5 V	0.7 V	0.5 V	0.7 V
Lock State B	0.5 V	0.7 V	0.5 V	0.7 V

USO TRP			-30 °C	+50 °C
---------	--	--	--------	--------

**Nominal Values at steady state:**

TM Name	TM Raw min.	TM Raw max.	TM value min	TM value max
DC Current	0.8 V	1.1 V	0.16 A	0.22 A
DC/DC Voltage	3.32 V	3.33 V	9.96 V	9.99 V
Output Power A	4.0 V	4.3 V	4.0 V	4.3 V
Output Power B	3.6 V	3.9 V	3.6 V	3.9 V
Oven Temp A	2.4 V	2.7 V	2.4 V	2.7 V
Oven Temp B	2.4 V	2.7 V	2.4 V	2.7 V
Lock State A	3.7 V	4.3 V	3.7 V	4.3 V
Lock State B	3.7 V	4.3 V	3.7 V	4.3 V
USO TRP			-20 °C	+50 °C

The data are valid under vacuum condition at BOL.

All values shall be constant under stable environment conditions; they only change versus environment temperature.

The Lock-State (e.g. Utune) will drift versus lifetime. When extrapolated, the value at EOL shall not exceed the range between 3.0V and 4.7V. This shall be reported to the PI on a regular base.

**3.4.4 Data Volume Calculation**

Estimate of the data volume (order of magnitude numbers):

**closed-loop:**

IFMS	Calculation (bytes)	One hour data recording @ 1 second sampling time
Overhead		18 kBytes
Ranging	110 x number of samples /hour	396 kBytes
Doppler	220 x number of samples/hour	792 kBytes
Meteo	100 x number of samples/hour	6 kbytes (1 min sampling time)

DSN ATDF	Calculation (bytes)	One hour data recording @ 1 second sampling time
Ranging Doppler	288 x number of samples/hour	1036 kBytes

**Open-loop (I+Q Channels):**

IFMS	Calculation (bytes)	Event volume
	36 Mbyte/min	2.2 Gbyte/1 hour

ROSETTA RSI: Rosetta Radio Science Investigations

Experiment User Manual

Document **RO-RSI-IGM-MA-3081**

Issue: 4

Revision: 2

Date: 25.04.2016

Page: 47 of 144


<b>DSN ODR</b>	<b>Calculation (bytes)</b>	<b>Event volume (tracking pass)</b>
occultations	0.5 Mbytes / minute	15 Mbytes total (duration 2x 15 minutes)
Bistatic radar	12.5 Mbytes / minute	750 Mbytes total (duration 1 hour)
Solar corona	0.5 Mbytes / minute	195 Mbytes total (6.5 hours)

### 3.4.5 End-to-End performance

The following is an excerpt from RO-RSI-IGM-TN-3057 [9].

#### 3.4.5.1 Discussion of Doppler noise sources

When evaluating error sources one has to analyze both ground station and space segment contributions and cannot concentrate only on the transponder quantization error.

**Thermal contribution:** Taking a 1 second integration interval, assuming a H2 Maser reference frequency source we obtain an r.m.s. velocity error of

$$\sigma_v = \frac{c \sqrt{\frac{2BN_0}{C}}}{4\pi f_d T} \quad (3-4)$$

due to thermal noise contribution. Assuming the noise band of the ground station PLL receiver,  $C/N_0$  the total carrier to noise power spectral density ratio,  $T$  the integration time,  $f_d$  the nominal downlink frequency and the  $c$  the speed of light in vacuum.

It is well justified to assume that the uplink  $C/N$  dominates over the downlink  $C/N$ , hence it is the downlink  $C/N$  which enters into formula (1). For S-Band we obtain with an estimated  $C/N_0$  23 dBHz at the ground station (3 AU), 1 sec integration time and  $2B = 1$  Hz loop bandwidth a velocity error of

**0.8 mm/s.**

We are correspondingly better at X- band due to an improved  $C/N_0$  .

Taking the totally accumulated phase error (thermal noise, NCO ground station quantization error, reference frequency instability and path delay instability at the Perth ground station, ref. [5,6], we receive at a corresponding velocity error of (naturally depending critically on link quality)

**1 mm/s for S-band and 0.3 mm/s for X-band.**

Additional noise sources are now given by the onboard transponder NCO quantization error noise contribution. The implementation of the NCO (32 bit word) will lead to a quantization error in frequency of 3mHz r.m.s. (applicable as well for S- as for X-band) corresponding to a velocity error of

**0.4 mm/s for S-band and 0.1 mm/s for X-band.**

Assuming an incremental error of  $d = 2\pi/2048$  in phase (12 bit word) and a uniform error distribution we obtain a variance of that error of

$$\frac{d}{\sqrt{12}} = 0.88 \text{ mrad r.m.s.}$$

This error contributes in the following way to the velocity error:

$$\sigma_v = \frac{c\sqrt{2}\sigma_\phi}{4\pi f_d T} \quad (3-5)$$

resulting in

**0.01 mm/s for S-band and 0.004 mm/s for X-band.**

On the basis of r.s.s. we obtain on the basis of a H2 maser at the ground station for an integration time of 1 second a

**total velocity error: 1.1 mm/s for S-band and 0.32 mm/s for X-band**

#### 3.4.5.2 Summary of error sources:

Error source	Velocity error $\sigma_v$	
	S-band	X-band
<b>Total phase error (thermal and ground station contribution)</b>	1.0 mm/s	0.3 mm/s
<b>Transponder quantization error in frequency</b>	0.4 mm/s	0.1 mm/s
<b>Transponder quantization error in phase</b>	0.01 mm/s	0.004 mm/s
<b>Total error (coherent mode)</b>	1.1 mm/s	0.32 mm/s

These Doppler errors are assumed for an integration time of 1 second and are comparable to those already observed from past missions. Considerable improvements can be achieved using longer integration times.

### **3.4.5.3 Doppler accuracy for longer integration times**

Taking all major error sources into account, the Doppler velocity error  $\sigma_{v0}$  at S-band and X-band is estimated in

Table 3.4-1 for a one second integration time. For longer integrations, the accuracy  $\sigma_0(\Delta t)$  scales with the square root of the integration time  $\Delta t$ :

$$\sigma_V(\Delta t) = \sigma_{V0} \frac{1}{\sqrt{\Delta t}} \quad (3-6)$$

Typical integration times used in the gravity science investigations are in the range between 60 seconds and 600 seconds for the asteroid flybys and for the determination of the nucleus mass, in particular in view of the very small orbital velocities and revolution periods about the nucleus.

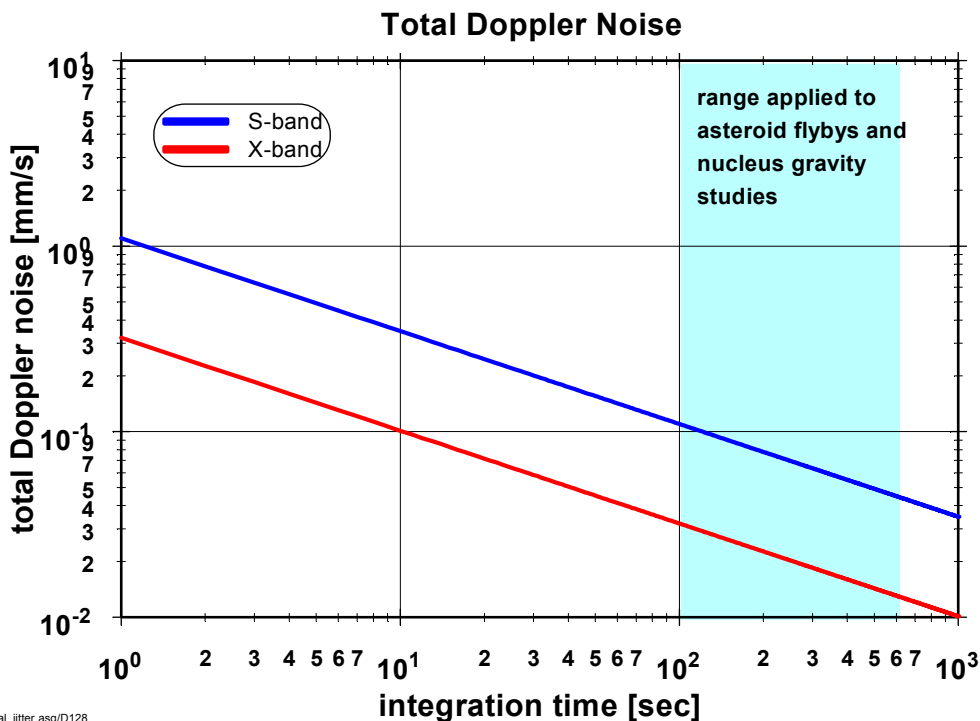


Figure 3.4-1: Total Doppler noise as a function of integration time  
 The error in the electron content from differential Doppler measurements (2) at one second integration time is computed to be in the order 0.02 hexem.

Table 3.4-1: Doppler velocity error budget

Error source	Velocity error $\sigma_v$	
	S-band	X-band
Phase error (thermal and ground station contribution)	1.0 mm/s	0.3 mm/s
Transponder quantization error in frequency	0.4 mm/s	0.1 mm/s
<b>Total error (coherent mode)</b>	<b>1.08 mm/s</b>	<b>0.32 mm/s</b>

Figure 3.4-2: Orbital Velocity and Spacecraft revolution period as function of distance to comet center of mass

## 4 Experiment Operations

### 4.1 Definitions and Configurations

#### 4.1.1 Spacecraft and Ground Station configurations

Two main spacecraft and ground station configurations are used: ONE and TWO describing one-way radio downlink(s) and two-way radio links, respectively. Further details are added to the acronyms as:

- S = single frequency downlink
- D = dual-frequency downlinks
- TCXO = driven by the transponder oscillator
- USO = driven by the onboard Ultrastable Oscillator
- -S = S-band uplink
- -X = X-band uplink

#### 4.1.2 ONES

This configuration acronym describes the X-band one-way downlink driven by the TXCO or the USO, ONES-TCXO or ONES-USO, respectively.

##### 4.1.2.1 ONES-TCXO

###### Spacecraft

Mode	Uplink	downlink	RNG	TM	Driven by
One-way	n/a	X-band	OFF	selectable	TCXO

###### Ground station

IFMS	Uplink	downlink	Sample rates (sec <sup>-1</sup> )					METEO
			RNG	DOP1	DOP2	AGC1	AGC2	
1	n/a	X-band	OFF	10	10	10	10	0.016
2	-	X-band	-	10	10	10	10	
3	-	X-band	-	10	10	10	10	

##### 4.1.2.2 ONES-USO

###### Spacecraft

Mode	Uplink	downlink	RNG	TM	Driven by
One-way	n/a	X-band	OFF	selectable	USO

###### Ground station

IFMS	Uplink	downlink	Sample rates (sec <sup>-1</sup> )					METEO
			RNG	DOP1	DOP2	AGC1	AGC2	
1	n/a	X-band	OFF	10	10	10	10	0.016
2	-	X-band	-	10	10	10	10	

3	-	X-band	-	10	10	10	10	
---	---	--------	---	----	----	----	----	--

### 4.1.3 ONED

#### 4.1.3.1 ONED-TCXO

##### Spacecraft

Mode	Uplink	downlink	RNG	TM	Driven by
One-way	n/a	X-band S-band	OFF OFF	Selectable Selectable	TCXO TCXO

##### Ground station

IFMS	Uplink	downlink	Sample rates (sec <sup>-1</sup> )					METEO
			RNG	DOP1	DOP2	AGC1	AGC2	
1	n/a	X-band	OFF	10	10	10	10	0.016
2	-	X-band	-	10	10	10	10	
3	-	S-band	-	10	10	10	10	

#### 4.1.3.2 ONED-USO

##### Spacecraft

Mode	Uplink	downlink	RNG	TM	Driven by
One-way	n/a	X-band S-band	OFF OFF	Selectable Selectable	USO USO

##### Ground station

IFMS	Uplink	downlink	Sample rates (sec <sup>-1</sup> )					METEO
			RNG	DOP1	DOP2	AGC1	AGC2	
1	n/a	X-band	OFF	10	10	10	10	0.016
2	-	X-band	-	10	10	10	10	
3	-	S-band	-	10	10	10	10	

#### 4.1.4 TWOS

##### Spacecraft

Mode	Uplink	downlink	RNG	TM	Driven by
Two-way coherent	X-band	X-band	ON	Selectable	G/S

##### Ground station

IFMS	Uplink	downlink	Sample rates (sec <sup>-1</sup> )					
			RNG	DOP1	DOP2	AGC1	AGC2	METEO
1	X-band	X-band	ON	1	1	1	1	0.016
2	-	X-band	-	1	1	1	1	
3	-	X-band	-	1	1	1	1	

#### 4.1.5 TWOD

##### 4.1.5.1 TWOD-X

##### Spacecraft

Mode	Uplink	downlink	RNG	TM	Driven by
Two-way coherent	X-band	X-band S-band	ON ON	Selectable Selectable	G/S

##### Ground station

IFMS	Uplink	downlink	Sample rates (sec <sup>-1</sup> )					
			RNG	DOP1	DOP2	AGC1	AGC2	METEO
1	X-band	X-band	ON	1	1	1	1	0.016
2	-	X-band	-	1	1	1	1	
3	-	S-band	-	1	1	1	1	

#### 4.1.5.2 TWOD-S

##### Spacecraft

Mode	Uplink	downlink	RNG	TM	Driven by
Two-way coherent	S-band	X-band S-band	ON ON	Selectable Selectable	G/S

##### Ground station

IFMS	Uplink	downlink	Sample rates (sec <sup>-1</sup> )					METEO
			RNG	DOP1	DOP2	AGC1	AGC2	
1	S-band	S-band	ON	1	1	1	1	0.016
2	-	S-band	-	1	1	1	1	
3	-	X-band	-	1	1	1	1	

## 4.2 RSI Operational Procedures

Due to the specific character of the RSI experiment the flight control procedures will have to be established compatible with the TTC subsystem, based on the RSI requests and agreed by the ROSETTA Project. The sections below define the S/C and G/S configurations and skeleton operational procedures.

RSI defined the following operational procedures:

CMD	Center of Mass Determination
PCx	Passive or Active Payload Checkout
DOT	Doppler Tracking
GMC	Gravity Mapping Campaign
OCP	Occultation Operations Procedures
BRP	Bistatic Radar Procedures
SCP	Solar Conjunction Procedures
AST	Asteroid Flyby Procedures

### 4.2.1 PCx *Passive or Active Checkout Number x*

Objective:	Monitor the sensitivity, drift and aging of the USO.
S/C Configuration:	ONED
Ground Segment Config.:	ONED-CL ONED-OL
Execution:	Every 6 month.
Requirements:	No S/C orbit correction within UCT Logging of thruster activities
Command Sequence:	ARFF030

#### **4.2.2 CMD            *Center of mass determination***

Objective: Calibration of the phase center displacement of the HGA by a sequence of slew manoeuvres to determine the center of mass of the Rosetta spacecraft w.r.t the HGA phase center

S/C Configuration: TWOD  
Ground Seg. Config.: TWOD-CL  
Execution: Cruise phase, before comet encounter, before/after asteroid flyby

Requirements: No S/C orbit correction within CMD  
Logging of thruster activity  
precise HGA earth pointing

Command Sequence: ARFF020

#### **4.2.3 DOT            *Doppler Tracking***

Objective: Gravity: Mass and density, higher gravity harmonics, moments of inertia  
comet orbit  
coma mass flux

S/C Configuration: TWOS; TWOD  
Ground Seg. Config.: TWOS-CL; TWOD-CL  
Execution: Comet approach Phase, Orbit Phase, Escort Phase  
Solar Conjunctions and Oppositions

Requirements: No S/C orbit correction within DOT  
Logging of thruster activity

Command Sequence: ARFF021; to be updated

**4.2.4 GMC Gravity Mapping Campaign**

Objective:	Nucleus gravity field
S/C Configuration:	TWOS; TWOD
Ground Seg. Config.:	TWOS-CL; TWOD-CL
Execution:	Beyond 3.0 AU heliocentric distance
Requirements:	Low circular, near-polar orbit 2 comet radii altitude 14 days GMC operations, depending on comet rotation rate Maximum tracking coverage (24 hours) Heliocentric distance beyond 3 AU No S/C orbit correction within GMC Minimum thruster activity and logging of thruster activity
Command Sequence:	TBW

**4.2.5 OCP Occultation Operations Procedures**

Objectives:	Near nucleus dust and plasma environment Nucleus internal structure
S/C Configuration:	ONES-USO; ONED-USO
Ground Seg. Config.:	ONES-CL; ONED-CL ONESS-OL; ONED-OL
Execution:	Planned occultation campaign Repeated every two months at comet
Requirements:	Establish one-way link 1/4 orbital period prior to occultation Re-establish two-way 1/4 orbital period after occultation Dedicated orbit optimised for occultations 7 days OCP operations, depending on orbit and occultation conditions No orbit correction within OCP Minimum thruster activity and logging of thruster activity
Command Sequence:	ARFF026; to be updated

**4.2.6 BRP      *Bistatic Radar Procedures***

Objective:	Nucleus surface properties
S/C Configuration:	ONES-USO
Ground Seg. Config.:	ONES-OL; ONES-POL
Execution:	Planned bistatic radar procedure Repeated periodically during prime mission
Requirements:	Pointing of HGA toward the comet Recording of RHC and LHC radio signals at the ground station No orbit correction during BRP Minimum thruster activity and logging of thruster activity
Command Sequence:	TBW

**4.2.7 AST      *Asteroid Flyby Procedures***

Objective:	Asteroid mass and bulk density
S/C Configuration:	TWOS; TWOD
Ground Seg. Config.:	TWOS-CL; TWOD-CL
Execution:	during asteroid flybys
Requirements:	Several hours continuous tracking coverage after the last correction manoeuvre before encounter, during flyby, and before the first correction manoeuvre after encounter
Command Sequence:	ARFF023/ARFF024/ARFF025; to be updated

**SCP      *Solor Corona Procedure***

Objective:	Sounding of the Solar Corona
S/C Configuration:	TWOD
Ground Seg. Config.:	TWODCL; TWOD-OL
Execution:	during solar conjunctions
Requirements:	≥ 4 hours continuous tracking; no S/C orbit correction within SCP; logging of thruster activity
Command Sequence:	ARFF022; to be updated

## 4.3 HGA Pointing Requirements

### 4.3.1 Overview

The Pointing requests for RSI are outlined in Table 4.2-1. Depending on the scientific operations, three different HGA pointing modes are distinguished. Pointing requests will be made in an EPS PTR-compatible syntax and are given below for the respective pointing scenarios. <Time or event> is an epoch during the mission. Additional parameters <value> (in sec.) are listed in Table 4.3-2.

Table 4.2-1 RSI Pointing Requests

RSI pointing mode	Applicable procedure
Earth pointing	DOT, SCP, OCP, GMC, AST, PCx
Comet pointing	BRP
Center of Mass	CMD

### 4.3.2 Earth inertial pointing

Earth inertial pointing is requested (and baselined) during most of the scientific operations during the Rosetta mission. It is also baselined during the commissioning phase. Applicable procedures are DOT SCP, OCP, GMC, PCx and AST.

Pointing Mode Request:

```
<Time or event> RSI INERT_START (\
                OBJECT=EARTH \
                DURATION=<value>
                POINTING_AXIS=HGA )
```

### 4.3.3 Comet pointing

For the bistatic radar experiment, the HGA pointing towards the comet is requested.

Pointing mode request:

```
<Time or event> RSI NADIR_START (\
                OBJECT=COMET \
                DURATION=<value>
                POINTING_AXIS=HGA )
```

### 4.3.4 Phase center pointing

In order to determine the phase center offset of the antenna with respect to the S/C center of mass, a slew of the S/C around two axes with the HGA pointing to Earth is requested:

```
<Time or event> RSI NADIR_START (\
                OBJECT=EARTH \
                DURATION=<value> \
                POINTING_AXIS=HGA \
                OFFSET_ANGLE=30 \
                SLEW_POLICY=SMOOTH ) \
<Time or event> RSI NADIR_START (\
                OBJECT=EARTH \
                DURATION=<value> \
                SLEW_AXIS= \
```

OFFSET\_ANGLE=-30 \  
SLEW\_POLICY=SMOOTH )

Table 4.3-2 Pointing Request Parameters

<b>Procedure</b>	<b>DURATION=&lt;value&gt;</b>
PCx	3x3600
DOT	8x3600
GMC	8x3600
OCP	8x3600
BRP	8x3600
SCP	8x3600
AST	10x3600

## 4.4 Mapping of Science Objectives to Operational Procedures

Table 4.4-1: Mapping of Science Objectives to Operational Procedures

Cometary Mass and Bulk Density	DOT, GMC
Cometary Gravity Field Coefficients	DOT, GMC
Cometary Moments of Inertia	DOT, GMC
Cometary Orbit	DOT
Nucleus Surface	BRP
Nucleus Internal Structure	OCC
Nucleus Size and Shape	OCC
Coma Plasma	OCC
Dust Grains	OCC
Coma Mass Flux	DOT
Asteroid Mass and Bulk Density	AST
Active and Passive Checkout	PCx
Solar Corona	SCP

## 4.5 Functions: Space Segment

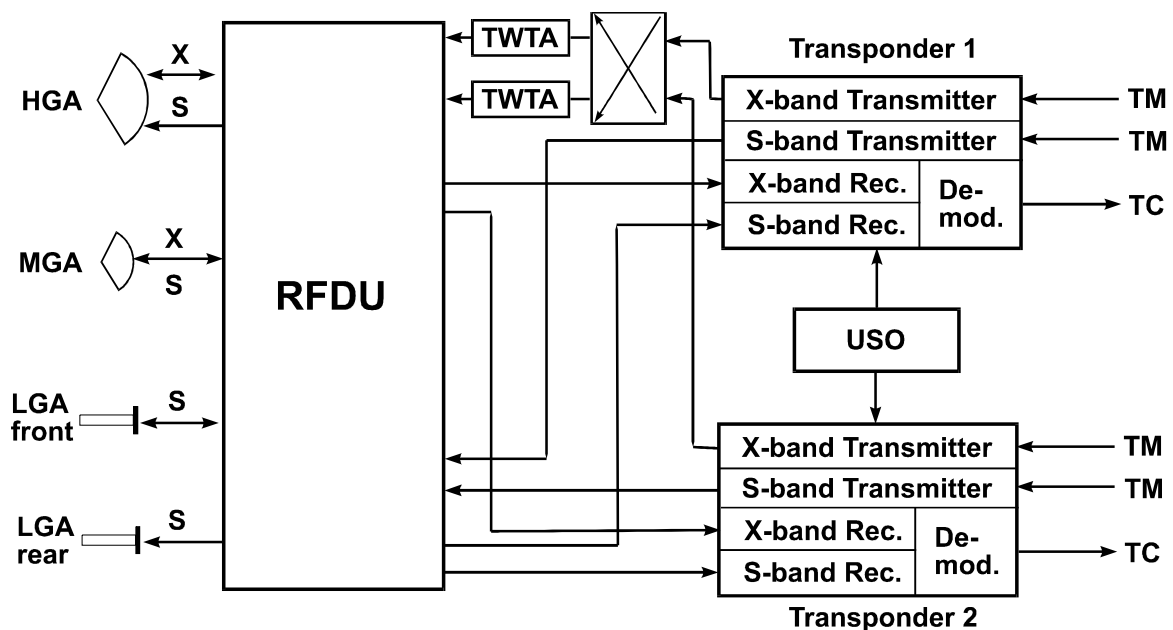
### 4.5.1 Design and Functional Description of the RF Subsystem

The Rosetta radio subsystem (Figure 4.5-1) is capable of receiving and transmitting radio signals via three dedicated antenna systems:

1. High Gain Antenna (HGA), a fully steerable parabolic dish of 2.20 m diameter
2. Medium Gain Antenna (MGA), a fixed parabolic dish of 0.60 m diameter
3. Two Low Gain Antennas (LGA), front and rear, S-band only

The HGA is the main antenna for receiving telecommands from and transmitting telemetry signals to ground. The MGA and LGA on Rosetta is considered as a back-up for emergency and near-earth operations only.

The two transponders consist of an S-band and X-band receiver and transmitter each. The spacecraft is capable of receiving one uplink signal at S-band (2100 MHz) via the LGAs/MGAs, or at either X-band (7100 MHz) or S-band via the HGA. The spacecraft can transmit via the HGA simultaneously two downlink signals at S-band (2300 MHz) and X-band (8400 MHz) or one downlink signal at S-band via the LGAs/MGAs. The radio frequency subsystem is equipped with an Ultrastable Oscillator (USO) dedicated to RSI operations. RSI will use the HGA for their measurements, only.



rosradio.cdr/D137

Figure 4.5-1: Block diagram of the Rosetta radio subsystem

ROSETTA RSI: **Rosetta Radio Science Investigations**  
**Experiment User Manual**

Document **RO-RSI-IGM-MA-3081**

Issue: 4

Revision: 2

Date: 25.04.2016

Page: 65 of 144

---

PAGE LEFT FREE

## 4.6 Functions: Ground Segment

### 4.6.1 Overview

#### 4.6.1.1 Ground Station

##### 4.6.1.1.1 Overview IFMS

The following description refers to the New Norcia ground station DSA 1. The dedicated Radio Science IFMS is an integral part of the receiving system (consisting of two IFMS with uplink capabilities) at the ESA ground station in New Norcia. Its configuration has to fulfill the requirements of the Radio Science experiments, it can however serve also as a complementary and redundant receiving unit for ESA's two prime IFMS units.

##### 4.6.1.1.2 System Description

According to MEX-MRS-IGM-RS-3014 [2] the following assumptions can be made with regard to the IFMS systems in the ground station:

1. The New Norcia ground station near Perth, Australia, will be equipped with two standard (operational) IFMSs and a third IFMS unit dedicated to the Radio Science observations
2. Two polarizations can be analyzed by one IFMS
3. Two downlink carriers at S-band and X-band can be received simultaneously, only one carrier will be modulated with telemetry
4. One, alternatively also two downlink carriers modulated with ranging signals can be received
5. Radio science open-loop measurements will be carried out simultaneously at S- and X-band<sup>1</sup> at the RS IFMS

The IFMS block diagram is shown in Figure 4.6-1. The configuration change from standard CL configuration to OL configuration will not involve any hardware changes.

A schematics including the digital signal processing part relevant for RSI is shown in Figure 4.6-2.

---

<sup>1</sup> There is the certain risk that there is no G/S equipment redundancy when performing radio science observations. The IFMS can quickly be reconfigured in the case of problems, so that that risk can be tolerated.

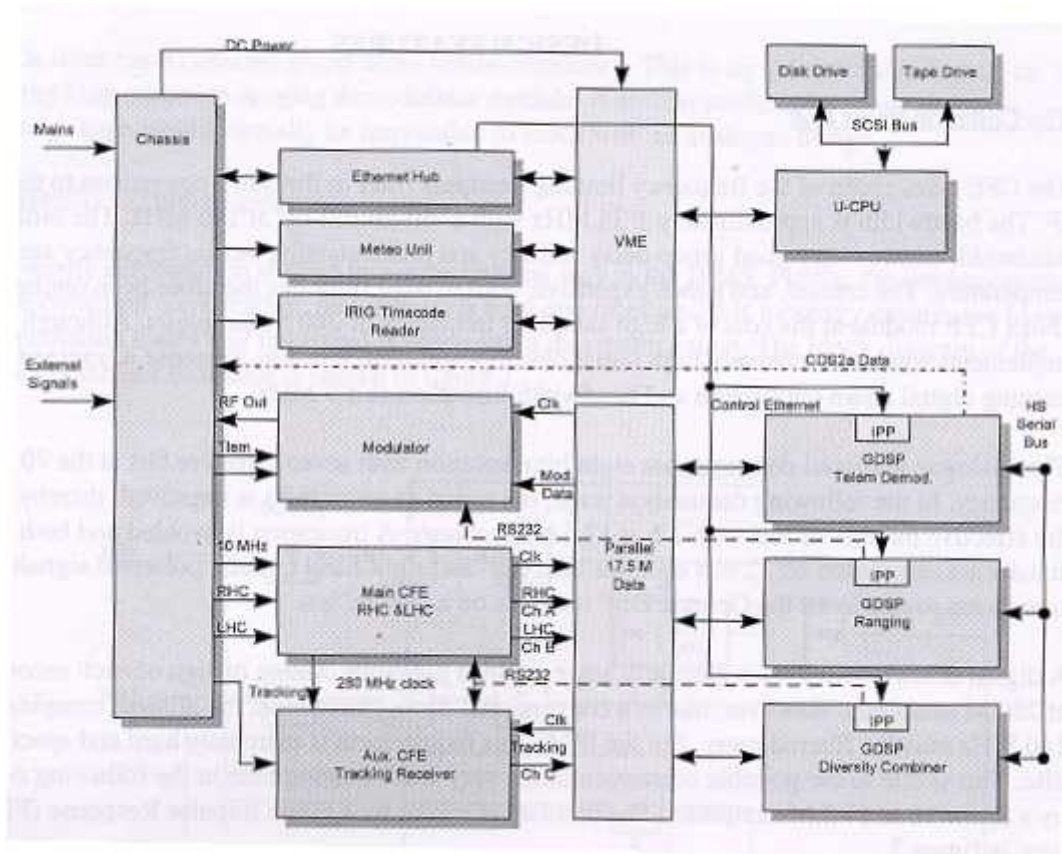


Figure 4.6-1: IFMS block diagram

## IFMS Open-Loop Processing for RSI

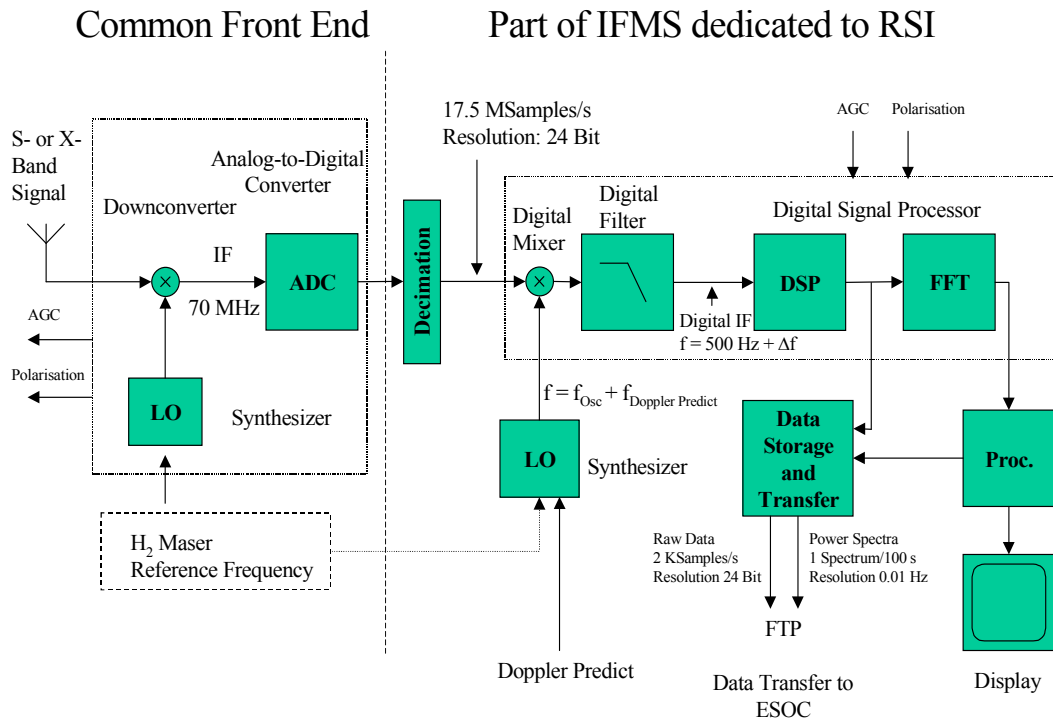


Figure 4.6-2: IFMS Open-Loop Digital Data Processing Part for RSI

According to reference [3,5] it is assumed that the IFMS operates on a 17.5 Mps 24-bit complex baseband stream (containing 12 bit words each for the I and Q channels) and resulting from filtering and decimating the 280 Mps 8-bit stream output by the Common Front End (CFE) Analogue to Digital converter. These channels are provided for both RCP and LCP polarisations.

The Radio Science raw data can be directly transferred to a mass storage device and/or processed by a Fast Fourier routine.

Data transfer rates from DSP to Data Storage (disk) is presently limited to 10 samples/s. Data Transfer to ESOC shall be done via FTP with a rate of 2 kps.

The Doppler predict has to be accurate enough to allow carrier signal analysis in the desired narrow frequency band.

The internally generated raw data stream consists of I and Q signals which are distributed on 8 parallel bits each for both left- and right-hand polarized signals which can be processed further and routed to a data dump and storage device ("PC" configured for MaRS/RSI, see also Fig. 2.6-2) in order to obtain higher data rates. Here, the absolute maximum data rate is limited to 10 Mb/s.

The incoming signals will be further processed in a diversity combiner providing the combined output together with an estimate for the electrical phase angle (MEX-MRS-IGM-RS-3014 [2]).

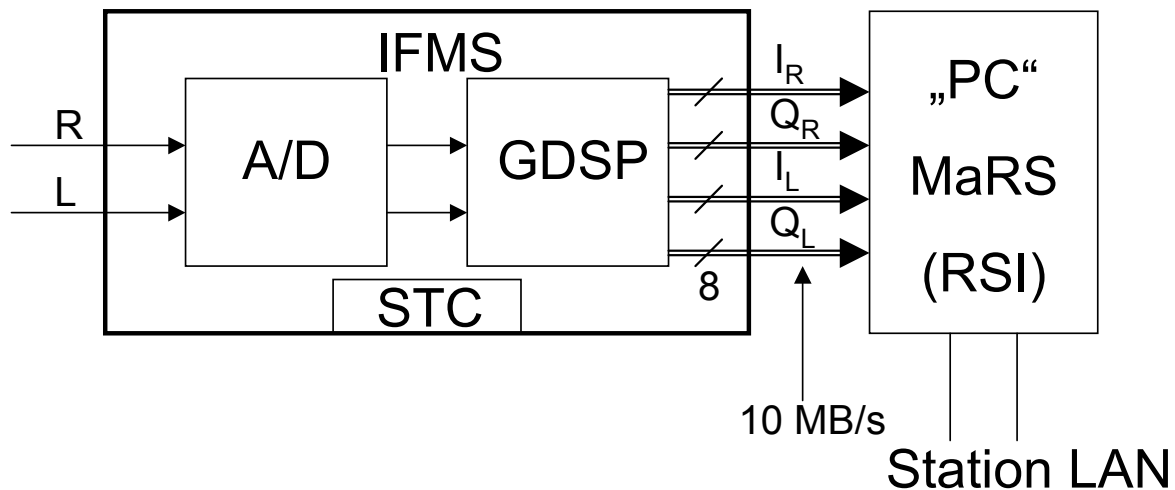


Figure 4.6-3: IFMS internal signal processing. The 8 bit resolution will be replaced by a 12 bit resolution.

RSI requires both the preservation of raw data for later data retrieval and the near real time data processing and conversion. These requests are further specified in section 6.

#### 4.6.1.1.3 IFMS Configurations

The following tables show the likely configuration scenarios for the IFMS system when Radio Science experiments will be conducted. All dual-frequency Doppler and ranging measurements must be performed by the standard ESA IFMS units with two downlink frequencies (TWOD) in order to allow compensation for the ionospheric/interplanetary TEC contribution.

The listed scenarios show that for all Radio Science operational cases, no telemetry modulation shall be applied to the downlink carrier analysed by the IFMS in order to preserve spectral cleanliness as much as possible.

Table 4.6-1: IFMS receiver system scenario 1

Functional use: **RSI gravity, mass flux, asteroid flyby**

Scenario1	IFMS A	IFMS B	IFMS RS
Uplink frequency	X	-	-
Downlink frequency	X	X	S
Telemetry modulation	Off	Off	Off
Receiver loop	CL	CL	CL
Observational parameters	Doppler AGC Meteo, Ranging	Doppler AGC	Amplitudes, ranging

Table 4.6-2: IFMS receiver system scenario 2

**Functional use: RSI solar corona sounding**

<b>Scenario 2</b>	<b>IFMS A</b>	<b>IFMS B</b>	<b>IFMS RS</b>
<b>Uplink frequency</b>	X		-
<b>Downlink frequency</b>	X	X	S
<b>Telemetry modulation</b>	Off	Off	Off
<b>Receiver loop</b>	CL	CL	CL/OL
<b>Observational parameters</b>	Doppler, Ranging AGC Meteo	Doppler, AGC	Doppler, AGC, ranging Open loop

Table 4.6-3: IFMS receiver system scenario 3

**Functional use: RSI bistatic radar (TBC)**

<b>Scenario 3</b>	<b>IFMS A</b>	<b>IFMS B</b>	<b>IFMS RS</b>
<b>Uplink frequency</b>	-	-	-
<b>Downlink frequency</b>	X	X	S
<b>Telemetry modulation</b>	Off	Off	Off
<b>Receiver loop</b>	CL	CL	OL
<b>Observational parameters</b>	Doppler AGC Meteo	Doppler AGC	Open loop LHC/RHC

Table 4.6-4: IFMS receiver system scenario 4

**Functional use: RSI occultations (cometary dust and grains) (1) (TBC)**

<b>Scenario 4</b>	<b>IFMS A</b>	<b>IFMS B</b>	<b>IFMS RS</b>
<b>Uplink frequency</b>	-	-	-
<b>Downlink frequency</b>	X	X	S
<b>Telemetry modulation</b>	Off	Off	Off
<b>Receiver loop</b>	CL	CL	OL
<b>Observational parameters</b>	Doppler Ranging AGC Meteo	Doppler AGC	Open loop LHC/RHC

## 4.6.2 Deep Space Network

### 4.6.2.1 Overview

Three Deep Space Communications Complexes (DSCCs) (near Barstow, CA; Canberra, Australia; and Madrid, Spain) comprise the DSN tracking network. Each complex is equipped with several antennas [including at least one each 70-m, 34-m High Efficiency (HEF), and 34-m Beam WaveGuide (BWG)], associated electronics, and operational systems. Primary activity at each complex is radiation of commands to and reception of telemetry data from active spacecraft. Transmission and reception is possible in several radio-frequency bands, the most common being S-band (nominally a frequency of 2100-2300 MHz or a wavelength of 14.2-13.0 cm) and X-band (7100-8500 MHz or 4.2-3.5 cm). Transmitter output powers of up to 400 kW are available

Ground stations have the ability to transmit coded and uncoded waveforms which can be echoed by distant spacecraft. Analysis of the received coding allows navigators to determine the distance to the spacecraft; analysis of Doppler shift on the carrier signal allows estimation of the line-of-sight spacecraft velocity. Range and Doppler measurements are used to calculate the spacecraft trajectory and to infer gravity fields of objects near the spacecraft.

Ground stations can record spacecraft signals that have propagated through or been scattered from target media.

The Deep Space Network is managed by the Jet Propulsion Laboratory of the California Institute of Technology for the U.S. National Aeronautics and Space Administration.

For more information on the Deep Space Network and its use in radio science see reports by Asmar & Renzetti (1993), Asmar & Herrera (1993), and Asmar et al (1995). For design specifications on DSN subsystems see [DSN810-5] [12].

### 4.6.2.2 DSN Radio Science Equipment

The Deep Space Communications Complexes (DSCCs) are an integral part of Radio Science instrumentation, along with the spacecraft Radio Frequency Subsystem. Their system performance directly determines the degree of success of Radio Science investigations, and their system calibration determines the degree of accuracy in the results of the experiments. The following paragraphs describe the functions performed by the individual subsystems of a DSCC. This material has been adapted from Asmar & Herrera (1993) and [JPLD-14027]; for additional information, consult [DSN810-5] [12]. Each DSCC includes a set of antennas, a Signal Processing Center (SPC), and communication links to the Jet Propulsion Laboratory (JPL). The general configuration is illustrated in Figure 4.6-4; antennas (Deep Space Stations, or DSS -- a term carried over from earlier times when antennas were individually instrumented) are also listed in the figure.

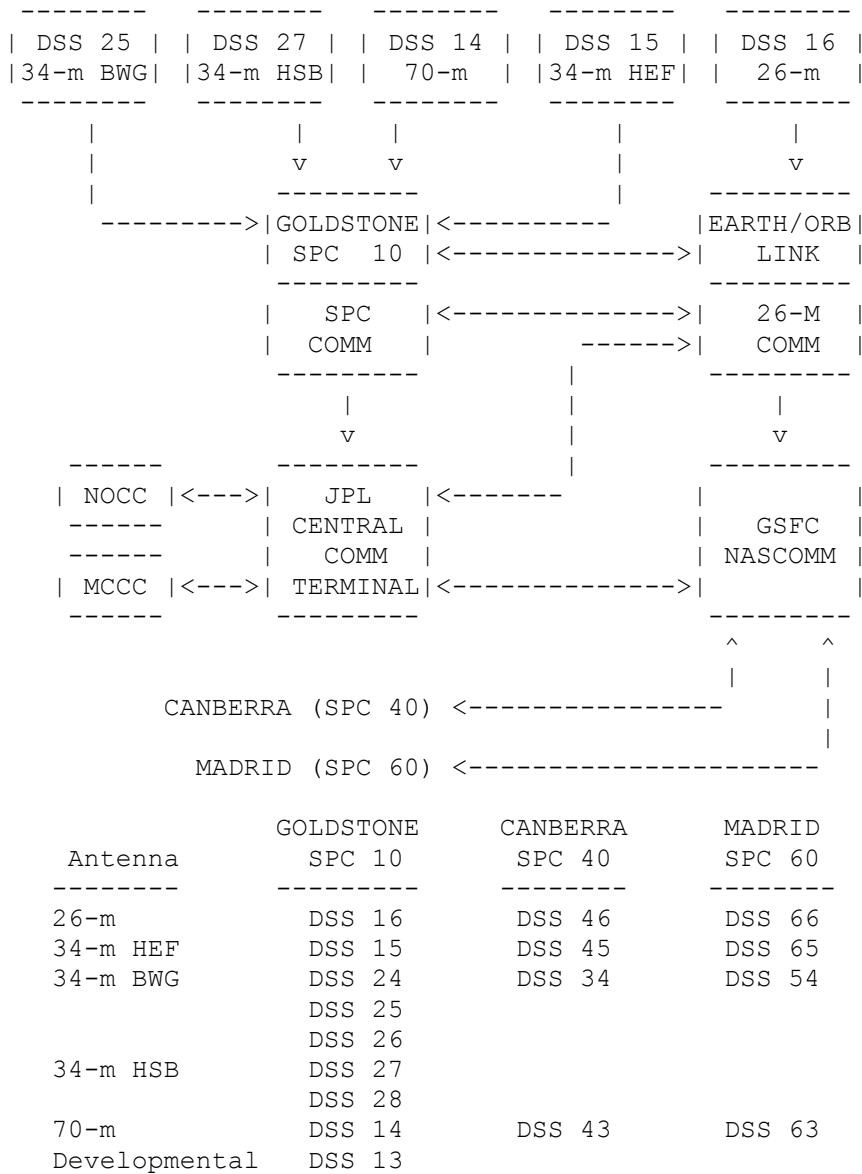


Figure 4.6-4: DSN Network

Subsystem interconnections at each DSCC are shown in figure Figure 4.6-5, and they are described in the sections that follow. The Monitor and Control Subsystem is connected to all other subsystems; the Test Support Subsystem can be.

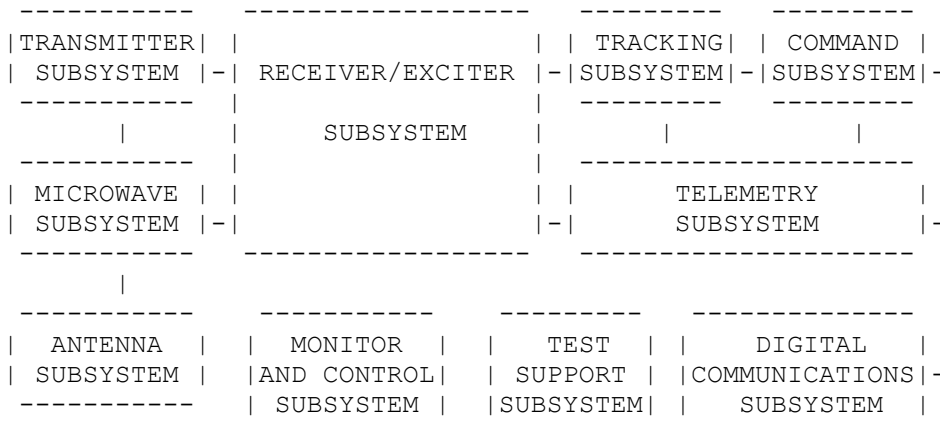


Figure 4.6-5: DSN subsystem schematics

**4.6.2.2.1 DSCC Monitor and Control Subsystem**

The DSCC Monitor and Control Subsystem (DMC) is part of the Monitor and Control System (MON) which also includes the ground communications Central Communications Terminal and the Network Operations Control Center (NOCC) Monitor and Control Subsystem. The DMC is the center of activity at a DSCC. The DMC receives and archives most of the information from the NOCC needed by the various DSCC subsystems during their operation. Control of most of the DSCC subsystems, as well as the handling and displaying of any responses to control directives and configuration and status information received from each of the subsystems, is done through the DMC. The effect of this is to centralize the control, display, and archiving functions necessary to operate a DSCC. Communication among the various subsystems is done using a Local Area Network (LAN) hooked up to each subsystem via a network interface unit (NIU).

DMC operations are divided into two separate areas: the Complex Monitor and Control (CMC) and the Link Monitor and Control (LMC). The primary purpose of the CMC processor for Radio Science support is to receive and store all predict sets transmitted from NOCC such as Radio Science, antenna pointing, tracking, receiver, and uplink predict sets and then, at a later time, to distribute them to the appropriate subsystems via the LAN. Those predict sets can be stored in the CMC for a maximum of three days under normal conditions. The CMC also receives, processes, and displays event/alarm messages; maintains an operator log; and produces tape labels for the DSP. Assignment and configuration of the LMCs is done through the CMC; to a limited degree the CMC can perform some of the functions performed by the LMC. There are two CMCs (one on-line and one backup) and three LMCs at each DSCC. The backup CMC can function as an additional LMC if necessary.

The LMC processor provides the operator interface for monitor and control of a link -- a group of equipment required to support a spacecraft pass. For Radio Science, a link might include the DSCC Spectrum Processing Subsystem (DSP) (which, in turn, can control the SSI), or the Tracking Subsystem. The LMC also maintains an operator log which includes operator directives and subsystem responses. One important Radio Science specific function that the LMC performs is receipt and transmission of the system temperature and signal level data from the

PPM for display at the LMC console and for inclusion in Monitor blocks. These blocks are recorded on magnetic tape as well as appearing in the Mission Control and Computing Center (MCCC) displays. The LMC is required to operate without interruption for the duration of the Radio Science data acquisition period.

The Area Routing Assembly (ARA), which is part of the Digital Communications Subsystem, controls all data communication between the stations and JPL. The ARA receives all required data and status messages from the LMC/CMC and can record them to tape as well as transmit them to JPL via data lines. The ARA also receives predicts and other data from JPL and passes them on to the CMC.

#### 4.6.2.2.2 DSCC Open-Loop Receiver (RIV)

The open loop receiver block diagram shown in Figure 4.6-6 is for the RIV system at 70-m and 34-m HEF and BWG antenna sites. Input signals at both S- and X-band are mixed to approximately 300 MHz by fixed-frequency local oscillators near the antenna feed. Based on a tuning prediction file, the POCA controls the DANA synthesizer, the output of which (after multiplication) mixes the 300 MHz IF to 50 MHz for amplification. These signals in turn are down converted and passed through additional filters until they yield output with bandwidths up to 45 kHz. The Output is digitally sampled and either written to magnetic tape or electronically transferred for further analysis.

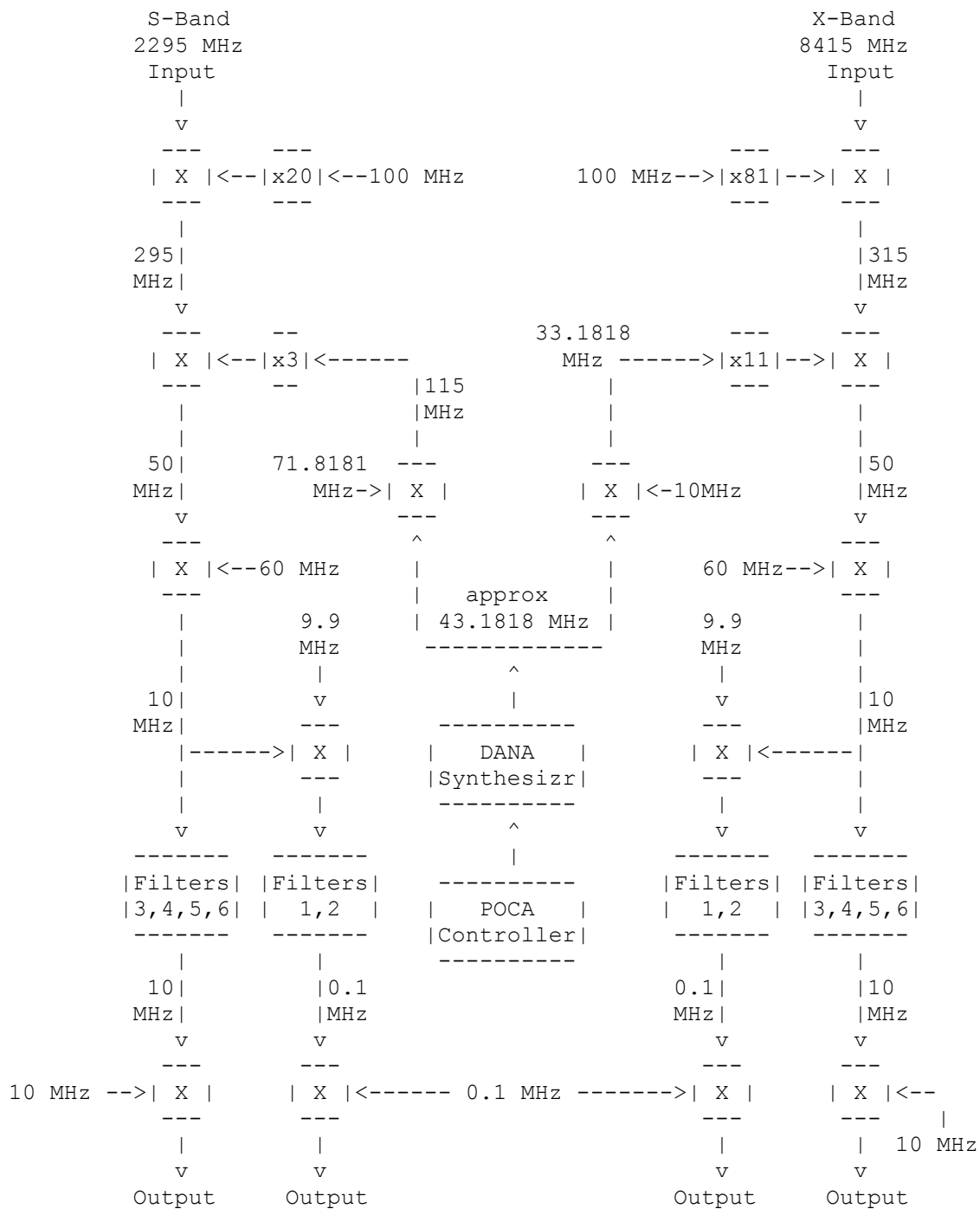


Figure 4.6-6: DSN open loop receiver block diagram

Reconstruction of the antenna frequency from the frequency of the signal in the recorded data can be achieved through use of one of the following formulas. Filters are defined below.

$$\begin{aligned}
 FS_{\text{ant}} &= 3 * SYN + 1.95 * 10^9 + 3 * (790/11) * 10^6 + F_{\text{rec}} && \text{(Filter 4)} \\
 &= 3 * SYN + 1.95 * 10^9 + 3 * (790/11) * 10^6 - F_{\text{samp}} + F_{\text{rec}} && \text{(Filters 1-3,5,6)}
 \end{aligned}$$

$$\begin{aligned}
 FX_{\text{ant}} &= 11 * SYN + 7.940 * 10^9 + F_{\text{samp}} - F_{\text{rec}} && \text{(Filter 4)} \\
 &= 11 * SYN + 7.940 * 10^9 - 3 * F_{\text{samp}} + F_{\text{rec}} && \text{(Filters 1,2,3,6)}
 \end{aligned}$$

where  $F_{S_{\text{ant}}}$ ,  $F_{X_{\text{ant}}}$  are the antenna frequencies of the incoming signals at S and X bands, respectively, SYN is the output frequency of the DANA synthesizer, commonly labeled the readback POCA frequency on data tapes,  $F_{\text{samp}}$  is the effective sampling rate of the digital samples, and  $F_{\text{rec}}$  is the apparent signal frequency in a spectrum reconstructed from the digital samples.

NB: For many of the filter choices (see below) the Output is that of a bandpass filter. The sampling rates in the table below are sufficient for the bandwidth but not the absolute maximum frequency, and aliasing results. The reconstruction expressions above are appropriate ONLY when the sample rate shown in the tables below is used.

#### 4.6.2.3 Operational Modes - DSN

- DSCC Antenna Mechanical Subsystem

Pointing of DSCC antennas may be carried out in several ways. For details see the subsection 'DSCC Antenna Mechanical Subsystem' in the 'Subsystem' section. Binary pointing is the preferred mode for tracking spacecraft; pointing predicts are provided, and the antenna simply follows those. With CONSCAN, the antenna scans conically about the optimum pointing direction, using closed-loop receiver signal strength estimates as feedback. In planetary mode, the system interpolates from three (slowly changing) RA-DEC target coordinates; this is 'blind' pointing since there is no feedback from a detected signal. In sidereal mode, the antenna tracks a fixed point on the celestial sphere. In 'precision' mode, the antenna pointing is adjusted using an optical feedback system. It is possible on most antennas to freeze z-axis motion of the subreflector to minimize phase changes in the received signal.

- DSCC Receiver-Exciter Subsystem

The diplexer in the signal path between the transmitter and the feed horns on all antennas may be configured so that it is out of the received signal path in order to improve the signal-to-noise ratio in the receiver system. This is known as the 'listen-only' or 'bypass' mode.

- **Closed-Loop vs. Open-Loop Reception**

Radio Science data can be collected in two modes: closed-loop, in which a phase-locked loop receiver tracks the spacecraft signal, or open-loop, in which a receiver samples and records a band within which the desired signal presumably resides. Closed-loop data are collected using Closed-Loop Receivers, and open-loop data are collected using Open-Loop Receivers in conjunction with the DSCC Spectrum Processing Subsystem (DSP). See the Subsystems section for further information.
- **Closed-Loop Receiver AGC Loop**

The closed-loop receiver AGC loop can be configured to one of three settings: narrow, medium, or wide. Ordinarily it is configured so that expected signal amplitude changes are accommodated with minimum distortion. The loop bandwidth is ordinarily configured so that expected phase changes can be accommodated while maintaining the best possible loop SNR.
- **Coherent vs. Non-Coherent Operation**

The frequency of the signal transmitted from the spacecraft can generally be controlled in two ways -- by locking to a signal received from a ground station or by locking to an on-board oscillator. These are known as the coherent (or 'two-way') and non-coherent ('one-way') modes, respectively. Mode selection is made at the spacecraft, based on commands received from the ground. When operating in the coherent mode, the transponder carrier frequency is derived from the received uplink carrier frequency with a 'turn-around ratio' typically of 240/221. In the non-coherent mode, the downlink carrier frequency is derived from the spacecraft on-board crystal-controlled oscillator. Either closed-loop or open-loop receivers (or both) can be used with either spacecraft frequency reference mode. Closed-loop reception in two-way mode is usually preferred for routine tracking. Occasionally the spacecraft operates coherently while two ground stations receive the 'downlink' signal; this is sometimes known as the 'three-way' mode.
- **DSCC Spectrum Processing Subsystem (DSP)**

The DSP can operate in four sampling modes with from 1 to 4 input signals. Input channels are assigned to ADC inputs during DSP configuration. Modes and sampling rates are summarized in the tables below:

Mode	Analog-to-Digital Operation
1	4 signals, each sampled by a single ADC
2	1 signal, sampled sequentially by 4 ADCs
3	2 signals, each sampled sequentially by 2 ADCs
4	2 signals, the first sampled by ADC #1 and the second sampled sequentially at 3 times the rate by ADCs #2-4

Table 4.6-5: DSN operational modes

8-bit Samples Sampling Rates (samples/sec per ADC)	12-bit Samples Sampling Rates (samples/sec per ADC)
50000	
31250	
25000	
15625	
12500	
10000	10000
6250	
5000	5000
4000	
3125	
2500	
	2000
1250	
1000	1000
500	
400	
250	
200	200

Table 4.6-6: DSN sampling rates

Input to each ADC is identified in header records by a Signal Channel Number (J1 - J4). Nominal channel assignments are shown below.

Signal Channel Number	Receiver Channel
J1	X-RCP
J2	S-RCP
J3	X-LCP
J4	S-LCP

Table 4.6-7: DSN Channel assignments

**PAGE LEFT FREE**

## 5 RSI Interface with RMOC

### 5.1 Operation Procedure Request

Radio Science Operations are requested by Operation Requests in a Syntax compatible with the Rosetta EPS. The syntax is specified in SOP-RSSD-SP-002 [3]. A detailed description of parameters will be given in the next issue of this manual. In the current baseline RSI OPRs are pre-processed by the Rosetta SOWT in ESTEC and forwarded to ESOC. Examples for OPRs can be extracted from the pointing requests given in section 4.3.

#### 5.1.1 EPS syntax

##### 5.1.1.1 Request handling

The experiment planning system EPS uses a CONFIGURATION FILE (\*.cfg) to determine how to handle operations requests. In the configuration file, the parameters CHECK\_GLOBAL\_<variable> usually do not need to be changed. Desired output files like errors, conflicts, power are given. Names of variables are generally self-explanatory. The most important output file options are MODULE\_STATES, which gives an ASCII configuration table of RSI modes almost identical to flight operations procedure tables. The option CONFLICTS must be included to identify possible misconfigurations of the telemetry system. If given, EPS will write all conflicts defined in the CONSTRAINTS section of the EDF to a file.

```
# Filename: rsi.cfg
#
# Author: Axel Hagermann
# Date: 28 August 2002
#
# (c) ESA/Estec
#
# Description: This is an EPS configuration file for RSI.
#
# $Id: config.example,v 1.2 2002/02/28 17:28:02 rosetta Exp $
#
# $Log: config.example,v $
# Revision 1.0 2002/08/28 rsi
# Initial revision
#
#
#Command_line: "-t 10 -s 120 -d 0"
#
```

Setting: CHECK\_GLOBAL\_ACTION FALSE  
Setting: CHECK\_GLOBAL\_PARAM FALSE  
Setting: CHECK\_GLOBAL\_UNIT FALSE

#

Output\_files: POWER\_AVG POWER\_PEAK POWER\_LOW MODULE\_STATES  
MS\_CHANGES\  
ACTIONS TIMELINE CONFLICTS

#

### 5.1.1.2 Definition of request formats

Operations request formats are defined in an experiment definition file (rsi.edf). Configurations of the experiment are defined as MODULES with various STATES (i.e. module USO\_state can have the states MUTE and ACTIVE. Module states are changed by pre-defined ACTIONS (e.g. the action USO\_UP powers the USO on. ACTIONS can also be used to set PARAMETERS (e.g. the parameter UL (=uplink) can have the values <X>, <S> and <\_> for X-band, S-band and no request respectively. A MODE comprises several module states. For example, the mode ONEWAY contains all individual module settings for a one-way radio link. Therefore, changing an instrument mode by an action will result in changing all module states defined in the mode. CONSTRAINTS can be inserted e.g. to prevent conflicts between modules states. In the case of RSI e.g., the use of IFMS A is heavily constrained. EDF- and ITL-files for RSI and MaRS are identical with the following exceptions:

- The 'Experiment name' variable is RSI or MRS respectively
- For MaRS, USO configuration is not possible, therefore USO-related items have no effect on the experiment

In the EDF as well as in the ITL, predefined experiment modes can be selected (cf. the following file). These modes can be selected in the ITL, but alternatively all settings can be made in 'DEFAULT' configuration (recommended).

In general, all entries in the EDF file are self-explanatory. Comments are marked by a hash <#> sign.

The RSI experiment definition file v.09. is quoted below for reference.

```
#  
# Filename: rsi.edf  
# Change record: #####  
# Author: Axel Hagermann  
# version 0.9  
# Date: 28-Aug-2002  
# Changes: Sampling rate definitions made, templates deleted,  
#  
# added a few more comments  
#  
#  
# based on experiment.template  
# Authors: Axel Hagermann & Raymond Hoofs  
# Date: 28-Jun-2002
```

```
#
# Authors: Peter van der Plas & Raymond Hoofs
# Date: 5 October 1999
#
# (c) ESA/Estec
#
# $Id: experiment.template,v 1.15 2002/02/22 14:21:06 rosetta Exp $
#
# <Experiments start here...>
#
Nr_of_experiments: 1
#
Experiment: RSI "Rosetta Radio Science Investigations"
#
# <Global properties start here...>
#
Global_actions: TM_bitrate \
                COHERENCY_ON COHERENCY_OFF \
                SC_LINK \
                USO_ACT USO_MUTE USO_UP \
                TM_ON TM_OFF \
                IFMS_A_Configure IFMS_B_Configure IFMS_RS_Configure \
                TRACKMODE \
                WAIT
Global_constraints: CHECK_TM_ON CHECK_IFMS_A_ACTION \
                  CHECK_TCXO
#
#
# <Modules start here...>
### Module definitions on S/C side #####
#
Module: Coherency "Up/downlink coherency definition"
Module_level: LEVEL1
Sub_modules:
Nr_of_module_states: 2
    Module_state: TWO_ "TWOx Configuration, i.e. coherency on"
    Module_state: ONE_ "ONEx Configuration, i.e. coherency off"
#
Module: SC_TRSP "S/C transponder downlink definition"
Module_level: LEVEL1
Sub_modules:
Nr_of_module_states: 3
    Module_state: S_x "X-Band D/L (default)"
    MS_power: 0 [Watts]
    Module_state: S_s "S-Band D/L"
    MS_power: 25 [Watts]
    Module_state: D_xs "Dual D/L"
    MS_power: 25 [Watts]
```

#

Module: USO\_pwr "USO Power"  
Module\_level: LEVEL1  
Sub\_modules:  
Nr\_of\_module\_states: 3  
    Module\_state: ON "On"  
    MS\_power: 3 [Watts]  
    Module\_state: OFF "Off"  
    MS\_power: 0 [Watts]  
    Module\_state: HEAT "Heating"  
    MS\_power: 7.5 [Watts]

#

Module: USO\_state "USO State"  
Module\_level: LEVEL1  
Sub\_modules:  
Nr\_of\_module\_states: 2  
    Module\_state: MUTE "Mute"  
    Module\_state: ACTIVE "Active"

#

Module: TCXO\_state "TCXO State"  
Module\_level: LEVEL1  
Sub\_modules:  
Nr\_of\_module\_states: 2  
    Module\_state: MUTE "Mute"  
    Module\_state: ACTIVE "Active"

#

Module: TM\_modulation "Telemetry modulation"  
Module\_level: LEVEL1  
Sub\_modules:  
Nr\_of\_module\_states: 2  
    Module\_state: ON "TM On"  
    Module\_state: OFF "TM Off"

#

Module: TM\_fsc "Telemetry subcarrier"  
Module\_level: LEVEL1  
Sub\_modules:  
Nr\_of\_module\_states: 2  
    Module\_state: 262 "262144 Hz subcarrier"  
    Module\_state: 8 "8192 Hz subcarrier"

#

Module: TM\_N "Subcarrier/Trans. symbol rate ratio"  
Module\_level: LEVEL1  
Sub\_modules:  
Nr\_of\_module\_states: 6  
    Module\_state: 5 "N=5"  
    Module\_state: 6 "N=6"  
    Module\_state: 8 "N=8"  
    Module\_state: 10 "N=10"  
    Module\_state: 12 "N=12"

Module\_state: 16 "N=16"

#etc...

### Module definition G/S side #####

Module: IFMS\_A\_UL "IFMS A Uplink"

Module\_level: LEVEL1

Sub\_modules:

Nr\_of\_module\_states: 3

Module\_state: X "X-Band uplink"

Module\_state: S "S-Band uplink"

Module\_state: \_ "No request"

#

Module: IFMS\_A\_DL "IFMS A Downlink"

Module\_level: LEVEL1

Sub\_modules:

Nr\_of\_module\_states: 5

Module\_state: X\_CL "X-Band closed-loop"

Module\_state: S\_CL "S-Band closed-loop"

Module\_state: X\_OL "X-Band open-loop"

Module\_state: S\_OL "S-Band open-loop"

Module\_state: \_ "No request"

#

Module: IFMS\_B\_UL "IFMS B Uplink"

Module\_level: LEVEL1

Sub\_modules:

Nr\_of\_module\_states: 3

Module\_state: X "X-Band uplink"

Module\_state: S "S-Band uplink"

Module\_state: \_ "No request"

#

Module: IFMS\_B\_DL "IFMS B Downlink"

Module\_level: LEVEL1

Sub\_modules:

Nr\_of\_module\_states: 5

Module\_state: X\_CL "X-Band closed-loop"

Module\_state: S\_CL "S-Band closed-loop"

Module\_state: X\_OL "X-Band open-loop"

Module\_state: S\_OL "S-Band open-loop"

Module\_state: \_ "No request"

#

Module: IFMS\_RS\_DL "IFMS RS Downlink"

Module\_level: LEVEL1

Sub\_modules:

Nr\_of\_module\_states: 5

Module\_state: X\_CL "X-Band closed-loop"

Module\_state: S\_CL "S-Band closed-loop"

Module\_state: X\_OL "X-Band open-loop"

Module\_state: S\_OL "S-Band open-loop"

Module\_state: \_ "No request"

#

Module: TRACKMODE "Tracking mode"

Module\_level: LEVEL1

Sub\_modules:

Nr\_of\_module\_states: 3

Module\_state: DOPPLER "Doppler only"

Module\_state: DOP\_RNG "Simultaneous Doppler and Range"

Module\_state: RANGE "Ranging only"

# Set sampling rate for IFMS #####

Module: SAMPLING\_OL "IFMS sampling rate open-loop (1/sec)"

Module\_level: LEVEL2

Sub\_modules:

Nr\_of\_module\_states: 6

Module\_state: 1000 "from here, Open-loop only"

Module\_state: 2000

Module\_state: 5000

Module\_state: 10000

Module\_state: 20000

Module\_state: 50000

Module: SAMPLING\_B "IFMS sampling rate closed-loop (1/sec)"

Module\_level: LEVEL2

Sub\_modules:

Nr\_of\_module\_states: 3

Module\_state: 1 "1 sample/sec"

Module\_state: 10

Module\_state: 100

# <Modes start here...>

#

#Nr\_of\_modes: <p>

Mode: MODE "Dummy mode"

Mode: DEFAULT "Dummy mode"

Mode: STDCONF "Standard configuration"

Module\_states: \

Coherency TWO\_ \

SC\_TRSP S\_x \

USO\_state MUTE \

TCXO\_state ACTIVE \

TM\_modulation ON \

IFMS\_A\_UL X \

IFMS\_A\_DL X\_CL \

IFMS\_B\_UL \_ \

IFMS\_B\_DL \_ \

IFMS\_RS\_DL \_

Mode: ONEWAY "Standard ONES configuration"

Module\_states: \

Coherency ONE\_ \  
USO\_state ACTIVE \  
TCXO\_state MUTE \  
TM\_modulation ON \  
IFMS\_A\_UL X \  
IFMS\_A\_DL X\_CL \  
IFMS\_B\_UL \_ \  
IFMS\_B\_DL \_ \  
IFMS\_RS\_DL \_

Mode: TWOWAY "Standard TWOS configuration"

Module\_states: \  
Coherency TWO\_ \  
TM\_modulation ON \  
IFMS\_A\_UL X \  
IFMS\_A\_DL X\_CL \  
IFMS\_B\_UL \_ \  
IFMS\_B\_DL \_ \  
IFMS\_RS\_DL \_

#####

# <Parameters start here...>

#

#Nr\_of\_parameters: <q>  
Parameter: FSCFREQ "Subcarrier frequency"  
Raw\_type: INT  
Parameter\_value: 262  
Parameter\_update: MSP 262  
Parameter\_value: 8  
Parameter\_update: MSP 8

#

Parameter: UL "Uplink"  
Eng\_type: TEXT  
Default\_value: \_  
Parameter\_value: \_  
Parameter\_update: MSP \_  
Parameter\_value: X  
Parameter\_update: MSP X  
Parameter\_value: S  
Parameter\_update: MSP S

#

Parameter: DL "Downlink"  
Eng\_type: TEXT  
Default\_value: \_  
Parameter\_value: \_  
Parameter\_update: MSP \_  
Parameter\_value: X\_CL  
Parameter\_update: MSP X\_CL

Parameter\_value: S\_CL  
Parameter\_update: MSP S\_CL  
Parameter\_value: X\_OL  
Parameter\_update: MSP X\_OL  
Parameter\_value: S\_OL  
Parameter\_update: MSP S\_OL

#

Parameter: SCLINK "S/C Transponder D/L mode"

Eng\_type: TEXT  
Default\_value: S\_x  
Parameter\_value: S\_x  
Parameter\_update: MSP S\_x  
Parameter\_value: S\_s  
Parameter\_update: MSP S\_s  
Parameter\_value: D\_xs  
Parameter\_update: MSP D\_xs

#

Parameter: TRKMOD

Eng\_type: TEXT  
Default\_value: DOPPLER  
Parameter\_value: DOPPLER  
Parameter\_update: MSP DOPPLER  
Parameter\_value: DOP\_RNG  
Parameter\_update: MSP DOP\_RNG  
Parameter\_value: RANGE  
Parameter\_update: MSP RANGE

Parameter: NRATIO "Symbol rate ratio"

Raw\_type: INT

Parameter: WAITTIME "Wait duration parameter"

Eng\_type: REAL  
Default\_value: 1.0 [secs]  
Unit: secs  
Eng\_limits: 1.0 3600.0 [secs]  
Resource: DURATION

Parameter: SAMPRATE "Sampling rate"

Raw\_type: INT

#

#

#####

###

# <Actions start here...>

### Action definitions #####

# USO-related

#

Action: USO\_UP "Bring the USO up: Heat for 20 min, then goto standby"

Action\_level: LEVEL1

Duration: 20 [minutes]  
Run\_type: RELATIVE  
Run\_actions: 00:00:00 uso\_heat \  
00:20:00 uso\_on

#

Action: uso\_heat "Heat the USO"  
Action\_level: LEVEL2  
Update\_when\_ready: MS USO\_pwr HEAT

#

Action: uso\_on "USO is up"  
Action\_level: LEVEL2  
Update\_when\_ready: MS USO\_pwr ON

#

Action: USO\_OFF "Power the USO off"  
Action\_level: LEVEL1  
Update\_when\_ready: MS USO\_pwr OFF  
Action\_constraints: CHECK\_TCXO

#

Action: USO\_ACT "Switch USO to ACTIVE mode"  
Action\_level: LEVEL1  
Update\_when\_ready: \  
MS USO\_state ACTIVE \  
MS TCXO\_state MUTE  
Action\_constraints: CHECK\_TM\_ON

#

Action: USO\_MUTE "Mute USO, unmute TCXO"  
Action\_level: LEVEL1  
Update\_when\_ready: \  
MS TCXO\_state ACTIVE \  
MS USO\_state MUTE  
Action\_constraints: CHECK\_TM\_ON

#

Action: COHERENCY\_ON "Go to Two-way mode"  
Action\_level: LEVEL1  
Update\_when\_ready: \  
MS Coherency TWO\_

#

Action: COHERENCY\_OFF "Go to One-way mode"  
Action\_level: LEVEL1  
Update\_when\_ready: \  
MS Coherency ONE\_

Action: SC\_LINK "S/C Transponder D/L mode"  
Action\_level: LEVEL1  
Action\_parameters: SCLINK  
Update\_when\_ready: \  
MSP SC\_TRSP SCLINK

#

# Telemetry related #####

#

Action: TM\_OFF "Switch telemetry modulation OFF"

Action\_level: LEVEL1

Update\_when\_ready: MS TM\_modulation OFF

#

Action: TM\_ON "Switch telemetry modulation ON"

Action\_level: LEVEL2

Update\_when\_ready: MS TM\_modulation ON

#

Action: TM\_Bitrate "Select Telemetry subcarrier &amp; bitrate ratio"

Action\_level: LEVEL2

Action\_parameters: FSCFREQ NRATIO

Update\_when\_ready: \

MSP TM\_fsc FSCFREQ \

MSP TM\_N NRATIO

#

Action: IFMS\_A\_Configure "Configure IFMS A"

Action\_level: LEVEL1

Action\_parameters: UL DL

Duration: 1 # "Duration is a dummy, but needed to raise the error flag"

Update\_when\_ready: \

MSP IFMS\_A\_UL UL \

MSP IFMS\_A\_DL DL

#

Action\_constraints: CHECK\_IFMS\_A\_ACTION

#

Action: IFMS\_B\_Configure "Configure IFMS B"

Action\_level: LEVEL1

Action\_parameters: UL DL

Update\_when\_ready: \

MSP IFMS\_B\_UL UL \

MSP IFMS\_B\_DL DL

#

Action: IFMS\_RS\_Configure "Configure Radio Science IFMS"

Action\_level: LEVEL1

Action\_parameters: DL

Update\_when\_ready: \

MSP IFMS\_RS\_DL DL

#

Action: WAIT "Wait a while"

Action\_level: LEVEL2

Action\_parameters: WAITTIME

#

Action: TRACKMODE "Set tracking mode (Doppler/Range)"

Action\_level: LEVEL1

Action\_parameters: TRKMOD

Update\_when\_ready: \

```
MSP TRACKMODE TRKMOD
#
Action: SET_SAMPLING_OL "Set sampling rate for open-loop recording"
Action_level: LEVEL1
Action_parameters: SAMPRATE
Update_when_ready: \
MSP SAMPLING_OL SAMPRATE
#
Action: SET_SAMPLING_CL "Set sampling rate for closed-loop recording"
Action_level: LEVEL1
Action_parameters: SAMPRATE
Update_when_ready: \
MSP SAMPLING_CL SAMPRATE
#
#####
# <Constraints start here...>

Constraint: CHECK_TM_ON "Warn when telemetry is OFF"
Constraint_type: TIME
Severity: WARNING
Condition: MS NOT TM_modulation ON
#
Constraint: CHECK_IFMS_A_ACTION "WATCH OUT! RSI IS TRYING TO MESS
WITH IFMS A!"
Constraint_type: TIME
Severity: WARNING
Condition: ACTION IS IFMS_A_Configure
#
Constraint: CHECK_TCXO "TCXO is inactive"
Constraint_type: TIME
Severity: ERROR
Condition: MS NOT TCXO_state ACTIVE
#
# Additional Check for IFMS A, can be called anytime
# Constraint: CHECK_IFMS_A_CONFIG "Is IFMS A in standard configuration?"
# Constraint_type:
# Severity: INFO
# Condition: MS NOT IFMS_A_DL X_CL
#AND (MS IS IFMS_A_UL X OR MS IS IFMS_A_UL _)
```

NB: Care must be taken to escape line-breaks within a single syntactic option with a backslash <\>

### 5.1.1.3 Issuing of requests

The actual operations request is performed in the instrument-timeline file (rsi.itl). Here the actions defined in the EDF are called. Subsequently module states are changed

as defined in the EDF. In the first lines, it must include a start and stop time and the initial module states. The actual requests are then entered in the syntax:

```
<timetag> <experiment> <action>
```

where <timetag> can be any epoch as specified in the EPS user manual. For valid epoch identifiers, see also the rosetta event definition file issued with the respective EPS release. For most operations requests, the experiment name is „RSI“. For pointing requests, „PTR“ is used as experiment identifier. <action> is the action defined in the EDF to be executed. Note that ACTION PARAMETERS are included in brackets. An example of an ITL:

```
#  
# Filename: input.example  
#  
# Author: Peter van der Plas  
# Date: 10 January 2000  
#  
# (c) ESA/Estec  
#  
# Description: This is an example input timeline file.  
#  
# $Id: input.example,v 1.7 2002/02/22 14:23:42 rosetta Exp $  
#  
# $Log: input.example,v $  
# Revision 1.7 2002/02/22 14:23:42 rosetta  
# SEPARATION parameter has relative time value.  
#  
# Revision 1.6 2002/02/19 16:13:41 rosetta  
# Added step numbers and source file info message.  
#  
# Revision 1.5 2001/07/11 13:00:21 rosetta  
# Updated to be compatible with the CRID issue B1.  
# New implementation of parameters, also on events.  
# New timing functionality and include file layout.  
# PTR information can now be embedded in the ITL.  
#  
# Revision 1.4 2000/10/31 17:20:35 rosetta  
# Removed all simulator state references.  
# Added the Start_timeline and Stop_timeline keywords.  
# Added the Event_time keyword.  
# Updated the use of arguments.  
# Direct DEFAULT updates are allowed now.  
# Include files can now be scheduled on events.  
#  
# Revision 1.3 2000/03/13 19:33:25 rosetta  
# Changed implementation of modules  
# Added module power and data rate  
# Added module level and sub-modules  
# Changed action type to action level  
# Various minor changes and document updates
```

```

#
# Revision 1.2 2000/02/21 16:51:54 rosetta
# Added use of include files and delta time values.
# More detailed description of arguments, labels and values.
#
# Revision 1.1 2000/01/10 12:30:17 rosetta
# Initial revision
#
#
Version: 00001
#
Ref_date: 21-February-2011
#
Start_time: 00:00:00
End_time: 02:00:00
#
Init_MODE: RSI DEFAULT
#
Init_MS: RSI USO_pwr OFF
#Init_MS: RSI TM_N 10
Init_MS: RSI Coherency TWO_
Init_MS: RSI SC_TRSP S_x
Init_MS: RSI USO_state MUTE
Init_MS: RSI TCXO_state ACTIVE
Init_MS: RSI TM_modulation ON
Init_MS: RSI IFMS_A_UL X
Init_MS: RSI IFMS_A_DL X_CL
Init_MS: RSI IFMS_B_UL _
Init_MS: RSI IFMS_B_DL _
Init_MS: RSI IFMS_RS_DL _

#
#000_00:10:00 RSI DEFAULT TM_bitrate ( \
# FSCFREQ = 8 \
# NRATIO = 6 )

#000_00:00:00 RSI DEFAULT
000_00:20:00 RSI DEFAULT USO_UP
000_00:30:00 RSI DEFAULT COHERENCY_OFF
000_00:35:00 RSI DEFAULT TM_OFF
000_00:50:00 RSI DEFAULT IFMS_B_Configure (UL=X DL=X_CL )
000_01:00:00 RSI DEFAULT USO_ACT
000_01:05:00 RSI DEFAULT USO_MUTE
000_01:10:00 RSI DEFAULT COHERENCY_OFF
000_01:15:00 RSI DEFAULT SC_LINK (SCLINK = D_xs)
000_01:20:00 RSI DEFAULT IFMS_A_Configure (UL=S DL=S_CL)
000_01:30:00 RSI DEFAULT TRACKMODE
(TRKMOD=DOP_RNG)
000_01:40:00 PTR NADIR ( OBJECT_TO_BE_POINTED = HGA \

```

OBJECT = EARTH )

## 5.2 Data retrieval

IFMS and auxiliary data will be made available on the DDS at ESOC as soon as feasible after the tracking pass depending on the data transfer time from Perth to ESOC.

## 5.3 Interface JPL/RSI

Radio science data observed and recorded at the DSN ground stations will be collected by the Multimission Radio Science Group at JPL and distributed to Cologne for further processing.

The digital samples from each RSR sub-channel are stored to disk in one second records in real time. In near real time the one second records are partitioned and formatted into a sequence of data units which are transmitted to JPL's Advanced Multi-Mission Operations System (AMMOS). The number of data units per one second data record depends on the bandwidth and sample size of the recorded data. Table 3-1 contains a list of valid configurations.

ROSETTA RSI: **Rosetta Radio Science Investigations**  
**Experiment User Manual**

Document **RO-RSI-IGM-MA-3081**

Issue: 4

Revision: 2

Date: 25.04.2016

Page: 95 of 144

---

PAGE LEFT FREE

## 6 Detailed Descriptions of Operational Procedures

### 6.1 Overview

activity name	description
PCx	Passive Checkout Number x
CMD	Center of Mass Determination
OCP	Occultation Operations Procedure
BRP	Bistatic Radar Procedure
SCP	Solar Conjunction Procedure
AST	Asteroid Flyby Procedure
GMC	Gravity Mapping Campaign
DOT	Doppler Tracking

## 6.2 PCx: Passive Checkout Number x

### 6.2.1 Objective

The objective of the PCx is the verification that the on-board USO is operating nominally. The ageing of the USO and its drift has to be monitored continuously during the mission.

### 6.2.2 Operations

The Passive Checkout takes place every 6 months in order to observe the proper functioning of the USO.

#### 6.2.2.1 Configuration

Exactly the same configuration can be used for the Active Payload Checkouts!

ROSETTA			
Instrument <b>RSI</b>		Originator Name <b>Tellmann</b>	Date <b>18.01.2006</b>
Mission Phase  Cruise	Activity ID RF-FCP-030 ARFF030	Activity Name  Passive Checkout Number x	
<b>Description of activity:</b>		<b>Passive Checkout Number x</b>	
<b>Duration of activity:</b>		<b>Data Recording time: 2 hours 30 minutes + 1 hour S-Band warm up</b>	
<b>Power demand:</b>		<b>S-Band transmitter (28 W) USO Power (5.5 W)</b>	
<b>Spacecraft pointing:</b>		<b>HGA Earth pointing</b>	
<b>Comments/other constraints:</b>			
<b>S-Band reception required</b> <b>USO required</b> <b>feasible ground stations: NNO</b> <b>DSN-HEF</b> <b>DSN-70 m</b>			
<b>sample rate</b>	:	<b>IFMS closed-loop</b>	<b>1 samples/sec</b>
		<b>DSN closed-loop</b>	<b>1 samples/sec</b>

**Spacecraft configuration****ONED-USO****X-uplink N/A****X- and S-band downlink****RNG OFF****TM switch ON/OFF****IFMS DAP Settings:****Configure Downlink Chain 1 for X-band ops****Configure Downlink Chain 2 for S-band ops****IFMS-1 configured for Input 1 (X-band prime)****IFMS-2 configured for Input 1 (X-band)****IFMS-3 configured for Input 2 (S-band)****IFMS-1 DAP Settings X/down****DOP1 set for 1 samples per second, 3600 samples per file****DOP2 set for 1 samples per second, 3600 samples per file****AGC1 set for 1 samples per second, 3600 samples per file****AGC2 set for 1 samples per second, 3600 samples per file****MET set for 1 sample per 60 seconds, 100 samples per file****IFMS-2 DAP Settings X/down****DOP1 set for 1 samples per second, 3600 samples per file****DOP2 set for 1 samples per second, 3600 samples per file****AGC1 set for 1 samples per second, 3600 samples per file****AGC2 set for 1 samples per second, 3600 samples per file****MET set for 1 sample per 60 seconds, 100 samples per file****IFMS-3 DAP Settings S/down****DOP1 set for 1 samples per second, 3600 samples per file****DOP2 set for 1 samples per second, 3600 samples per file****AGC1 set for 1 samples per second, 3600 samples per file****AGC2 set for 1 samples per second, 3600 samples per file****MET set for 1 sample per 60 seconds, 100 samples per file**

<b>S/C onboard time (OBT)</b>	<b>Ground receive time (GRT)</b>	<b>Duration [h]</b>	<b>event</b>
---	--	-------------------------	--------------

Assumption is that spacecraft is in TWOS-X configuration with USO ON but MUTE after AOS and first check of TM

**T0 is predicted start of first data recording**

OWLT is the one-way light time

Assumption is that commands are preprogrammed and executed automatically on board

T0 - OWLT - 01:00			command S-band transmitter POWER ON
T0 - OWLT - 00:02			Command USO ACTIVE
T0 - OWLT - 00:01			Command S-band D/L ON Command Cohereny OFF Command Ranging OFF
	T0 - 00:01		AOS of X-band and S-band non-coherent D/L
	T0	01:00	Start of Radio Science activities: Configuration: ONED-USO, TM ON, RNG OFF Start recordings: IFMS: DOP1,2; AGC 1,2; MET
T0 - OWLT + 01:00		00:30	Command TM OFF
T0 - OWLT + 01:30		01:00	Command TM ON
T0- OWLT+ 02:30			Stop all recordings
T0 - OWLT + 02:30			Command S-band transmitter OFF Command USO MUTE Command Coherency ON
Accepted:	PI	RSI Project	ESOC

**Configuration Control**

Issue	Rev.	Date	Changes	Author
1	0	19.01.2006	All	ST

## 6.3 CMD: Center of Mass Determination

### 6.3.1 Objective

The objective of the CMD is the precise determination of the center of mass of the S/C. The center of mass is needed in order to calculate the phase center offset of the HGA which needs to be accounted for during Doppler measurements. As the center of mass of the S/C varies during the mission (e.g. due to the consumption of propellant), the operations should be repeated.

### 6.3.2 Operations

The Center of Mass Determination will be performed once during the Commissioning Phase and may be performed again during cruise before the asteroid flybys and before starting routine operations at the comet.

#### 6.3.2.1 Configuration

ROSETTA

Instrument <b>RSI</b>		Originator Name <b>Tellmann</b>	Date <b>20.01.2006</b>
Mission Phase Asteroid flyby Routine	Activity ID RF-FCP-020 ARFF020	Activity Name Center of Mass Determination: CMD	
<b>Description of activity:</b>		<b>Center of Mass Determination CMD</b>	
<b>Duration of activity:</b>		<b>Data Recording time: flexible + 1 hour S-Band warm up</b>	
<b>Power demand:</b>		<b>S-Band transmitter (28 W)</b>	
<b>Spacecraft pointing:</b>		<b>HGA Earth pointing</b>	

**Comments/other constrains:****S-Band reception required**

feasible ground stations: NNO  
 DSN-HEF  
 DSN-70 m

sample rate	:	IFMS closed-loop	1 samples/sec
		DSN closed-loop	1 samples/sec

**Spacecraft configuration**

TWOD-X  
 X-uplink  
 X- and S-band downlink  
 RNG ON  
 TM OFF

**IFMS DAP Settings:**

Configure Downlink Chain 1 for X-band ops  
 Configure Downlink Chain 2 for S-band ops  
 IFMS-1 configured for Input 1 (X-band prime)  
 IFMS-2 configured for Input 1 (X-band)  
 IFMS-3 configured for Input 2 (S-band)

**IFMS-1 DAP Settings X/up & X/down**

DOP1 set for 1 samples per second, 3600 samples per file  
 DOP2 set for 1 samples per second, 3600 samples per file  
 AGC1 set for 1 samples per second, 3600 samples per file  
 AGC2 set for 1 samples per second, 3600 samples per file  
 MET set for 1 sample per 60 seconds, 100 samples per file

**IFMS-2 DAP Settings X/down**

DOP1 set for 1 samples per second, 3600 samples per file  
 DOP2 set for 1 samples per second, 3600 samples per file  
 AGC1 set for 1 samples per second, 3600 samples per file  
 AGC2 set for 1 samples per second, 3600 samples per file  
 MET set for 1 sample per 60 seconds, 100 samples per file

**IFMS-3 DAP Settings S/down**

DOP1 set for 1 samples per second, 3600 samples per file  
 DOP2 set for 1 samples per second, 3600 samples per file  
 AGC1 set for 1 samples per second, 3600 samples per file  
 AGC2 set for 1 samples per second, 3600 samples per file  
 MET set for 1 sample per 60 seconds, 100 samples per file

Ranging Recording			
S/C onboard time (OBT)	Ground receive time (GRT)	Duration [h]	event
Assumption is that spacecraft is in TWOS-X configuration with USO ON but MUTE after AOS and first check of TM <b>T0 is predicted start of first data recording</b> <b><math>\Delta T</math> is the slew time of the S/C</b> OWLT is the one-way light time Assumption is that commands are preprogrammed and executed automatically on			
T0 - OWLT - 01:00			command S-band transmitter POWER ON
T0 - OWLT - 00:01			Command S-band D/L ON
	T0 - 00:01		AOS of X-band and S-band coherent D/L
	T0	15	Start of Radio Science activities: Configuration: TWOD-X, TM ON, RNG ON Start recordings: IFMS: DOP1,2; AGC 1,2; MET,RNG
T0- OWLT+ 00:15		$\Delta T$	Start S/C slew
T0 - OWLT + 00:15 + $\Delta T$			Stop S/C slew
T0 - OWLT + 00:15 + $\Delta T$		15	Continue Doppler and Ranging Recording
	T0 - 00:30 $\Delta T$		Stop all recordings

T0 – OWLT + 00:30 ΔT			Command S-band transmitter OFF Command TM ON
Accepted:	PI	RSI Project	ESOC

**Configuration Control**

Issue	Rev.	Date	Changes	Author
1	0	20.01.2006	All	ST

## 6.4 Doppler Tracking: DOT

### 6.4.1 Objective

#### 6.4.1.1 Cometary Orbit

Two-way coherent and simultaneous X/X and X/S radio tracking of the Rosetta orbiter during the comet orbiting phase provides essential information on the position and velocity of the cometary nucleus with respect to the Earth and hence also to the Sun. The geocentric distance of the comet is directly obtained from range measurements after removing periodic contributions due to the orbiter motion. Likewise the right ascension and declination may be deduced from the daily variations of the Doppler signal caused by the rotation of the Earth, according to the Hamilton & Melbourne (1966) algorithm. In practice, the comet position will be adjusted as part of the spacecraft orbit determination, which solves for the state vectors of both the spacecraft and the comet.

Following Thurman (1990), right ascension is typically accurate to 100 nrad for a Doppler measurement accuracy of  $10^{-4}$  m/s, while a degraded accuracy of 200-1000 nrad applies for the declination determination within a band of  $5^\circ < |\delta| < 20^\circ$ . Range measurements in contrast are accurate to about 10 m disregarding media effects, which is well below the dimension of the nucleus.

#### 6.4.1.2 Coma Mass Flux

A S/C orbiting the nucleus in the coma environment, is subject to drag forces due to the gas and dust impinging onto its surface. These forces, accumulated over the spacecraft cross sectional area exposed to the forces and over a certain time interval, are detectable in the Doppler frequency shifts of the radio signal.

Gill et al. (1996) estimated the perturbing acceleration due to gas jets to be in the range  $10^{-9}$  m/s<sup>2</sup> to  $10^{-7}$  m/s<sup>2</sup> depending on gas production (heliocentric distance) and spacecraft distance to the nucleus.

Cometary activity, i. e. the emission of gas and dust from the nucleus, usually happens when the comet is in the perihelion arc of its orbit. Water ice sublimation due to sun heating governs the material emission inside 2 – 3 AU solar distance, while other species may dominate in the distant orbit part. Recent IR and optical observations point towards the presence of some low-level activity of the coma in short-periodic comets far from the sun, so that material emission may take place even at large distances from the sun. In this case, *Rosetta* may encounter a dust / gas cloud when approaching the comet at a solar distance of  $\approx 4.8$  AU.

Due to nucleus rotation, a „diurnal“ variation of the emission may produce high activity on the dayside and low activity on the nightside of the nucleus. Maximum activity of an emission region may be shifted to post-meridional hour angles due to the temporal inertia of thermal conductivity and gas diffusion in the surface layers. This effect causes the net force of jets on the comet to deviate from the Sun-comet line, thus producing notable impact on the cometary orbital elements.

From a combined analysis of the cometary orbit and the observed jets, the net mass flux may be derived. Modelling the external drag forces acting on Rosetta allows the determination of the mass flux. Combining these derived forces with the

results of the GIADA and ROSINA experiments allows the determination of the density and velocity of gas and dust in the jets.

### 6.4.2 Operation

DOT will be performed at two frequencies when ever possible in orbit. The goal is the determination of the perturbing forces on the spacecraft by the outgassing mass flux in order to derive the gas production rate.

#### 6.4.2.1 Configuration

ROSETTA

Instrument <b>RSI</b>		Originator Name <b>Tellmann</b>	Date <b>20.01.2006</b>
Mission Phase Routine	Activity ID RF-FCP-021 ARFF021 (to be updated)	Activity Name Doppler Tracking Procedure (DOT)	
<b>Description of activity:</b>		Doppler Tracking Procedure	
<b>Duration of activity:</b>		Data Recording time: 10 hours + 1 hour S-Band warm up	
<b>Power demand:</b>		S-Band transmitter (28 W)	
<b>Spacecraft pointing:</b>		HGA Earth pointing	
<b>Comments/other constrains:</b>			
S-Band reception required feasible ground stations: NNO DSN-HEF DSN-70 m			
sample rate : IFMS 1 samples/sec DSN closed-loop 1 samples/sec			
<b>Spacecraft configuration</b>			
TWOD-X X uplink X- and S-band downlink RNG ON on X-band and S-band TM ON			

**IFMS DAP Settings:**

Configure Downlink Chain 1 for X-band ops  
 Configure Downlink Chain 2 for S-band ops  
 IFMS-1 configured for Input 1 (X-band prime)  
 IFMS-2 configured for Input 1 (X-band)  
 IFMS-3 configured for Input 2 (S-band)

**IFMS-1 DAP Settings X/down**

DOP1 set for 1 samples per second, 3600 samples per file  
 DOP2 set for 1 samples per second, 3600 samples per file  
 AGC1 set for 1 samples per second, 3600 samples per file  
 AGC2 set for 1 samples per second, 3600 samples per file  
 MET set for 1 sample per 60 seconds, 100 samples per file

**IFMS-2 DAP Settings X/down**

DOP1 set for 1 samples per second, 3600 samples per file  
 DOP2 set for 1 samples per second, 3600 samples per file  
 AGC1 set for 1 samples per second, 3600 samples per file  
 AGC2 set for 1 samples per second, 3600 samples per file  
 MET set for 1 sample per 60 seconds, 100 samples per file

**IFMS-3 DAP Settings S/down**

DOP1 set for 1 samples per second, 3600 samples per file  
 DOP2 set for 1 samples per second, 3600 samples per file  
 AGC1 set for 1 samples per second, 3600 samples per file  
 AGC2 set for 1 samples per second, 3600 samples per file  
 MET set for 1 sample per 60 seconds, 100 samples per file

**RNG Recording**

S/C onboard time (OBT)	Ground receive time (GRT)	Duration [h]	event
------------------------	---------------------------	--------------	-------

Assumption is that spacecraft is in TWOS configuration with USO ON but MUTE after AOS and first check of TM

**T0 is predicted start of first Doppler Recording**

OWLT is the one-way light time

Assumption is that commands are preprogrammed and executed automatically on board

T0 - OWLT - 01:00			command S-band transmitter POWER ON
T0 - OWLT - 00:01			command S-band d/I ON

T0 - OWLT - 00:01			Command RNG ON on X-band and S-band
	T0	10:00	Start of Radio Science activities: Configuration: TWOD-X, TM ON, RNG ON Start recordings: IFMS: DOP1,2; AGC 1,2; MET, RNG
	T0 + 10:00		Stop all recordings
T0 – OWLT + 10:00			Command S-band transmitter OFF Command RNG OFF
Accepted:	PI	RSI Project	ESOC

### Configuration Control

Issue	Rev.	Date	Changes	Author
1	0	19.01.2006	All	ST
1	1	20.01.2006	All	ST

#### 6.4.2.2 Constraints

Any spacecraft orbit correction manoeuvres shall not be performed within the observation period. Furthermore, spacecraft attitude thruster activities should be avoided or kept at a minimum. In case of thruster activities, a logging of relevant thrust parameters has to be performed.

The orbital ground track of Rosetta should cover the comets surface in a uniform way, as to derive gravity information with uniform accuracy. Hence a near-circular polar orbit is required as close to the comet as possible e.g. at an altitude of 2 cometary radii. Non-gravitational perturbations should be kept at a minimum, therefore the heliocentric distance of the comet should exceed 3 AU. Close passes to active areas of the comet should be avoided.

#### 6.4.2.3 Accuracy

Figure 6.4-1 shows the required tracking time to resolve perturbing acceleration due to mass flux on the spacecraft as a function of Doppler integration time for the upper and lower bounds of expected accelerations. Values for a  $2\sigma$  (50% error) and  $10\sigma$  (10% error) signal are shown.

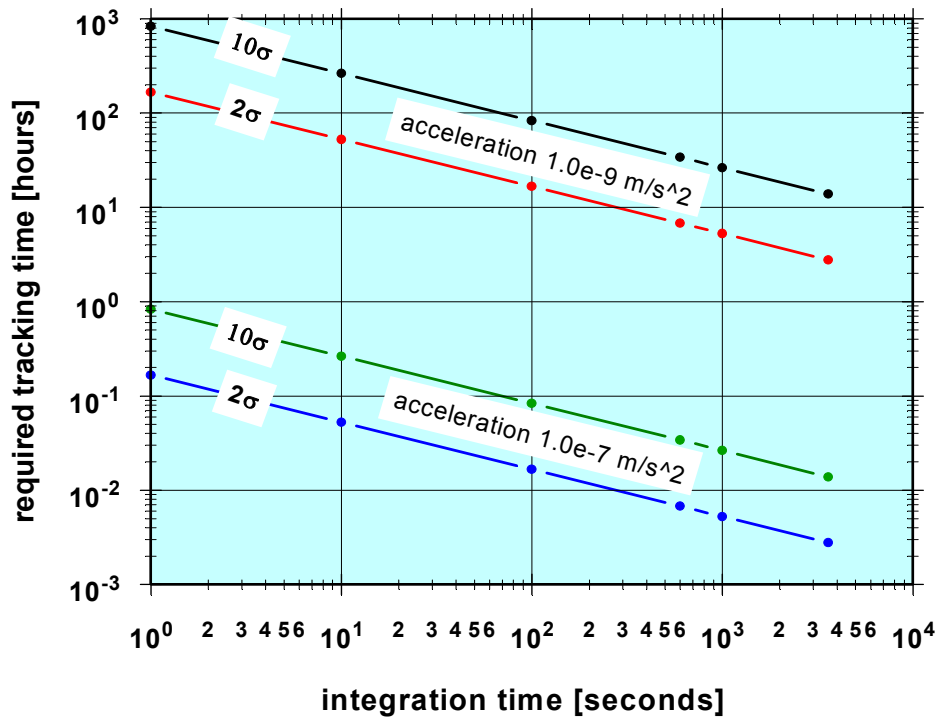


Figure 6.4-1: Required tracking time as a function of Doppler integration time to resolve perturbing acceleration from the Doppler noise background for 2σ and a 10σ signal.

## 6.5 GMC: Gravity mapping Campaign

### 6.5.1 Objectives

#### 6.5.1.1 Cometary Mass and Bulk Density

The determination of the cometary mass and the bulk density addresses the prime objective of the ROSETTA mission. The mass  $M$  of the comet can be derived from the gravitational coefficient  $GM$ , that may be estimated from tracking data, spanning several orbital revolutions. The bulk density of the comet  $\rho$  can be derived from the cometary mass together with estimates of the comet volume. The latter is a result of the OSIRIS experiment with possible contributions from RSI.

#### 6.5.1.2 Gravity Field Coefficients

The gravity field coefficients characterise the deviations of the external gravity field of celestial bodies from that of point masses. Thereby, these coefficients carry information about the internal structure of the nucleus. Gravity field coefficients, together with other information like shape, topography and moments of inertia therefore can help to disentangle the cometary interior or constrain respective models.

Besides the scientific relevance of gravity field coefficients, the knowledge of the cometary gravity field plays also an important role for the Rosetta flight operations.

#### 6.5.1.3 Cometary Moments of Inertia

The moments of inertia tensor of the cometary nucleus depend on the internal mass distribution and may likewise be used to constrain models of the nucleus structure. While five out of six independent elements of the inertia tensor are directly related to the second-order gravity field coefficients derived by the RSI experiment, the full tensor may be derived from an analysis of the cometary rotation under the action of gravitational and non-gravitational external forces. Using auxiliary data from OSIRIS, the rotation may be modelled to determine the inertia tensor and the principal moments of inertia.

As described above, the full inertia tensor may be described by the second-order gravity field coefficients  $C_{20}$ ,  $C_{22}$ ,  $C_{21}$ ,  $S_{22}$ ,  $S_{21}$ , as well as the z-component of the inertia tensor  $I_{zz}$ , that may be derived from observed rotation rates  $\omega$  and a modelling of external torques  $T$  due to gas jets according to Euler's equation.

### 6.5.2 Description

In contrast to DOT, which is a routine procedure during the entire mission, GMC is a special observation campaign to take place at times when the comet is very far from the sun and its coma is not active.

### 6.5.3 Operations

#### 6.5.3.1 Configuration

Operations will be conducted using a coherent simultaneous dual-frequency two-way tracking link (TWOD). Coherency of the transponded signal is mandatory for Doppler data acquisition. Dual-frequency operations are mandatory for an a posteriori calibration of ionospheric and interplanetary plasma effects and removal from the Doppler data. Two-way tracking is required to make use of the high-precision ground station frequency reference.

Instrument <b>RSI</b>		Originator Name <b>Carone</b>	Date <b>20.01.2006</b>
Mission Phase Routine	Activity ID TBW	Activity Name Gravity Mapping Campaign GMC	
<b>Description of activity:</b>		global gravity with TM OFF	
<b>Duration of activity:</b>		3.0 h $\leq$ TD $\leq$ 6.0 h TD = duration of radio science activities Duration requested by RSI	
<b>Power demand:</b>		28 Watts S-band transmitter 5.5 Watts USO power	
<b>Spacecraft pointing:</b>		HGA Earth pointing	
<b>Comments/other constrains:</b> Ground stations: NNO DSN – HEF DSN 70 m S-band reception required Sample rate: 1 sample/sec TM OFF			
<b>Spacecraft configuration</b> TWOD-X X-band uplink X- and S-band downlink RNG S-band ON RNG X-band ON TM OFF			

**IFMS DAP Settings:**

Configure Downlink Chain 1 for X-band ops  
 Configure Downlink Chain 2 for S-band ops  
 IFMS-1 configured for Input 1 (X-band prime)  
 IFMS-2 configured for Input 1 (X-band)  
 IFMS-3 configured for Input 2 (S-band)

**IFMS-1 DAP Settings X/up/down**

RNG set for 1 sample per second, 3600 samples per file  
 (only for TWOS and TWOD)  
 DOP1 set for 1 samples per second, 3600 samples per file  
 DOP2 set for 1 samples per second, 3600 samples per file  
 AGC1 set for 1 samples per second, 3600 samples per file  
 AGC2 set for 1 samples per second, 3600 samples per file  
 MET set for 1 sample per 60 seconds, 100 samples per file

**IFMS-2 DAP Settings X/down**

DOP1 set for 1 samples per second, 3600 samples per file  
 DOP2 set for 1 samples per second, 3600 samples per file  
 AGC1 set for 1 samples per second, 3600 samples per file  
 AGC2 set for 1 samples per second, 3600 samples per file  
 MET set for 1 sample per 60 seconds, 100 samples per file

**IFMS-3 DAP Settings S/down**

RNG set for 1 sample per second, 3600 samples per file  
 (only for TWOD if available)  
 DOP1 set for 1 samples per second, 3600 samples per file  
 DOP2 set for 1 samples per second, 3600 samples per file  
 AGC1 set for 1 samples per second, 3600 samples per file  
 AGC2 set for 1 samples per second, 3600 samples per file  
 MET set for 1 sample per 60 seconds, 100 samples per file

S/C onboard time (OBT)	Ground receive time (GRT)		Event
			T0 = start of radio science activities in GRT
Assumption is that spacecraft is in TWOS configuration after AOS and first check of TM <b>T0 is start of radio science activities in GRT = S/C ET + OWLT</b> OWLT is the one-way light time Assumption is that commands are pre-programmed and executed automatically on board Only one IFMS file start at the start of track			
T0 -01:10 - OWLT			Command S-band transmitter POWER ON

T0 -00:10 - OWLT			Command S-band d/I ON
T0 - 00:05 - OWLT			Command TM OFF
	T0 - 00:05	5	AOS of S-band and X-band coherent
	T0		Start of radio science activities TWOD-X Start RNG recordings: IFMS: on IFMS-1 and IFMS-3 (if available) DSN: at X-band and S-band Start recordings: IFMS : DOP1, DOP2, AGC1, AGC2, MET on all IFMS DSN: CL Doppler recording at X-band and S-band
	T0+TD		Stop all recordings
T0+TD -OWLT			Command TM ON
T0+TD -OWLT +00:05			Command S-band d/I OFF

### Configuration Control

Issue	Rev.	Date	Changes	Author
1	0	29.10.04	All	LC
1	1	20.01.06	Title	ST

## 6.6 OCP: Occultation Operations Procedure

### 6.6.1 Objectives

Occultations can be used to constrain the size and shape of the comet. The precisely known orbit of the S/C together with the observed times of the disappearance and reappearance of the one-way radio signal allow for a precise reconstruction of the cometary shape.

The radio link grazes very close to the nucleus immediately before occultation and immediately after exit from occultation. This allows it to search for a anticipated population of large dust grains (in the cm – dm size interval).

### 6.6.2 Description

This investigation is done during occultations. Since the derivation of the nucleus shape requires repeated occultations, occultations should be scheduled in sequence (occultation campaigns). Also, it is expected that occultations will not occur as single events, but as a sequence of individual occultations.

#### 6.6.2.1 Nucleus Size and Shape

Observations of the exact time of ingress and egress of the one-way downlink signal from occultation campaigns yield important quantitative constraints on the size and shape of the nucleus. Accurate measurements of the ingress and egress occultation times determine the length of the occultation chord for a known S/C trajectory, hence constrain the size of the nucleus. Repeated measurements for different occultation track geometries constrain the nucleus shape.

These observations complement the optical observations carried out by OSIRIS and may become important in the case that the surface is obscured by dust, or are permanently on the night side.

#### 6.6.2.2 Nucleus internal Structure

Because the comet is a relatively small celestial body, its interior may be penetrable by microwaves. The refractive properties of the nucleus will modify the propagation of a radio signal in a way that might enable sensing of the nucleus structure. Both, hints for the internal structure of the comet, as well as constraints on the bulk refractive index of the comet can be derived from these nucleus-sounding experiments. The typical occasions for a radio-sounding experiment of this type are during occultations when the S/C is behind the cometary nucleus, as seen from the Earth.

#### 6.6.2.3 Coma Plasma and Dust Grains

The RSI experiment will attempt to isolate the electron of the cometary ionosphere as it evolves on the comets approach to perihelion. The total electron content will contain the usual terrestrial contribution, a slowly increasing interplanetary contribution and the contribution by the cometary ionosphere. The electron density in the photochemically dominated part will be proportional to the square-root of the solar EUV flux and hence varies inversely with the distance of the comet from the Sun. Hence it should be possible to separate the cometary contribution from the other contributions by its magnitude at least close to 1 AU.

Analysis of Earth-based radar observations of comets Iras-Araki-Alcock and Halley revealed a spectral component almost surely caused by particles streaming away from the nucleus with a few m/s velocity. Their radius must be larger than a few mm to interact efficiently with the radar wavelength ( $\approx 3.5$  cm and 12.9 cm), and could probably be as large as 10 cm. The echo bandwidth implies a cloud that probably extends nearly 1000 km from the nucleus. Additional observations in the infrared (by IRAS) and in the optical wavelength band strengthen the hypothesis of the existence of large dust grains around the cometary nucleus.

The investigation of the lower cometary ionosphere and the search for large dust grains are performed during occultation orbits. During the ingress and egress phase of occultations, the ray path sounds the regions of interest, close to the cometary nucleus.

Neutral and ionized species within the coma constitute refractive media that potentially affect the phase and amplitude of the direct signal during occultation of Rosetta by the coma. Observations at two coherently related wavelengths is necessary for unambiguous separation of the contribution of each species. The separation relies on the wavelength dependence of the observed phase, being proportional to  $\lambda$  for plasma and to  $\lambda^{-1}$  for the neutral gas.

Another observable of a cometary coma sounding experiment is the signal attenuation along the direct path from the S/C to the Earth. Characterised in terms of the optical depth  $\tau(\lambda)$ . On the one hand, its value at X-band,  $\tau(3.6$  cm), reflects the contribution of all particles of radius greater than a few mm. On the other, its differential value  $\tau(3.6$  cm) -  $\tau(13$  cm) is diagnostic of the population of particles in the mm-dm size range. The exact size range depends on the refractive index of the particles.

### 6.6.3 Operations

#### 6.6.3.1 Configuration

##### 6.6.3.1.1 Occultation Operations Procedure for Occultation Ingress: OCP\_INGRESS

ROSETTA

Instrument <b>RSI</b>		Originator Name <b>Tellmann</b>	Date <b>20.01.2006</b>
Mission Phase Routine	Activity ID RF-FCP-026 (to be updated)	Activity Name <b>Occultation Operations Procedure OCP_INGRESS</b>	
<b>Description of activity:</b>		<b>Occultation OCP for Occultation Ingress</b>	
<b>Duration of activity:</b>		<b>Data recording time: flexible + 1 hour S-band warm up</b>	
<b>Power demand:</b>		<b>S-Band transmitter (28 W) USO-power (5.5 W)</b>	

<b>Spacecraft pointing:</b>	HGA Earth pointing
<p><b>Comments/other constrains:</b></p> <p><b>S-Band reception required</b>  <b>feasible ground stations: NNO</b>  <b>DSN-HEF</b>  <b>DSN-70 m</b></p> <p><b>sample rate (minimum): IFMS 10 samples/sec</b>  <b>DSN open-loop</b>  <b>DSN closed-loop 10 samples/sec</b></p> <p><b>TM OFF</b></p>	
<p><b>Spacecraft configuration</b></p> <p><b>ONED-USO</b>  <b>No uplink; X- and S-band downlink</b>  <b>RNG OFF, TM OFF (if feasible)</b></p>	
<p><b>IFMS DAP Settings:</b></p> <p><b>Configure Downlink Chain 1 for X-band ops</b>  <b>Configure Downlink Chain 2 for S-band ops</b>  <b>IFMS-1 configured for Input 1 (X-band prime)</b>  <b>IFMS-2 configured for Input 1 (X-band)</b>  <b>IFMS-3 configured for Input 2 (S-band)</b></p> <p><b>IFMS-1 DAP Settings X/down</b>  <b>DOP1 set for 10 samples per second, 3600 samples per file</b>  <b>DOP2 set for 10 samples per second, 3600 samples per file</b>  <b>AGC1 set for 10 samples per second, 3600 samples per file</b>  <b>AGC2 set for 10 samples per second, 3600 samples per file</b>  <b>MET set for 1 sample per 60 seconds, 100 samples per file</b></p>	
<p><b>IFMS-2 DAP Settings X/down</b>  <b>DOP1 set for 10 samples per second, 3600 samples per file</b>  <b>DOP2 set for 10 samples per second, 3600 samples per file</b>  <b>AGC1 set for 10 samples per second, 3600 samples per file</b>  <b>AGC2 set for 10 samples per second, 3600 samples per file</b>  <b>MET set for 1 sample per 60 seconds, 100 samples per file</b></p> <p><b>IFMS-3 DAP Settings S/down</b>  <b>DOP1 set for 10 samples per second, 3600 samples per file</b>  <b>DOP2 set for 10 samples per second, 3600 samples per file</b>  <b>AGC1 set for 10 samples per second, 3600 samples per file</b>  <b>AGC2 set for 10 samples per second, 3600 samples per file</b>  <b>MET set for 1 sample per 60 seconds, 100 samples per file</b></p>	

S/C onboard time (OBT)	Ground receive time (GRT)		event
<p>Assumption is that spacecraft is in TWOS configuration with USO ON but MUTE after AOS and first check of TM</p> <p><b>T0 is predicted start of geometrical occultation at GRT</b></p> <p><b>DT is the data recording time</b></p> <p>OWLT is the one-way light time</p> <p>Assumption is that commands are preprogrammed and executed automatically on board</p>			
T0 – OWLT - 01:08 – DT			command S-band transmitter POWER ON
T0 - OWLT - 00:08 - DT			command S-band d/l ON
T0 - OWLT - 00:07 - DT			command TM OFF (if feasible)
T0 - OWLT - 00:06 - DT			command USO UNMUTE
T0 - OWLT - 00:05 - DT			command Coherency OFF
	T0 – 00:05 - DT	5	AOS of S-band and X-band non-coherent
	T0 - DT		<p>Start of Radio Science activities:            Configuration: ONED-USO, TM OFF, RNG OFF            Start recordings: IFMS: DOP1,2; AGC 1,2; MET            DSN: Open loop            RHC, RHC-S</p>
	T0		Start of predicted geometrical occultation
	T0 + 00:05		Stop all recordings

T0 - OWLT+ 00:05			command S-band d/I OFF	
T0 – OWLT + 00:05			Command USO MUTE	
Accepted:	PI	RSI Project	ESOC	

### Configuration Control

Issue	Rev.	Date	Changes	Author
1	0	20.01.06	All	ST
0				

#### 6.6.3.1.2 Occultation Operations Procedure for Occultation Egress: OCP\_EGRESS

ROSETTA

Instrument <b>RSI</b>		Originator Name <b>Tellmann</b>	Date <b>20.01.2006</b>
Mission Phase Routine	Activity ID RF-FCP-026 (to be updated)	Activity Name <b>Occultation Operations Procedure OCP_EGRESS</b>	
<b>Description of activity:</b>		Occultation OCP for Occultation Egress	
<b>Duration of activity:</b>		Data recording time: flexible + 1 hour S-band warm up	
<b>Power demand:</b>		S-Band transmitter (28 W) USO-power (5.5 W)	
<b>Spacecraft pointing:</b>		HGA Earth pointing	

**Comments/other constrains:****S-Band reception required**

feasible ground stations: **NNO**  
**DSN-HEF**  
**DSN-70 m**

sample rate (minimum): **IFMS 10 samples/sec**  
**DSN open-loop**  
**DSN closed-loop 10 samples/sec**

**TM OFF (if feasible)**

**Spacecraft configuration****ONED-USO**

**Uplink N/A; X- and S-band downlink**  
**RNG OFF, TM OFF (if feasible)**

**IFMS DAP Settings:**

**Configure Downlink Chain 1 for X-band ops**  
**Configure Downlink Chain 2 for S-band ops**  
**IFMS-1 configured for Input 1 (X-band prime)**  
**IFMS-2 configured for Input 1 (X-band)**  
**IFMS-3 configured for Input 2 (S-band)**

**IFMS-1 DAP Settings X/down**

**DOP1 set for 10 samples per second, 3600 samples per file**  
**DOP2 set for 10 samples per second, 3600 samples per file**  
**AGC1 set for 10 samples per second, 3600 samples per file**  
**AGC2 set for 10 samples per second, 3600 samples per file**  
**MET set for 1 sample per 60 seconds, 100 samples per file**

**IFMS-2 DAP Settings X/down**

**DOP1 set for 10 samples per second, 3600 samples per file**  
**DOP2 set for 10 samples per second, 3600 samples per file**  
**AGC1 set for 10 samples per second, 3600 samples per file**  
**AGC2 set for 10 samples per second, 3600 samples per file**  
**MET set for 1 sample per 60 seconds, 100 samples per file**

**IFMS-3 DAP Settings S/down**

**DOP1 set for 10 samples per second, 3600 samples per file**  
**DOP2 set for 10 samples per second, 3600 samples per file**  
**AGC1 set for 10 samples per second, 3600 samples per file**  
**AGC2 set for 10 samples per second, 3600 samples per file**  
**MET set for 1 sample per 60 seconds, 100 samples per file**

S/C onboard time	Ground receive time		event
------------------------	---------------------------	--	-------

(OBT)	(GRT)		
<p>Assumption is that spacecraft is in <b>ONES-TCXO configuration (earth occultation)</b> with USO ON but MUTE</p> <p><b>T1 is predicted end of geometrical occultation at GRT</b></p> <p><b>DT is the data recording time</b></p> <p>OWLT is the one-way light time</p> <p>Assumption is that commands are preprogrammed and executed automatically on board</p>			
T1 – OWLT - 01:08			command S-band transmitter POWER ON
T1 - OWLT - 00:08			command S-band d/l ON
T1 - OWLT - 00:07			command TM OFF (if feasible)
T1 - OWLT - 00:06			command USO UNMUTE
	T1		AOS of S-band and X-band non-coherent
	T1		Start of Radio Science activities: Configuration: ONED-USO, TM OFF, RNG OFF Start recordings: IFMS: DOP1,2; AGC 1,2; MET DSN: Open loop 5000 samples/sec RHC, RHC-S
	T1 + DT		Stop all Recordings
T1 - OWLT+ DT			command S-band d/l OFF
T1 – OWLT + DT			Command USO MUTE Command TM ON Command Coherency ON

Accepted:	PI	RSI Project	ESOC
-----------	----	-------------	------

**Configuration Control**

Issue	Rev.	Date	Changes	Author
1	0	20.01.06	All	ST
0				

## 6.7 BRP: Bistatic Radar Procedure

### 6.7.1 Objective

The scientific objectives of this investigation are the determination of the dielectric properties and roughness of the comet surface from scattering and polarisation studies of bistatic radar echoes reflected from the nucleus surface and received on Earth.

### 6.7.2 Description

The circularly polarised one-way downlink carrier signal from the S/C, impinging on the nucleus at the angle of incidence  $\gamma$ , is transformed into a linearly polarised signal when specularly reflected from the comet's surface at the Brewster angle  $\gamma = \gamma_B$ . The dielectric constant (surface permittivity)  $\varepsilon$  of the cometary surface can be inferred from determinations of the Brewster angle  $\gamma_B$  according to the relation  $\varepsilon = \tan^2 \gamma_B$ . If the comet's reflectivity is governed by an icy conglomerate with an index of refraction close to that of water, one expects to find  $\gamma_B = 50^\circ$ . A very dusty surface would raise  $\gamma_B$  to values around  $60^\circ$ .

The total power contained in the bistatic radar echoes will be recorded for an estimate of the radio albedo of the comet's surface. The broadening of the echo frequency spectrum is related to the roughness of the surface on scales of the radio wavelength.

From the varying total power within a rotation period and from the periodical variation of the echo spectrum position, the determination of nucleus rotation, precession, and nutation rates is feasible within a tracking pass.

### 6.7.3 Operations

#### 6.7.3.1 Configuration

Rosetta			
Instrument	<b>RSI</b>	Originator Name <b>Carone</b>	Date <b>29.10.2004</b>
Mission Phase Routine	Activity ID TBW	Activity Name <b>Bistatic Radar Procedure BRP</b>	
<b>Description of activity:</b>		<b>Bistatic Radar</b>	
<b>Duration of activity:</b>		<b>3 hours of spacecraft time (s/c operations only) 7 hours of ground station time (includes noise calibration)</b>	
<b>Power demand:</b>		<b>S-Band transmitter power (28 W) USO-power (8 W)</b>	

<b>Spacecraft pointing:</b>		<b>BSR-INERT: surface inertial pointing</b> <b>BSR-SPOT: surface spot pointing</b> <b>BSR-SPEC: surface specular pointing</b>	
<b>Comments/other constrains:</b> <b>DSN 70-m station required</b> Each BSR activity consists of these activities in sequence: <ol style="list-style-type: none"> <li>1. BNOISE</li> <li>2. BCAL</li> <li>3. BSLW</li> <li>4. BSR-INERT or BSR-SPOT or BSR-SPEC</li> <li>5. BSLW</li> <li>6. BCAL</li> <li>7. BNOISE</li> </ol>			
<b>Spacecraft configuration</b> <b>ONED-USO:</b> <b>X- and S-band downlink</b> <b>RNG OFF</b> <b>TM OFF</b>			
<b>IFMS DAP Settings</b>  None  <b>DSN RSR open-loop settings:</b> <b>RSR1: RCP X-band; sample rate 50000 samples/sec</b> <b>RSR2: LCP X-band; sample rate 50000 samples/sec</b> <b>RSR3: RCP S-band; sample rate 50000 samples/sec</b> <b>RSR4: LCP S-band; sample rate 50000 samples/sec</b>			
<b>Sequence of Events</b>			
S/C onboard time (OBT)	Ground receive time (GRT)		event
	T0 – 03:00	BNOISE	Start of noise calibration activities in the ground station No s/c signal required
	T0		Stop of calibration activities Pointing of antenna towards s/c position

Assumption is that spacecraft is in TWOS configuration after AOS and first check of TM USO is ON but MUTE

**T0 is the time of the start of radio science operation in GRT**

OWLT is the one-way light time

Assumption is that commands are pre-programmed and executed automatically on board

T0 – OWLT - 01:02		BCAL	command S-band transmitter POWER ON
T0- OWLT- 0:02			command S-band d/l ON
T0- OWLT- 0:01			command USO UNMUTE
T0 - OWLT			command coherency OFF
	T0		Stop uplink AOS of X-band and S-band non-coherent D/L
	T0 + 00:05		Start open-loop recordings at four RSR channels
	T0 + 00:35		Stop recordings
T0 – OWLT + 00:35		BSLW	Start of s/c slew to requested BSR pointing
T0 – OWLT + 01:05			End of s/c slew
T0 – OWLT +01:05		BSR- INERT or BSR- SPOT or BSR- SPEC	Start s/c pointing sequence: inertial, spot or specular
	T0 + 01:05		Start open-loop recordings at four RSR channels
	T0 + 02:05		Stop recordings
T0 – OWLT + 02:05			End s/c pointing sequence

T0 – OWLT + 02:05		BSLW	Start s/c slew to HGA Earth pointing	
T0 – OWLT + 02:35			Stop s/c slew	
	T0 + 02:35	BCAL	Start open-loop recordings at four RSR channels	
	T0 + 03:05		Stop recordings	
T0 – OWLT + 03:05			Command S-band D/L OFF Command S-band transmitter POWER OFF	
	T0 + 03:05		Start X-band uplink	
T0 + 03:05 + OWLT			s/c acquires X-band uplink	
T0 + 03:08 + OWLT			command coherency ON	
T0 + 03:09 + OWLT			command USO MUTE	
	T0 + 03:10 + 2 OWLT		s/c transferred to other receiving antenna	
	T0 + 03:10 + 2 OWLT	BNOISE	Start of noise calibration activities in ground station No spacecraft signal required	
	T0 + 04:10 + 2 OWLT		Stop activities	
Accepted:		PI	RSI Project	ESOC

**Configuration Control**

Issue	Rev.	Date	Changes	Author
-------	------	------	---------	--------

ROSETTA RSI: Rosetta Radio Science Investigations  
Experiment User Manual

Document **RO-RSI-IGM-MA-3081**

Issue: 4

Revision: 2

Date: 25.04.2016

Page: 125 of 144

---

1	0	29.10.04	All	LC
1	1	20.01.06	Title	ST

## 6.8 SCP: Solar Conjunction Procedure

### 6.8.1 Objectives

The scientific objectives are the determination of the total electron content of the solar corona, the solar wind speed, the turbulence spectrum, and the identification of coronal mass ejections.

### 6.8.2 Description

The total electron content and its temporal changes, the solar wind speed, and the turbulence spectrum can be derived from measurements of dual-frequency differential group time delay (ranging) and the differential Doppler shift.

### 6.8.3 Operations

#### 6.8.3.1 Configuration

Instrument <b>RSI</b>		Originator Name <b>Carone</b>	Date <b>20.01.2006</b>
Mission Phase <b>Routine</b>	Activity ID <b>RF-FCP-022</b> (to be updated)	Activity Name <b>Solar Conjunction Procedure SCP</b>	
<b>Description of activity:</b>		Solar Corona Sounding with X-band uplink	
<b>Duration of activity:</b>		TD >= 4.0 h TD = duration of radio science activities Duration requested in MREQ	
<b>Power demand:</b>		28 Watts S-band transmitter	
<b>Spacecraft pointing:</b>		HGA Earth pointing	
<b>Comments/other constrains:</b> During superior or inferior solar conjunction phase as defined by radio science as superior solar conjunction $\pm 10^\circ$ elongation from the solar disc Ground stations: NNO DSN – HEF DSN 70 m S-band reception required Sample rate: 1 sample/sec TM ON			

**Spacecraft configuration**

TWOD-X  
 X-band uplink  
 X- and S-band downlink  
 RNG S-band ON  
 RNG X-band ON  
 TM ON

**IFMS DAP Settings:**

**Configure Downlink Chain 1 for X-band ops**  
**Configure Downlink Chain 2 for S-band ops**  
**IFMS-1 configured for Input 1 (X-band prime)**  
**IFMS-2 configured for Input 1 (X-band)**  
**IFMS-3 configured for Input 2 (S-band)**

**IFMS-1 DAP Settings X/up/down**

**RNG set for 1 sample per second, 3600 samples per file**  
**(only for TWOS and TWOD)**  
**DOP1 set for 1 samples per second, 3600 samples per file**  
**DOP2 set for 1 samples per second, 3600 samples per file**  
**AGC1 set for 1 samples per second, 3600 samples per file**  
**AGC2 set for 1 samples per second, 3600 samples per file**  
**MET set for 1 sample per 60 seconds, 100 samples per file**

**IFMS-2 DAP Settings X/down**

**DOP1 set for 1 samples per second, 3600 samples per file**  
**DOP2 set for 1 samples per second, 3600 samples per file**  
**AGC1 set for 1 samples per second, 3600 samples per file**  
**AGC2 set for 1 samples per second, 3600 samples per file**  
**MET set for 1 sample per 60 seconds, 100 samples per file**

**IFMS-3 DAP Settings S/down**

**RNG set for 1 sample per second, 3600 samples per file**  
**(only for TWOD if available)**  
**DOP1 set for 1 samples per second, 3600 samples per file**  
**DOP2 set for 1 samples per second, 3600 samples per file**  
**AGC1 set for 1 samples per second, 3600 samples per file**  
**AGC2 set for 1 samples per second, 3600 samples per file**  
**MET set for 1 sample per 60 seconds, 100 samples per file**

S/C onboard time (OBT)	Ground receive time (GRT)	Event
		T0 = start of radio science activities in GRT

Assumption is that spacecraft is in TWOS configuration after AOS and first check of TM  
**T0 is start of radio science activities in GRT = S/C ET + OWLT**  
 OWLT is the one-way light time  
 Assumption is that commands are pre-programmed and executed automatically on board  
 Only one IFMS file start at the start of track

T0-01:05 - OWLT			Command S-band transmitter POWER ON
T0-00:05 - OWLT			Command S-band d/I ON
	T0-00:05	5	AOS of S-band and X-band coherent
	T0		Start of radio science activities TWOD-X Start RNG recordings: IFMS: on IFMS-1 and IFMS-3 (if available) DSN: at X-band and S-band Start recordings: IFMS : DOP1, DOP2, AGC1, AGC2, MET on all IFMS DSN: CL Doppler recording at X-band and S-band
	T0+TD		Stop all recordings
T0 -OWLT +TD			Command S-band d/I OFF

### Configuration Control

Issue	Rev.	Date	Changes	Author
1	0	29.10.04	All	LC
1	1	20.01.06	Title	ST

## 6.9 AST: Asteroid Flyby Procedures

### 6.9.1 Objective

Spacecraft fly-bys at asteroids offer an unique way to determine the mass of the asteroid. Together with knowledge on the volume of the body, derived from imaging data of the onboard camera system, the bulk density of asteroids may be derived.

This has impressively been demonstrated with the NEAR spacecraft, that passed asteroid 253 Mathilde on July 27, 1997. Based on pre- and post-encounter Doppler tracking data the asteroid mass was determined with an accuracy of about 6%.

### 6.9.2 Description

2-way coherent and simultaneous X/X and X/S Doppler tracking of the Rosetta orbiter from pre- and post-encounter arcs provides information on the asteroid mass.

As a rule of thumb, the fractional error in the mass depends on the fly-by velocity  $v$ , the closest approach distance  $b$  to the center of the mass, the asteroids mass  $GM$ , and the Doppler velocity variance  $\sigma(\rho)$ , according to (Anderson et al., 1992)

$$\frac{\sigma(GM)}{GM} = \sigma(\rho) \frac{bv}{GM} \quad (6-1)$$

For coherent X/X-band Doppler data with an integration time of 100 s we expect  $\sigma(\rho) = 0.03\text{mm/s}$ .

### 6.9.3 Operations

#### 6.9.3.1 Configuration

Instrument <b>RSI</b>		Originator Name <b>Tellmann</b>	Date <b>20.01.2006</b>
Mission Phase Routine	Activity ID RF-FCP-023 RF-FCP-024 RF-FCP-025 ARFF023 ARFF024 ARFF025 (to be updated)	Activity Name <b>Asteroid Flyby AST</b>	
<b>Description of activity:</b>		Gravity measurement at Asteroid with TM OFF	
<b>Duration of activity:</b>		TD >= 8.0 h TD = duration of radio science activities	

<b>Power demand:</b>	28 Watts S-band transmitter
<b>Spacecraft pointing:</b>	HGA Earth pointing
<b>Comments/other constrains:</b>	
<p>Ground stations: NNO  DSN – HEF  DSN 70 m  S-band reception required  Sample rate: 1 sample/sec  TM ON</p>	
<b>Spacecraft configuration</b>	
<p>TWOD-X  X-band uplink  X- and S-band downlink  RNG S-band ON  RNG X-band ON  TM OFF</p>	
<b>IFMS DAP Settings:</b>	
<p><b>Configure Downlink Chain 1 for X-band ops</b>  <b>Configure Downlink Chain 2 for S-band ops</b>  <b>IFMS-1 configured for Input 1 (X-band prime)</b>  <b>IFMS-2 configured for Input 1 (X-band)</b>  <b>IFMS-3 configured for Input 2 (S-band)</b></p>	
<p><b>IFMS-1 DAP Settings X/up/down</b>  <b>RNG set for 1 sample per second, 3600 samples per file</b>  <b>(only for TWOS and TWOD)</b>  <b>DOP1 set for 1 samples per second, 3600 samples per file</b>  <b>DOP2 set for 1 samples per second, 3600 samples per file</b>  <b>AGC1 set for 1 samples per second, 3600 samples per file</b>  <b>AGC2 set for 1 samples per second, 3600 samples per file</b>  <b>MET set for 1 sample per 60 seconds, 100 samples per file</b></p>	
<p><b>IFMS-2 DAP Settings X/down</b>  <b>DOP1 set for 1 samples per second, 3600 samples per file</b>  <b>DOP2 set for 1 samples per second, 3600 samples per file</b>  <b>AGC1 set for 1 samples per second, 3600 samples per file</b>  <b>AGC2 set for 1 samples per second, 3600 samples per file</b>  <b>MET set for 1 sample per 60 seconds, 100 samples per file</b></p>	
<p><b>IFMS-3 DAP Settings S/down</b>  <b>RNG set for 1 sample per second, 3600 samples per file</b>  <b>(only for TWOD if available)</b>  <b>DOP1 set for 1 samples per second, 3600 samples per file</b></p>	

DOP2 set for 1 samples per second, 3600 samples per file AGC1 set for 1 samples per second, 3600 samples per file AGC2 set for 1 samples per second, 3600 samples per file MET set for 1 sample per 60 seconds, 100 samples per file			
S/C onboard time (OBT)	Ground receive time (GRT)		Event T0 = start of radio science activities in GRT
Assumption is that spacecraft is in TWOS configuration after AOS and first check of TM <b>T0 is start of radio science activities in GRT = S/C ET + OWLT</b> OWLT is the one-way light time Assumption is that commands are pre-programmed and executed automatically on board Only one IFMS file start at the start of track			
T0 -01:10 - OWLT			Command S-band transmitter POWER ON
T0 -00:10 - OWLT			Command S-band d/I ON
T0 -00:05 - OWLT			Command TM OFF (if feasible)
	T0 -00:05		AOS of S-band and X-band coherent
	T0		Start of radio science activities TWOD-X Start RNG recordings: IFMS: on IFMS-1 and IFMS-3 (if available) DSN: at X-band and S-band Start recordings: IFMS : DOP1, DOP2, AGC1, AGC2, MET on all IFMS DSN: CL Doppler recording at X-band and S-band
	T0+TD		Stop all recordings
T0+TD -OWLT			Command TM ON
T0+TD -OWLT +00:05			Command S-band d/I OFF

### Configuration Control

Issue	Rev.	Date	Changes	Author
1	0	22.10.04	All	ST
1	1	20.01.2006	Duration	ST

ROSETTA RSI: Rosetta Radio Science Investigations  
Experiment User Manual

Document **RO-RSI-IGM-MA-3081**

Issue: 4

Revision: 2

Date: 25.04.2016

Page: 132 of 144

---


PAGE LEFT FREE

## 7 Flight Operation Procedures (FOP); Sequence-of-Events

### 7.1 Definitions

ESOC prepared the following Flight Operations Procedures (FOP) which configure the spacecraft and the ground station and create command sequences for the configuration according to RSI requirements (ARFFxxxA) and the reconfiguration after the end of activity (ARFFxxxB).

#### 7.1.1 Format of FOP file names

##### RF-FCP-xxx

	description
RF	RSI instrument acronym
FCP	Flight Control Procedure
xxx	procedure number

#### 7.1.2 RSI FOP procedures

FOP	description
RF-FCP-010	Telemetry Configuration for RSI operations to be deleted
RF-FCP-011	RSI UCT ONES to be deleted
RF-FCP-012	RSI UCT ONED to be deleted
RF-FCP-013	RSI TVT Proc-1 to be deleted
RF-FCP-014	RSI TVT Proc-2 to be deleted
RF-FCP-015	RSI TVT Proc-3 to be deleted
RF-FCP-016	RSI TVT Proc-4 to be deleted
RF-FCP-017	RSI TVT Proc-6 to be deleted
RF-FCP-018	RSI TVT Proc-7 to be deleted
RF-FCP-019	RSI TVT Proc-5 to be deleted
RF-FCP-020	Centre of Mass Determination CMD
RF-FCP-021	RSI Doppler Tracking Procedure DOT to be updated
RF-FCP-022	Solar Conjunction Procedure SCP to be updated
RF-FCP-023	Asteroid Flyby Procedure (Pre Encounter (E-24hr)) AST
RF-FCP-024	Asteroid Flyby Procedure (Encounter (E)) AST to be updated
RF-FCP-025	Asteroid Flyby Procedure (Post Encounter (E+24hr+10h15m TBC)) AST

RF-FCP-026	Occultation Procedure OCP to be updated
RF-FCP-030	RSI Passive Checkout procedure PCx
RF-FCP-xxx	Bistatic Radar Procedures BRP tbw
RF-FCP-xxx	Gravity Mapping Campaign GMC tbw

### 7.1.3 Format of Command Sequence Files

#### ARFFxxxQ

	description
A	Command Sequence
RF	RSI instrument acronym
F	Flight Control Procedure
xxx	procedure number (see 6.3.2)
Q	A = start of RSI configuration B = reconfiguration after RSI activity

### 7.1.4 Command sequence files

FOP	calls	
	Start RSI configuration	reconfiguration
RF-FCP-010	ARFF010A	ARFF010B
RF-FCP-011	ARFF011A	ARFF011B
RF-FCP-012	ARFF012A	ARFF012B
RF-FCP-013	ARFF013A	ARFF013B
RF-FCP-014	ARFF014A	ARFF014B
RF-FCP-015	ARFF015A	ARFF015B
RF-FCP-016	ARFF016A	ARFF016B
RF-FCP-017	ARFF017A	ARFF017B
RF-FCP-018	ARFF018A	ARFF018B
RF-FCP-019	ARFF019A	ARFF019B
RF-FCP-020	ARFF020A	ARFF020B
RF-FCP-021	ARFF021A	ARFF021B
RF-FCP-022	ARFF022A	ARFF022B
RF-FCP-023	ARFF023A	ARFF023B
RF-FCP-024	ARFF024A	ARFF024B
RF-FCP-025	ARFF025A	ARFF025B
RF-FCP-026	ARFF026A	ARFF026B
RF-FCP-030	ARFF030A	ARFF030B

## 8 Commissioning Results

The following chapter summarizes the results from the NEVP Commissioning in March, May and October 2004 using the ESA ground station in New Norcia (NNO) and the results from the first Passive Checkouts performed in April 2005 and September 2005.

### 8.1 NEVP Commissioning

An overall view of the NEVP results can be found in ROS-RSI-IGM-TR-3117 [13] and also in ROS-RSI-IGM-RP-3123 [17].

### 8.2 Passive Checkout Results

An overall view of the Commissioning results and the Passive Checkout Results can be found in ROS-RSI-IGM-RP-3123 [17].

## 9 References

Anderson, J.D., Armstrong, J.W., Estabrook, F.B., Hellings, R.W., Lau, E.K. and Wahlquist, H.D., Pioneer 10 search for gravitational waves - No evidence for coherent radiation from Geminga, *Nature*, 308, 158-160, 1984.

Anderson, J.D., Krisher, T. and Borutzki, S. et al., Radio range measurements of coronal electron densities at 13 and 3.6 cm wavelengths, *Astrophys. J.*, 323, L141-L143, 1987.

Anderson, J.D., Armstrong, J.W., Campbell, J.K., Estabrook, F.B., Krisher, T.P. and Lau, E.L., Gravitation and celestial mechanics investigations with Galileo, *Space Sci. Rev.*, 60, 591-610, 1992.

Anderson, J.D., S.G. Turyshev, S.W. Asmar, M.K. Bird, A.S. Konopliv, T.P. Krisher, E.L. Lau, G. Schubert and W.L. Sjogren, Radio science investigation on a Mercury Orbiter mission, *Planet. Space Sci.* 45, 21-29, 1997.

Anderson, J.D., Lau, E.L., Asmar, S.W., Bird, M.K., Clark, B.C., Giampieri, G., Gilliland, K.V., Pätzold, M., *J. Geophys. Res.*, 109, doi:10.1029/2004JE002323, Stardust dynamic science at comet 81P/Wild 2, 2004.

Andreev, V.I. and Gavrik, A.L., Distribution of electron density at comet P/Halley from radio science data, *Kosmicheskie Issledovaniya*, 28, 293-303, 1990.

Asmar, S.W., and R.G. Herrera, Radio Science Handbook, JPL D-7938 Volume 4, Jet Propulsion Laboratory, Pasadena, CA, 22 January 1993.

Asmar, S.W., R.G. Herrera, and T. Priest, Radio Science Handbook, JPL D-7938 Volume 6, Jet Propulsion Laboratory, Pasadena, CA, 1995.

Bär, A. H. Boehnhardt and H. Drechsel, ESTEC Contract Report, 1999.

Barucci, M. A. et al., Asteroid target selection for the new Rosetta mission baseline, *Astronomy & Astrophysics* 430, 313-317, 2005

Bertotti, B., Ambrosini, R., Asmar, S.W., Brenkle, J.P., Comoretto, G., Giampieri, G., Iess, L., Messeri, A., and Wahlquist, H.D., The gravitational wave experiment, *Astron. Astrophys. Supp. Ser.*, 92, 431-440., 1992.

Bird, M.K., Volland, H., Pätzold, M., Edenhofer, P., Asmar, S.W. and Brenkle, J.P., The coronal electron density distribution determined from dual-frequency ranging measurements during the 1991 solar conjunction of the Ulysses spacecraft, *Astrophys. J.*, 426, 373-381, 1994.

Bird, M.K., Pätzold, M., Edenhofer, P., Asmar, S.W., McElrath, T.P., Coronal radio sounding with Ulysses: Solar wind electron density near 0.1 AU during the 1995 conjunction, *Astron. Astrophys.* 316, 437 - 448, 1996.

Bird, M.K., M. Allison, S.W. Asmar, D.H. Atkinson, I.M. Avruch, R. Dutta-Roy, Y. Dzierma, P. Edenhofer, W.M. Folkner, L.I. Gurvits, D.V. Johnston, D. Plettemeier, S.V. Pogrebenko, R.A. Preston and G.L. Tyler, The vertical profile of winds on Titan, *Nature* XXX, in press, 2005

Boehnhardt, H., Babion, J. and West, R.M., An optimized detection technique for faint moving objects on a star-rich background, *Astron. Astrophys.* 320, 642, 1996.

Boehnhardt, H., A. Fiedler, M. Geffert and J. Sanner, ESTEC Contract Report, 1997.

Boehnhardt, H., C. Delahodde, T. Sekiguchi, O. Hainaut, J. Spyromilio, J. Tarengi, R.M. West, R. Amestica, R. Schulz, and G. Schwehm, VLT Kueyen observations of Rosetta target comet 46P/Wirtanen near aphelion, *Astron. Astrophys.*, in press, 1999.

Bougher, S.W., S. Engel, D.P. Hinson, and J.R. Murphy, MGS radio science electron density profiles: Interannual variability and implications for the Martian neutral atmosphere, *J. Geophys. Res.*, 109, E03010, doi:10.1029/2003JE002154, 2004.

Campbell, D.B., Harmon, J.K. and Shapiro, I.I., Radar observations of comet Halley, *Astrophys. J.* , 338 , 1094-1105, 1989.

Elliot, J.L., and P.D. Nicholson, "The Rings of Uranus," *Planetary Rings*, R. Greenberg and A. Brahic (Eds.), U. of Arizona Press, Tucson, p. 25, 1984.

Elliot, J.L., Dunham, E.W. , Bosh, A.S. , Slivan, S.M. , Young, L.A. , Wasserman, L.H. and Millis, R.L., Pluto's atmosphere, *Icarus*, 77, Issue 1, Pages 148-170, January, 1989.

Eshleman, V. R., The Radio Occultation Method for the Study of Planetary Atmospheres, *Planet. Space Sci.*, Vol. 21, pp. 1521-1531, 1973.

Eshleman, V. R. and G. L. Tyler, "Radio Occultation: Problems and Potential Solutions," Presented at the Jupiter Conf., Tucson, AZ, 19 May, 1975. Published in TECH. RPT. 3241-3, SU-SEL-78-032, 1975.

Eshleman, V.R., G.L. Tyler, J.D. Anderson, G. Fjeldbo, G.S. Levy, G.E. Wood, and T.A. Croft, "Radio Science Investigations with Voyager," *Space Sci. Rev.*, Vol. 21, p. 207, 1977.

Fjeldbo, G., Bistatic Radar Methods for Studying Planetary Ionospheres and Surfaces, Stanford Electronics Laboratory, Stanford University, SU-SEL-64-025, 1964.

Gill, E., Montenbruck, O. and Pätzold, M., Perturbation forces acting on the Rosetta spacecraft in a close orbit around comet P/Wirtanen, AAS paper 96-150, Houston, 1996.

Häusler B. et al., Venus Express Radio Science Experiment VeRa, *ESA-Special Publication, in press*, 2006.

Harmon, J.K., Campbell, D.B., Hine, A.A., Shapiro, I.I. and Marsden, B.G., Radar observations of comet Iras-Araki-Alcock, *Astrophys. J.*, 338, 1071-1093, 1989.

Harmon, J.K., S.J. Ostro, L.A.M. Benner, K.D. Rosema, R.F. Jurgens, R. Winkler, D.K. Yeomans, D. Choate, R. Cormier, J.D. Giorgini, D.L. Mitchell, P.W. Chodas, R. Rose, D. Kelley, M.A. Slade and M.L. Thomas, Radar detection of the nucleus and coma of Comet Hyakutake (C/1996 B2), *Science* 278, 1921, 1997.

Hinson, D. P., R. A. Simpson, J. D. Twicken, G. L. Tyler, and F. M. Flasar, Initial Results from Radio Occultation Measurements with Mars Global Surveyor, *Journal of Geophysical Research (Planets)*, vol. 104, no. E11, pp. 26297-27012, 1999.

Hinson, D. P., M. D. Smith, and B. J. Conrath, Comparison of atmospheric temperatures obtained through infrared sounding and radio occultation by Mars Global Surveyor, *J. Geophys. Res.*, 109, E12002, doi:10.1029/2004JE002344, 2004a.

Hinson, D. P., and R. J. Wilson, Temperature inversions, thermal tides, and water ice clouds in the Martian tropics, *J. Geophys. Res.*, 109, E01002, doi:10.1029/2003JE002129, 2004b.

JPL, JPL's HORIZONS System, <http://ssd.jpl.nasa.gov/horizons.html>, November 2005

Kamoun, P., D.B. Campbell, S.J. Ostro, G.H. Pettengill, and I.I. Shapiro, Comet Encke: Radar detection of the nucleus, *Science* 216, 293, 1982.

Kamoun, P., D. Campbell, G. Pettengill and I. Shapiro, Radar observations of three comets and detection of one: P/Grigg-Skjellerup, *Planet. Space Sci.* 47, 23-28, 1999.

Kursinski, E. R., G. A. Hajj, K. R. Hardy, J. T. Schofield, and R. Linfield, Observing Earth's Atmosphere with Radio Occultation Measurements, *Journal of Geophysical Research*, Vol. 102, No. D19, pp 23429-23465, 1997a.

Kursinski, E. R., G. A. Hajj, T. Schofield, R. P. Linfield, Observing Earth's atmosphere with radio occultation measurements using the Global Positioning System, *Journal of Geo. Research*, vol. 102, no. D19, 23,429-23,465, 30 October 1997b.

Lamy, P.L., I. Toth, L. Jorda, H.A. Weaver and M. A'Hearn, The nucleus and inner coma of Comet 46P/Wirtanen, *Astron. Astrophys.* 335, L25-L29, 1998.

Lamy, P.L., Toth, I., Weaver, H., Jorda, L., & Kaasalainen, M. 2003, AAS/Division for Planetary Sciences Meeting 35.

Lazzarin M. et al., Visible spectral properties of asteroid 21 Lutetia, target of Rosetta Mission, *Astronomy & Astrophysics* 425, L25-L28, 2004

Lipa, B. J. and G. L. Tyler, "Statistical and Computational Uncertainties in Atmospheric Profiles from Radio Occultations: Mariner 10 at Venus," *ICARUS*, vol. 39, no. 2, pp. 192-208, August, 1979.

Marouf, E.A., Tyler, G.L. and Eshleman, V.R., Theory of radio occultation by Saturn's rings, *Icarus* , 49 , 161-193, 1982.

Marouf, E. A., Tyler, G.L., Zebker, H.A., Simpson, R.A. and Eshleman, V.R., Particle size distributions in Saturn's rings from Voyager 1 radio occultations, *Icarus* , 54 , 189-211, 1983.

Marouf, E. A. and Bird, M.K., Rosetta and bistatic-radar detectability of cometary nuclei, (Abstract) AGU Fall Meeting, San Francisco, CA, December 11-15, 1995.

Marsden, B.G. and Williams, G.V., *Catalogue of Cometary orbits* , Tenth Ed., IAU Central Bureau for Astronomical telegrams, Cambridge, MA, 1995.

Miller, J.K., Williams, B.G., Bollman, W.E., Davis, R.P., Helfrich, C.E., Scheeres, D.J., Synnott, S.P., Wang, T.C. and Yeomans, D.K., Navigation analysis for Eros rendezvous and orbital phases, *Journ. Astronautical Sci.* , 43 , 453-476, 1995.

Muhleman, D.O. and Anderson, J.D., Solar wind electron density from Viking dual-frequency radio measurements, *Astrophys. J.* , 247 , 1093-1101, 1981.

Ostro, S. J., Radar observations of asteroids and comets, *Pub. Astron. Soc. Pacific* , 97 , 877-884, 1985.

Ostro, S. J., Campbell, D.B., Simpson, R.A., Hudson, R.S., Chandler, J.F., Rosema, K.D., Shapiro, I.I., Standish, E.M., Winkler, R., Yeomans, D.K., Velez, R. and Goldstein, R.M., Europa, Ganymede, and Callisto: new radar results from Arecibo and Goldstone, *Journ. Geophys. Res.* , 97 , 18,227-18,244, 1992.

Pätzold, M., Bird, M.K., Volland, H., Edenhofer, P. and Buschert, H., Dynamics of the Giotto spacecraft in the inner dust coma of comet P/Halley; Part 1: Observations, *Z. Flugwiss. Weltraumforsch.* , 15 , 89-96, 1991a.

Pätzold, M., Bird, M.K., Volland, H., Edenhofer, P. and Buschert, H., Dynamics of the Giotto spacecraft in the inner dust coma of comet P/Halley; Part 2: Interpretations, *Z. Flugwiss. Weltraumforsch.* , 15 , 159-164, 1991b.

Pätzold, M., Bird, M.K. and Edenhofer, P., The change of Giotto's dynamical state during the P/Grigg-Skjellerup flyby caused by dust particle impacts, *Journ. Geophys. Res.* , 98, 20911-20920, 1993.

Pätzold, M., Bird, M.K., Edenhofer, P., Asmar, S.W. and McElrath, T.P., Dual-frequency radio sounding of the solar corona during the 1995 conjunction of the Ulysses spacecraft, *Geophys. Res. Lett.*, 22 , 3313-3316, 1995.

Pätzold, M., Karl, J., Bird, M.K., Coronal radio sounding with Ulysses: Phase scintillation spectra in coronal holes and streamers, *Astron. Astrophys.* 316, 449 - 456, 1996.

Pätzold, M., Neubauer, F.M., Andreev, V.E. and Gavrik, A.I., Detection of the inner plasma pile-up region at comet Halley during the VEGA-1 flyby by the radio sounding experiment, *Journ. Geophys. Res.* 102, 2213-2222, 1997.

Pätzold, M., and M.K. Bird, Velocity changes of the Giotto spacecraft during the comet flybys: on the interpretation of perturbed Doppler data, *Aerosp. Sci. Technol.* 5, 235-241, 2001a.

Pätzold, M., J. Schwinger, A. Wennmacher, B. Häusler, W. Eidel, K. Aksnes, H. Boehnhardt and N. Thomas, Gravity determination of a comet nucleus: Rosetta at P/Wirtanen, *Astron. Astrophys.* 375, 651 - 660, 2001b.

Pätzold, M., A. Wennmacher, B. Häusler, W. Eidel, T. Morley, N. Thomas and J.D. Anderson, Mass and density determinations of 140 Siwa and 4979 Otawara during the Rosetta flybys, *Astron. Astrophys.* 370, 1122 - 1127, 2001c.

Pätzold M. et al., Mars Express Orbiter Radio Science, *ESA-Special Publication*, SP-1240, 2004.

Pätzold M. et al., Mars Express Orbiter Radio Science, *ESA-Special Publication*, SP-xxx, in preparation, 2006.

Richter, K. and Keller, H.U., On the stability of dust particle orbits around cometary nuclei, *Icarus* 14 , 355-371, 1995.

Scheeres, D.J. (1995), Analysis of orbital motion around 433 Eros, *Journ. Astronautical Sci.* , 43 , pp. 427-452.

Simpson, R.A. and Tyler, G.L., Viking bistatic radar experiment: summary of first-order results emphasizing north polar data, *Icarus* , 46 , 361-389, 1981.

Simpson et al., 2006, accepted

Standish, E.M., Planet X – No Dynamical Evidence in the Optical Observations. *Astron. J.*, 105(5), 2000-2006, 1993.

Tyler, G.L., Brewster Angle of the Lunar Crust, *Nature*, 219, 1243-1244, 1968a.

Tyler, G.L., Oblique-scattering Radar Reflectivity of the Lunar Surface: Preliminary Results from Explorer 35, *J. Geophys. Res.*, 73, 7609 – 7620, 1968b.

Tyler, G.L. and Howard, H.T., Dual-frequency bistatic-radar investigations of the Moon with Apollos 14 and 15, *Journ. Geophys. Res.* , 78 , 4852-4874, 1973.

Tyler, G. L., Marouf, E.A., Simpson, R.A., Zebker, H.A. and Eshleman, V.R., The microwave opacity of Saturn's rings at wavelengths of 3.6 and 13 cm from Voyager 1 radio occultation, *Icarus* , 54 , 160-188, 1983.

Tyler, G.L., Sweetnam, D.N., Anderson, J.D. , Campbell, J.K. , Eshleman, V.R., Hinson, D.P. , Levy, G.S. , Lindal, G.F. , Marouf, E.A. , Simpson, R.A. ,Voyager 2 radio science observations of the Uranian system: Atmosphere, rings, and satellites. *Science*, 233, 79-84, 1986.

Tyler, G.L., Radio propagation experiments in the outer solar system with Voyager, *Proceedings of the IEEE* , 75 , 1404-1431, 1987.

Tyler, G.L. , Sweetnam, D.N. , Anderson, J.D , Borutzki, S.E. , Campbell, J.K. , Eshleman, V.R. , Gresh, D.L. , Gurrola, E.M. , Hinson, D.P. , Kawashima, N. , Kursinski, E.R. , Levy, G.S. , Lindal, G.F , Lyons, J.R. , Marouf, E.A. , Rosen, P.A. , Simpson, R.A , and Wood, GE. ; Voyager radio science observations of Neptune and Triton. *Science*, 246, 1466-1473, 1989.

Tyler, G.L., Ford, P.G., Campbell, D.B., Elachi, C., Pettengill, G.H., and Simpson, R.A., Magellan: Electrical and physical properties of Venus' surface: *Science*, v. 252, p. 265-270, 1991.

Tyler, G.L., Simpson, R.A., Maurer, M.J. and Holmann, E., Scattering properties of the Venusian surface: Preliminary results from Magellan, *Journ. Geophys. Res.* , 97 , 13115-13140, 1992a.

Tyler, G. L., G. Balmino, D. P. Hinson, W. L. Sjogren, D. E. Smith, R. T. Woo, S. M. Asmar, M. J. Connally, C. L. Hamilton, R. A. Simpson, Radio Science Investigations with Mars Observer, *Journal of Geophysical Research (Planets)*, vol. 97, no. E5, May 25, 1992b.

Tyler, G. L., G. Balmino, D. P. Hinson, W. L. Sjogren, D. E. Smith, R. A. Simpson, S. W. Asmar, P. Priest, and J. D. Twicken, Radio science observations with Mars Global Surveyor: Orbit insertion through one Mars year in mapping orbit, *J. Geophys. Res.*, 106(E10), 23,327-23,348, 2001.

Ware, R., M. Exner, et al., GPS sounding of the atmosphere from low Earth orbit - preliminary results, *Bull. Am. Meteorol. Soc.*, 77, 19-40, 1996.

Yakovlev, O.I. & Efimov, A.I., Studies of Reflection of Meter-Length Radio Waves, *Dokladi Akademii Nauk SSSR*, 174, 583-584.

Yeomans, D.K., Physical interpretations from the motions of comets Halley and Giacobini-Zinner, *ESA SP-250 II* , pp. 419-425, 1986.

Yeomans, D.K., Barriot, J.-P., Bunham, D.W., Farquar, R.W., Giorgini, J.D., Helfrich, C.E., Konopliv, A.S., McAdams, J.V., Miller, J.K., Owen, W., Jr., Scheeres, D.J., Synnott, S.P. and Williams, B.G., Estimating the Mass of Asteroid Mathilde from Tracking Data during the Near Flyby, *Science* 278, 2106-2109, 1997.

Yeomans, D.K., Antreasian, P.G., Cheng, A., Dunham, D.W., Farquhar, R.W., Gaskell, R.W., Giorgini, J.D., Helfrich, C.E., Konopliv, A.S., McAdams, J.V., Miller, J.K., Owen Jr., W.M., Thomas, P.C., Veverka, J., Williams, B.G., Estimating the Mass of Asteroid 433 Eros During the NEAR Spacecraft Flyby, *Science* Vol. 285. no. 5427, pp. 560 – 561, 1999.

Yeomans, D.K., Antreasian, P.G., Barriot, J.-P., Chesley, S.R., Dunham, D.W., Farquhar, R.W., Giorgini, J.D., Helfrich, C.E., Konopliv, A.S., McAdams, J.V., Miller, J.K., Owen, W.M., Scheeres, D.J., Thomas, P.C., Veverka, J., and Williams, B.G., Radio Science Results during the NEAR- Shoemaker Spacecraft Rendezvous with Eros. *Science* 289, 2085 – 2088, 2000.

Yuen, J. H., Ed., Deep Space Telecommunications Systems. New York, Plenum, 1983.